

**University of Piraeus**

**School of Maritime and Industrial Studies**



**Department of Industrial Management and Technology**

**PhD Thesis**

**Optimization of biomass exploitation within a  
framework of process combination**

**Salapa Ioanna**

**Consultants:**

**Professor Dimitrios Karalekas**

**Professor Dimitrios Sidoras (Supervisor)**

**Assistant Professor Christina Siontorou**

**Piraeus 2018**

# Acknowledgments

Firstly, I would like to express my sincere gratitude to my advisor Prof. Dimitrios Sdiras for the continuous support of my PhD study and related research, for his patience, motivation, and immense knowledge. His guidance helped me in all the time of research and writing of this thesis.

Besides my advisor, I would like to thank Assistant Professor Christina Siontorou who continuously supported my work and encouraged me and Emeritus Professor Fragiskos Batzias for his insightful comments. I am also grateful to Mrs Aggeliki Geronti for the assistance and Dr. Dorothea Politi for the feedback and cooperation.

My sincere thanks also goes to Assistant Professor Evangelos Topakas who gave me access to the Biotechnology Laboratory in the School of Chemical Engineering, NTUA. In addition I would like to express my gratitude to my fellow doctoral students in the Biotechnology Laboratory for the acceptance and especially to Constantinos Katsimpouras for the cooperation. Without their precious support it would not be possible to conduct this research.

I would like to thank my friends for their understanding and encouragement. Last but not the least, I would like to thank my family: my parents, my brother and grandmother for supporting me spiritually throughout writing this thesis and life in general.

# Table of Contents

Table of Figures .....	v
List of Tables .....	viii
Preface.....	xii
Introduction.....	xvi
1 Lignocellulosic biomass.....	1
1.1 Composition and chemical structure.....	1
1.1.1 Cellulose .....	1
1.1.2 Hemicellulose .....	3
1.1.3 Lignin.....	6
1.1.4 Ash.....	8
1.1.5 Pectin.....	8
1.2 The use of lignocellulosic biomass .....	10
2 Lignocellulosic biomass and the biorefinery concept.....	12
2.1 Biorefinery definition.....	12
2.2 Lignocellulosic biorefinery .....	13
2.3 Pretreatment processes .....	14
2.3.1 Physical pretreatment.....	15
2.3.2 Chemical pretreatment .....	16
2.3.3 Physico-chemical pretreatment.....	18
2.3.4 Biological pretreatment.....	20
3 Organosolv fractionation .....	21
3.1 Overview of organosolv fractionation .....	21
3.2 Biorefinery and the organosolv fractionation process .....	21
3.3 Organosolv fractionation processes .....	24
4 Process simulation and mathematical models.....	28
4.1 Organosolv fractionation .....	28
4.1.1 Generalized pseudo-first-order kinetic model .....	28
4.1.2 Severity factor .....	29
4.1.3 Design of experiments and Response surface methodology.....	30
4.2 Adsorption kinetic-study.....	34
4.2.1 Pseudo-first-order model .....	34
4.2.2 Pseudo-second-order model.....	34
4.2.3 Intra-particle diffusion model .....	35
4.3 Applicability of various adsorption isotherm models on adsorption.....	36
4.3.1 Freundlich model .....	36
4.3.2 Langmuir model.....	36
4.3.3 Sips model.....	37
4.3.4 Redlich-Peterson model .....	38
4.3.5 Temkin model .....	38
4.3.6 Dubinin-Radushkevich model .....	38
4.3.7 Toth model .....	39
4.3.8 Unilan model.....	39
5 Materials and Methods.....	40
5.1 Materials .....	40
5.2 Modification processes .....	41
5.3 Organosolv pretreatment.....	42
5.3.1 Wheat straw organosolv pretreatment with various catalysts.....	42

5.3.2	Acetone organosolv pretreatment process of barley straw .....	42
5.4	Analyses .....	43
5.4.1	Organosolv liquors .....	43
5.4.2	Composition of fractionated solids .....	44
5.4.3	Enzymatic digestibility .....	44
5.5	Pretreatment effect on lignocellulosic feedstock adsorptivity .....	44
5.5.1	Kinetic experiments .....	45
5.5.2	Isothermal experiments .....	45
6	Results and discussion .....	46
6.1	Organosolv pretreatment with various solvents .....	46
6.1.1	Compositional analysis .....	47
6.1.2	Enzymatic digestibility .....	54
6.1.3	Fermentability of pretreated solids for ethanol production.....	57
6.1.4	Adsorption capacity .....	61
6.2	Acetone organosolv pretreatment of barley straw .....	76
6.2.1	Compositional analysis .....	77
6.2.2	Enzymatic digestibility .....	78
6.2.3	Simulation based on CSF.....	80
6.2.4	Simulation based on RSM .....	85
6.2.5	Optimization .....	92
6.2.6	Adsorption capacity .....	95
7	Conclusions - Aspects for further research.....	108
7.1	Conclusions.....	108
7.2	Aspects for further research .....	110
	References.....	111
	Appendix.....	131

## Table of Figures

<b>Fig. 1.1</b> Molecular chain structure of cellulose (Zugenmaier, 2001) .....	2
<b>Fig. 1.2</b> Haworth cellulose formula (Ott et al., 1956).....	2
<b>Fig. 1.3</b> Different crystalline parts of cellulose microfibrils (Karimi et al., 2013).....	3
<b>Fig. 1.4</b> Basic hemicellulose units .....	4
<b>Fig. 1.5</b> Lignin basic structural units .....	6
<b>Fig. 1.6</b> Schematic structural formula for lignin (Adler, 1977).....	7
<b>Fig. 1.7</b> Schematic structure of pectin showing the four pectic polysaccharides homogalacturonan (HG), xylogalacturonan (XGA), rhamnogalacturonan I (RG-I) and rhamnogalacturonan II (RG-II) linked to each other. ....	9
<b>Fig. 1.8</b> Thermochemical and biochemical processing of lignocellulosic biomass (Menon & Rao, 2012).....	11
<b>Fig. 2.1</b> Biorefinery and its role in the transformation of biomass.....	12
<b>Fig.2.2</b> Lignocellulosic biomass potential products (Kamm et al., 2006).....	13
<b>Fig. 3.1</b> Organosolv-based lignocellulosic biorefinery (Salapa et al., 2017) .....	22
<b>Fig .5.1</b> The 3.75-L batch reactor PARR 455.....	41
<b>Fig. 5.2</b> The HPLC, Agilent 1260.....	43
<b>Fig. 6.1</b> Organosolv pretreatment temperature (a) and pressure (b) profiles vs. time at 160 °C for 20 min.....	48
<b>Fig. 6.2</b> Organosolv pretreatment temperature (a) and pressure (b) profiles vs. time at 180 °C for 20 min.....	49
<b>Fig. 6.3</b> Effects of organic solvent, temperature and time on lignin removal; organosolv pretreatments catalyzed by 23 mol m <sup>-3</sup> H <sub>2</sub> SO <sub>4</sub> ; organic solvents: ethanol (1-4), methanol (5-8), butanol (9-12), acetone (13-16), diethylene glycol (17-20). ....	51
<b>Fig. 6.4</b> Glucose and total reducing sugars (TRS) concentration after (a) 8 and (b) 72 h of enzymatic hydrolysis of pretreated samples using an enzyme load of 9 g kg <sup>-1</sup> of dry matter DM Cellic® CTec2 at 130 g kg <sup>-1</sup> dry solids in the total liquid mass.....	55
<b>Fig. 6.5</b> Cellulose conversion (%) achieved after 72 h of enzymatic hydrolysis and relative ethanol yield (%). ....	60
<b>Fig. 6.6</b> Curves according to the Pseudo-second-order kinetic model for untreated and organosolv pretreated with ethanol wheat straw.....	65

<b>Fig. 6.7</b> Curves according to the Pseudo-second-order kinetic model for untreated and organosolv pretreated with methanol wheat straw.....	65
<b>Fig. 6.8</b> Curves according to the Pseudo-second-order kinetic model for untreated and organosolv pretreated with butanol wheat straw. ....	66
<b>Fig. 6.9</b> Curves according to the Pseudo-second-order kinetic model for untreated and organosolv pretreated with acetone wheat straw. ....	66
<b>Fig. 6.10</b> Curves according to the Pseudo-second-order kinetic model for untreated and organosolv pretreated diethylene glycol wheat straw.....	67
<b>Fig. 6.11</b> Kinetic parameter $q_e$ according to the pseudo-second order model; organosolv pretreatments catalyzed by $23 \text{ mol m}^{-3} \text{ H}_2\text{SO}_4$ ; organic solvents: ethanol (1-3), methanol (4-6), butanol (7-9), acetone (10-12), diethylene glycol (13-15). ....	68
<b>Fig. 6.12</b> Sips plots for the adsorption of MB by untreated and organosolv pretreated with ethanol wheat straw.....	72
<b>Fig. 6.13</b> Sips plots for the adsorption of MB by untreated and organosolv pretreated with methanol wheat straw. ....	72
<b>Fig. 6.14</b> Sips plots for the adsorption of MB by untreated and organosolv pretreated with butanol wheat straw. ....	73
<b>Fig. 6.15</b> Sips plots for the adsorption of MB by untreated and organosolv pretreated with acetone wheat straw. ....	73
<b>Fig. 6.16</b> Sips plots for the adsorption of MB by untreated and organosolv pretreated with diethylene glycol wheat straw.....	74
<b>Fig. 6.17</b> Effect of organosolv pretreatment based on Sips maximum adsorption capacity ( $q_m$ ); organosolv pretreatments catalyzed by $23 \text{ mol m}^{-3} \text{ H}_2\text{SO}_4$ ; organic solvents: ethanol (1-3), methanol (4-6), butanol (7-9), acetone (10-12), diethylene glycol (13-15).....	75
<b>Fig. 6.18</b> Glucose and total reducing sugars (TRS) concentration after (a) 8 and (b) 72 h of enzymatic hydrolysis of pretreated samples using an enzyme load of $9 \text{ g kg}^{-1}$ of dry matter DM Cellic® CTec2 at $130 \text{ g kg}^{-1}$ dry solids in the total liquid mass.....	79
<b>Fig. 6.19</b> Removed lignin (%) as a function of the combined severity factor logarithm. ...	80
<b>Fig. 6.20</b> Total glucose and total xylose as a function of the combined severity factor logarithm.....	81
<b>Fig. 6.21</b> Enzymatic cellulose to glucose conversion(%) after 72 h, as a function the combined severity factor logarithm. ....	82
<b>Fig. 6.22</b> Response surface graphs for the effect of sulfuric acid concentration and reaction time on lignin removal.....	87

<b>Fig. 6.23</b> Response surface graphs for the effect of sulfuric acid concentration and reaction temperature on lignin removal. ....	87
<b>Fig. 6.24</b> Response surface graphs for the effect of reaction time and temperature on lignin removal. ....	88
<b>Fig. 6.25</b> Response surface graphs for the effect of sulfuric acid concentration and reaction time temperature on total xylan concentration.....	89
<b>Fig. 6.26</b> Response surface graphs for the effect of sulfuric acid concentration and reaction temperature on total xylan concentration.....	89
<b>Fig. 6.27</b> Response surface graphs for the effect reaction time and temperature on total xylan concentration.....	90
<b>Fig. 6.28</b> Response surface graphs for the effect of sulfuric acid concentration and reaction time. ....	91
<b>Fig. 6.29</b> Response surface graphs for the effect of sulfuric acid concentration and reaction temperature on cellulose to glucose conversion. ....	91
<b>Fig. 6.30</b> Response surface graphs for the effect of reaction time and temperature on cellulose to glucose conversion. ....	92
<b>Fig. 6.31</b> Curves of kinetic models for untreated barley straw.....	98
<b>Fig. 6.32</b> Curves of kinetic models for pretreated barley straw at 140 °C for 0 min with 10 mol/m <sup>3</sup> H <sub>2</sub> SO <sub>4</sub> (exp1).....	98
<b>Fig. 6.33</b> Curves of kinetic models for pretreated barley straw at 160 °C for 20 min with 23 mol/m <sup>3</sup> H <sub>2</sub> SO <sub>4</sub> (exp7).....	99
<b>Fig. 6.34</b> Curves of kinetic models for pretreated barley straw at 160 °C for 40 min with 35 mol/m <sup>3</sup> H <sub>2</sub> SO <sub>4</sub> (exp13).....	99
<b>Fig. 6.35</b> Kinetic parameter $q_e$ according to the pseudo-second order model with respect to the CSF.....	101
<b>Fig. 6.36</b> Plots for isotherm models for untreated barley straw.....	105
<b>Fig. 6.37</b> Plots for isotherm models for pretreated at 140 °C for 0 min with 10 mol/m <sup>3</sup> H <sub>2</sub> SO <sub>4</sub> (exp1) barley straw. ....	105
<b>Fig. 6.38</b> Plots for isotherm models for pretreated at 160 °C for 20 min with 23 mol/m <sup>3</sup> H <sub>2</sub> SO <sub>4</sub> (exp7) barley straw. ....	106
<b>Fig. 6.39</b> Plots for isotherm models for pretreated at 160 °C for 40 min with 35 mol/m <sup>3</sup> H <sub>2</sub> SO <sub>4</sub> (exp13) barley straw. ....	106
<b>Fig. 6.40</b> Sips plots for the adsorption of MB by acetone organosolv pretreated barley straw.....	107

## List of Tables

<b>Table 3.1</b> Fractionation processes .....	24
<b>Table 4.1</b> Response-surface designs.....	32
<b>Table 5.1</b> Composition of untreated barley and wheat straw (mass fraction (%) on dry solid). .....	40
<b>Table 6.1</b> Organosolv pretreatment of wheat straw at varying temperature, reaction time and solvent. ....	47
<b>Table 6.2</b> Composition of pulps and raw wheat straw (mass fraction (%) on dry solid)...	50
<b>Table 6.3</b> Mass balance (expressed as mass fraction of the initial dry cellulose).....	52
<b>Table 6.4</b> Mass balance (expressed as mass fraction of the initial dry xylan). ....	53
<b>Table 6.5</b> Cellulose conversion (%) achieved after 72 h of enzymatic hydrolysis of organosolv pretreated wheat straw samples using an enzyme load of 9 g kg <sup>-1</sup> of dry matterDM Cellic® CTec2 at 130 g kg <sup>-1</sup> dry solids in the total liquid mass. ....	56
<b>Table 6.6</b> Effect of different organosolv pretreatment conditions on maximum ethanol production, ethanol productivity, and relative ethanol yield (calculated as percentage of maximum theoretical yield). ....	59
<b>Table 6.7</b> Pseudo-first-order kinetic model parameters. ....	62
<b>Table 6.8</b> Pseudo-second-order kinetic model parameters.....	63
<b>Table 6.9</b> Initial adsorption factor $R_i$ and kinetic behavior based on the intra-particle diffusion model. ....	64
<b>Table 6.10</b> Parameters of Freundlich isotherm model of MB adsorption on modified and untreated wheat straw. ....	69
<b>Table 6.11</b> Parameters of Langmuir isotherm model of MB adsorption on modified and untreated wheat straw. ....	70
<b>Table 6.12</b> Parameters of Sips isotherm model of MB adsorption on modified and untreated wheat straw. ....	71
<b>Table 6.13</b> Box-Behken experimental design and the combined severity factor.....	76
<b>Table 6.14</b> Liquor composition (% on initial polysaccharides). ....	77
<b>Table 6.15</b> Composition of pulps and untreated barley straw (mass fraction (%) on dry pulp). ....	78
<b>Table 6.16</b> Estimated t-values and p-values for the regression coefficients obtained from the combined severity factor. ....	83
<b>Table 6.17</b> Analysis of variance for polynomial models derived from the combined severity factor.....	84
<b>Table 6.18</b> Estimated t-values and p-values for the regression coefficients. ....	85
<b>Table 6.19</b> Analysis of variance for polynomial models. ....	86
<b>Table 6.20</b> Pseudo-first-order kinetic model parameters. ....	96
<b>Table 6.21</b> Pseudo-second-order kinetic model parameters.....	97
<b>Table 6.22</b> Initial adsorption factor $R_i$ and kinetic behavior based on the intra-particle diffusion model. ....	100
<b>Table 6.23</b> Parameters of Freundlich isotherm model of MB adsorption on modified and untreated barley straw with regard to the CSF.....	102
<b>Table 6.24</b> Parameters of Langmuir isotherm model of MB adsorption on modified and untreated barley straw with regard to the CSF.....	103
<b>Table 6.25</b> Parameters of Sips isotherm model of MB adsorption on modified wheat straw and untreated barley straw with regard to the CSF.....	104

---

## Nomenclature

---

A	Temkin isotherm model constant
ANOVA	Statistical analysis of variance
b	Temkin constant related to the heat adsorption
B	Dubinin-Radushkevich isotherm model constant related to the mean free energy of adsorption ( $\text{mol}^2 \text{kJ}^{-2}$ )
$C_0$	Initial dye concentration (mg/L)
$C_e$	The equilibrium concentration of dye in solution (mg/L)
$C_{ij}$	Concentrations expressed in w/w units based on initial quantity of dry component in the reacting system
CSF	Combined severity factor
DF	Degrees of Freedom
DOE	Design of experiments
E	Activation energy (kJ/mol)
F	Fisher's variance ratio
k	Reaction rate constant ( $\text{min}^{-1}$ )
$k_1$	The rate constant of sorption ( $\text{min}^{-1}$ )

$k_2$	The rate constant of pseudo-second-order adsorption model ( $\text{g mg}^{-1} \text{min}^{-1}$ )
$K_F$	Freundlich isotherm constant related to adsorption capacity ( $\text{mg g}^{-1} (\text{L mg})^{1/n}$ )
$K_L$	Langmuir equilibrium constant ( $\text{L/mg}$ )
$k_p$	The rate constant of intra-particle diffusion model ( $\text{mg/g min}^{0.5}$ )
$K_S$	Sips equilibrium constant ( $\text{L mg}^{-1})^{1/n_S}$
$K_T$	Toth equilibrium constant
MB	Methylene blue
MS	Mean Square
$n$	Freundlich isotherm constant related to adsorption intensity
$n_S$	Sips isotherm model exponent
$q_e$	The amount of dye adsorbed at equilibrium time ( $\text{mg/g}$ )
$q_m$	Maximum adsorption capacity ( $\text{mg/g}$ )
$q_t$	The amount of dye adsorbed at any time 't' ( $\text{mg/g}$ )
R	Universal gas constant ( $\text{J mol}^{-1} \text{K}^{-1}$ )
$R_o^*$	Combined severity factor (including pH effect for non-isothermal reaction conditions)
$R^2$	Coefficient of determination factor
$R_i$	The initial adsorption factor of the intra-particle diffusion model

$R_L$	Langmuir dimensionless separation factor
$R_o$	Severity parameter
$R^*_o$	Combined severity factor (including pH effect)
RSM	Response surface methodology
S	Unilan constant
SA	Sulfuric acid
SEE	Standard Error of Estimate
SigF	Significance of F
SS	Sum of squares
SSF	Saccharification and fermentation process
t	Reaction time (min)
T	Reaction temperature (°C)
$T_{ref}$	Reference temperature (usually 100 °C)
TRS	Total reducing sugars
UWS	Untreated wheat straw
X	Cellulose conversion (%)
Y	Relative ethanol yield (%)

# Preface

This PhD Thesis was carried out from July 2012 to January 2018 and it is submitted for the degree of Philosophiae Doctor at the Department of Industrial Management and Technology in the School of Maritime and Industrial Studies of University of Piraeus. The focus of the Thesis has been the effective biomass exploitation within the biorefinery concept.

Lignocellulose feedstock basically encompasses forest woody feedstocks (softwoods and hardwoods), agricultural residues and herbaceous or municipal solid wastes. Lignocellulose feedstock is abundant, low in cost and its availability does not impact land use. Some pilot and demo plants, for ethanol production in operation in Europe and USA, use wood residues, switchgrass, cereal straw, corn stover, sugar cane bagasse etc. The three main components of lignocellulose are cellulose, hemicellulose and lignin, of which only cellulose and hemicellulose contain sugars such as glucose and xylose that can be used for ethanol production. However, cellulose and hemicellulose are polymers of which the sugars are not readily available for fermentation. The breakdown of these complex sugars into their monomeric forms, glucose and xylose, is necessary before the sugars can be fermented into ethanol or other biobased products. Consequently the crucial step for lignocellulosic ethanol production is the pretreatment process which breaks down the complex sugars. Several pretreatment methods have been proposed over the years each one having certain advantages and disadvantages. Organosolv pretreatment process of wheat and barley straw was chosen and evaluated herein, within the biorefinery concept.

During my doctoral studies, the results of the research work have been published, as follows:

## Journals with ISI Impact Factor

1. Salapa I., Katsimpouras C., Topakas E., Sidiras D., 2017. Organosolv pretreatment of wheat straw for efficient ethanol production using various solvents. *Biomass and Bioenergy* **100**, 10–16. doi:10.1016/j.biombioe.2017.03.011. [ISI Impact Factor 3.219](#).
2. Salapa I., Topakas E., Sidiras D., 2018. Simulation and optimization of barley straw organosolv pretreatment. *Industrial Crops & Products* **113**, 80-88, doi: 10.1016/j.indcrop.2018.01.018. [ISI Impact Factor 3.181](#).

### **Journals without ISI Impact Factor**

1. F.A. Batzias, D.K. Sidiras, C.G. Siontorou, A.N. Bountri, D.V. Politi, O.N. Kopsidas, I.G. Konstantinou, G.N. Katsamas, I.S. Salapa, S.P. Zervopoulou. Experimental design for estimating parameter-values of modelling crude oil adsorption on thermo-chemically modified lignocellulosic biomass. *International Journal of Arts and Sciences* 7(3) (2014) 205-222.
2. D.K. Sidiras, I.S. Salapa, “Organosolv pretreatment as a major step of lignocellulosic biomass refining” in "Biorefinery I: Chemicals and Materials From Thermo-Chemical Biomass Conversion and Related Processes", Nicolas Abatzoglou, Universite de Sherbrooke, Canada Sascha Kersten, University of Twente, The Netherlands Dietrich Meier, Thunen Institute of Wood Research, Germany Eds, ECI Symposium Series, (2015).  
[http://dc.engconfintl.org/biorefinery\\_I/18](http://dc.engconfintl.org/biorefinery_I/18)
3. D.K. Sidiras, F.A. Batzias, C.G. Siontorou, I.G. Konstantinou, I.Salapa, S.P. Zervopoulou, “Modeling of pollutant adsorption on novel modified biomass as a means of seawater decontamination” in "Biorefinery I: Chemicals and Materials From Thermo-Chemical Biomass Conversion and Related Processes", Nicolas Abatzoglou, Universite de Sherbrooke, Canada Sascha Kersten, University of Twente, The Netherlands Dietrich Meier, Thunen Institute of Wood Research, Germany Eds, ECI Symposium Series, (2015).  
[http://dc.engconfintl.org/biorefinery\\_I/16](http://dc.engconfintl.org/biorefinery_I/16)
4. F.A. Batzias, D.K. Sidiras, C.G. Siontorou, I.G. Konstantinou, G.N. Katsamas, I.S. Salapa, S.P. Zervopoulou. Modeling with parameter identification of pollutant adsorption on novel modified biomass as a means of lake/river water decontamination. *International Journal of Arts & Sciences*, 08(08) (2015) 347–374.

## Conferences

- (1) Batzias F. A., *Salapa I. S.*, Siontorou C. G., On the tradeoff between reliability and uncertainty when combining bioreactors for wastewater treatment, 8th WSEAS International Conference on Cellular and Molecular Biology, Biophysics and Bioengineering, December 29-31 2012, Montreux, Switzerland.
- (2) D.K. Sidiras, F.A. Batzias, C.G. Siontorou, A.N. Bountri, D.V. Politi, O.N. Kopsidas, I.G. Konstantinou, G.N. Katsamas, I.S. Salapa, S.P. Zervopoulou. Factorial Experimental Design for Determining Biomass Thermochemical Treatment and Pure Hydrocarbons Adsorption Parameters. 22nd European Biomass Conference and Exhibition. Hamburg, Germany, 23 - 26 June 2014, pp. 1043 - 1057.
- (3) *Salapa I. S.*, Sidiras D. K., Methylene blue adsorption on maleic acid pretreated wheat straw, 23<sup>rd</sup> European Biomass Conference & Exhibition, June 1-4 2015, Vienna, Austria pp. 403-409.
- (4) D.K. Sidiras, F.A. Batzias, C.G. Siontorou, I.G. Konstantinou, G.N. Katsamas, I.S. Salapa, S.P. Zervopoulou. Techno-economic optimization of the modification process of lignocellulosic biomass to adsorbent material at laboratory scale. 23<sup>rd</sup> European Biomass Conference and Exhibition, Vienna, Austria, 1-4 June 2015, pp. 410-424.
- (5) *Salapa I.S.*, Sidiras D.K., Organosolv pretreatment of barley straw within the biorefinery concept. 24th European Biomass Conference and Exhibition, 6-9 June 2016, pp. 1187 – 1192, Amsterdam, The Netherlands. 6-9 June 2016, pp. 1187 – 1192, DOI:10.5071/24thEUBCE2016-3CV.2.4
- (6) Sidiras D. K., *Salapa I.S.*, Politi D.V., Organosolv modified wheat straw as adsorbent for basic dyes in water bodies, 2<sup>nd</sup> World Congress on Mechanical, Chemical, and Material Engineering (MCM'16) August 22 – 23 2016, Budapest, Hungary. pp. 106-1 - 106-8.

- (7) Sidiras D. K., *Salapa I.S*, Politi D.V., Giakoumakis G., Organosolv treated barley straw for industrial Liquid waste cleaning, 25<sup>th</sup> European Biomass Conference & Exhibition, June 12-15 2017, Stockholm, Sweden. pp. 1253 - 1258.

The journal papers (without ISI impact factor) No 1, 3 and 4 and the conference papers No 2 and 4 have been co-financed by the European Union (European Social Fund – ESF) and Greek national funds through the Operational Program "Education and Lifelong Learning" of the National Strategic Reference Framework (NSRF) - Research Funding Program: THALES. Investing in knowledge society through the European Social Fund. - Project: **THALIS – University Of Piraeus – Development Of New Material From Waste Biomass For Hydrocarbons Adsorption In Aquatic Environments.**

# Introduction

A short description of the PhD Thesis follows. The Thesis consists of two parts: the theoretical and the experimental. The theoretical part includes chapters 1 to 4. More specifically in chapter 1 An introduction referred to the lignocellulosic biomass composition and chemical structure is presented. Furthermore, several uses of lignocellulosic biomass are analyzed along with its intertwined nature hindering complete exploitation.

In chapter 2, the biorefinery concept is introduced. However in order to achieve total utilization of the key lignocellulosic components (cellulose, hemicelluloses and lignin) a crucial step is the pretreatment. Pretreatment processes are categorized and the most commonly used are described in detail.

In chapter 3, the proposed organosolv pretreatment process is described. The integration of the organosolv pretreatment process in a biorefinery pilot plant along with a literature survey about various solvent/water mixtures and the fractionation results are presented.

In chapter 4, three approaches to simulate the fractionation process are described. The generalized pseudo-first order kinetic model, the Severity factor and the Response surface methodology. Moreover, the most widely used kinetic and isotherm models proposed to elucidate the mechanism of adsorption are also presented.

The experimental part includes chapters from 5 and 6. More specific, in chapter 5 the materials used in modification experiments and in adsorbency experiments are presented. Furthermore, the experimental procedure, the laboratory equipments and the analytical techniques of these experiments are also presented.

In chapter 6, the results of the organosolv fractionation process of materials such as wheat and barley straw towards enzymatic digestibility are presented. The influence of the most important process parameters is investigated in an attempt to achieve process optimization. Furthermore, the adsorption capacity of the untreated and pretreated wheat and barley straw, are extensively studied using several kinetic and isotherm equations and models. Finally, in chapter 7, general conclusions and aspects for further research are presented.

# 1 Lignocellulosic biomass

## 1.1 Composition and chemical structure

Lignocellulosics constitutes the most abundant source of unutilized biomass and their availability does not necessarily impact land use. There are several types of raw materials that are differentiated by their origin, composition and structure. Forest woody feedstocks (softwoods and hardwoods), agricultural residues, herbaceous and municipal solid wastes are some of those types.

Lignocellulosic biomass mainly consists of 30-50% cellulose, 15-35% hemicellulose and 10-20% lignin (Petersen, 1984; Badger, 2000; Mielenz, 2001; Girio et al., 2010). Apart from the three basic chemical compounds that lignocellulose consists of; water is also present in the complex. Furthermore, minor amounts of proteins, minerals and other components can be found in the lignocellulose composition as well.

Cellulose molecules arrange regularly and determine the framework of the plant's cell wall while fibers are filled with hemicellulose and lignin. There is different bonding among cellulose, hemicellulose, and lignin. Cellulose and hemicellulose or lignin molecules are linked together mainly by hydrogen bonds. In addition to the hydrogen bonds, there is the chemical bonding between hemicellulose and lignin, which results in the lignin, when isolated from natural lignocelluloses, containing a small amount of carbohydrates. The chemical bonds among the hemicellulose and lignin mainly refer to the chemical bonds between galactose residues, arabinose residues on the side chains of hemicellulose molecules and lignin (Chen, 2014).

### 1.1.1 Cellulose

One of the key components in the plant cell wall, which determines the wall structure, is cellulose. The "ideal" cellulose is a linear polymer composed of individual anhydroglucose units (also called glucopyranose units) linked at the 1 and 4 positions through glucosidic bonds with the beta configuration.

Cellulose mainly contains carbon (44.44%), hydrogen (6.17%), and oxygen (49.39%). Moreover, its chemical formula, as presented in Fig. 1.1, is  $(C_6H_{10}O_5)_n$ ; n, called the degree of polymerization, representing the number of glucose groups and ranging from hundreds to thousands or even tens of thousands. The glucose residue is tilted toward its neighbors by  $180^\circ$ , thus it would be more accurate to consider the cellulose as a polymer of cellobiose

(Fig.1.1), and not glucose as Haworth's formula showed (Fig.1.2) (Lee et al. 1994; Pérez and Samain, 2010).

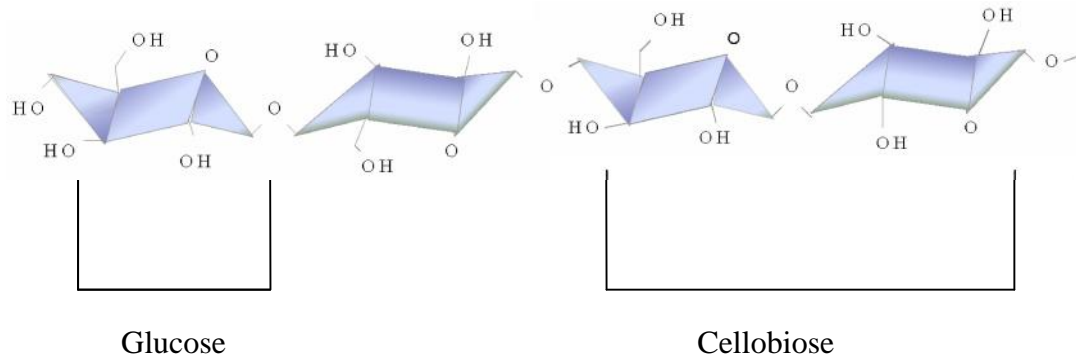


**Fig. 1.1** Molecular chain structure of cellulose (Zugenmaier, 2001)

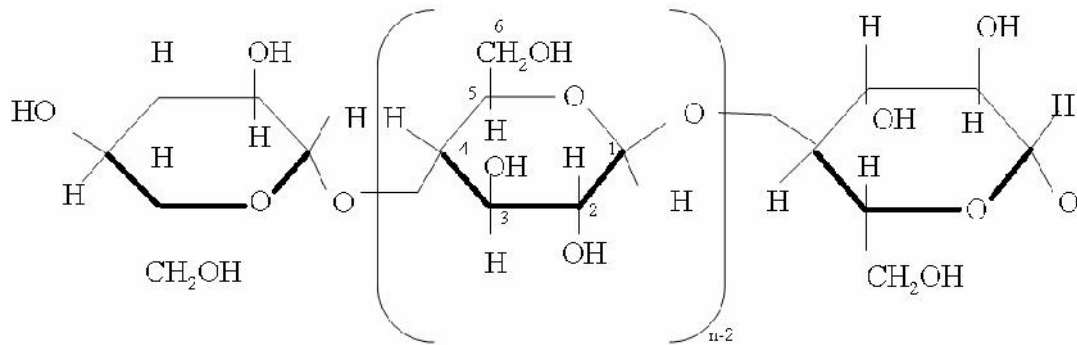


**Fig. 1.2** Haworth cellulose formula (Ott et al., 1956)

The stabilization and crystallinity of cellulose derive mainly from the presence of hydroxyl groups (OH) (Festucci-Buselli et al., 2007). Large amounts of hydroxyl groups in the crystalline phase are available in each glucose molecule forming many hydrogen bonds; these hydrogen bonds construct a huge network that directly contributes the compact crystal structure (Zhang et al., 2008). In most conditions, the cellulose is wrapped by hemicellulose (dry matter accounting for 20–35 %) and lignin (dry matter accounting for 5–30 %).

The crystallization of cellulose exhibits pleomorphism. There are five kinds of crystal modification in solid cellulose, whose characteristics can be reflected by characteristics of their unit cells. Under certain conditions, cellulose crystals can be converted into many crystal variants. Type I is the crystal form of the natural cellulose. Types II, III, IV, and X

are those crystal forms of “artificial” cellulose under artificial processing. Now, the commonly accepted cell structure of type I is the monoclinic unit cell model introduced by Meyer and Misch in 1937 (Zhan, 2005). The cellulose molecules in lignocelluloses are in the form of fibrils, where the fibrils are composed of microfibrils. Microfibrils in turn are composed of elementary fibrils that are further associated with hemicellulose and lignin. Each microfibril is suggested to contain approximately 36 glucose chains (Ding and Himmel 2006). The microfibrils consist of three groups of glucose chains; true crystal chains (core chains), subcrystalline chains (transition chains), and “subcrystalline or noncrystalline” chains (surface chains) as shown in Fig. 1.3 (Ding and Himmel 2006; Festucci-Buselli et al. 2007). From them the true-crystal chains are the most resistant part of cellulose for chemical and biological hydrolysis.

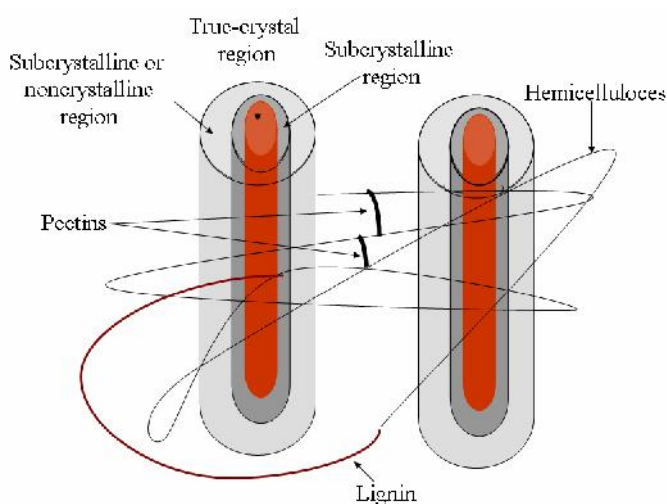


**Fig. 1.3** Different crystalline parts of cellulose microfibrils (Karimi et al., 2013)

### 1.1.2 Hemicellulose

Hemicellulose, also called polyoses, a heteropolymer of polysaccharides and polyuronides, is available in almost all lignocellulosic materials along with cellulose. The cellulosic fabric in the primary and secondary cell walls of plants forms a continuous but also porous (or sponge like) with communicating interstices system. In these elongated spaces are deposited the amorphous cell-wall constituents, mainly lignin and polysaccharides that are described as hemicelluloses. These noncellulosic unoriented components similarly form a more or less continuous interpenetrating system and thus having a stiffening effect on the wall as a whole (Ott et al., 1956).

The polysaccharide part of hemicellulose contains different polymers of hexosans (mannan, glucosan, galactan, and rhamnan) and pentosans (xylan and arabinan) (Fig. 1.4). Polyuronides parts contain hexuronic acids and methoxyl, acetyl, and free carboxylic groups. Polyuronides appear to be more sensitive to chemical and biological attacks than polysaccharide (Norman, 1934; Billa and Monties, 1991).

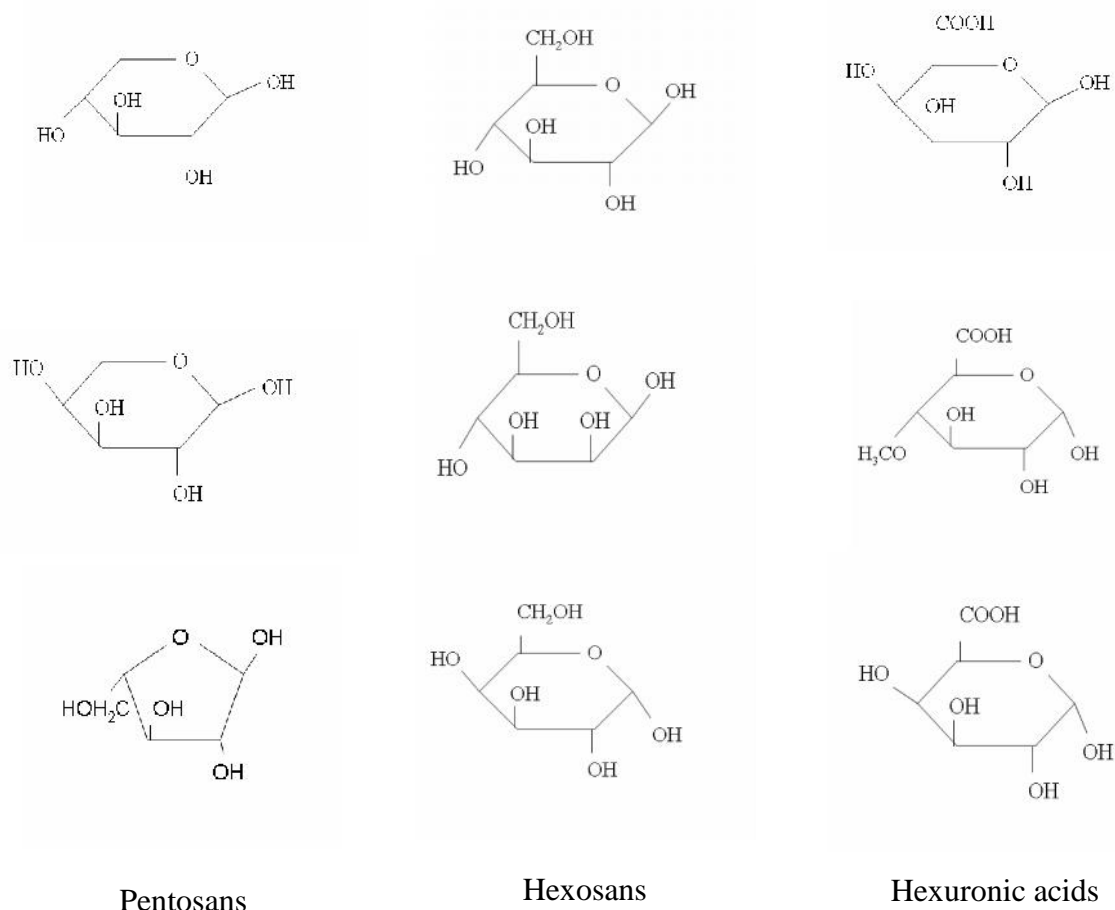


**Fig. 1.4** Basic hemicellulose units

In general xyloglucan, galactoglucomannans, arabinoglucuronoxylan, xylan, glucuronoxylan, arabinoxylan, mannan, and glucomannan are the key polymers in hemicelluloses. The main monomeric sugar in softwoods hemicelluloses is mannose which is highly acetylated and contains galactose side groups. While xylose is dominant in hardwoods and agriculture residues which is less acetylated and contains arabinose side groups (Fry, 1989). The typical molecular structure of hemicellulose of Gramineae is mainly composed of  $\beta$ -D-xylopyranosyl, which is linked by  $\beta$ -1,4-glucosidic bonds. Branch chains consist of L-arabinofuranosyl and D-glucuronopyranosyl, respectively, on C3 and C2 of the main chain; there are also branch chains composed of xylosyl and acetyl (xylosyl

acetate). The degree of polymerization of hemicellulose in Gramineae is less than 100 (Xu et al., 2003).

Unlike cellulose, which is crystalline and recalcitrant to hydrolysis, hemicellulose has an amorphous structure with short chain polymers as a side chain. Thus making hemicellulose more easily degraded in acidic medium than cellulose (Girio et al. 2010; Peng et al. 2012).

### 1.1.3 Lignin

Lignin is one of the most abundant organic polymers in plants, just after cellulose. It is a very complex polymer playing a cementing role to connect cells while at the same time enhancing the mechanical strength properties, and rendering the plant resistant against diseases and biodegradation by microorganisms. Lignin is sometimes referred as glue between hemicellulose and cellulose components; whereas other times as glue between lignin and cellulose. Anyway, hemicellulose and lignin are known to cover the surface of cellulose, which adds structural strength to the cellulose matrix (Pérez and Samain 2010).

Lignin is a cross-linked polymer which is basically composed of phenylpropane units connected by C–C and C–O linkages. Lignin includes three basic structural monomers: p-phenyl monomer (H type) derived from coumaryl alcohol, guaiacyl monomer (G type) derived from coniferyl alcohol, and syringyl monomer (S type) derived from sinapyl alcohol (Fig. 1.5). Due to the different monomers, lignin can be divided into three types: syringyl lignin polymerized by syringyl propane, guaiacyl lignin polymerized by guaiacyl propane, and hydroxy-phenyl lignin polymerized by hydroxy-phenyl propane

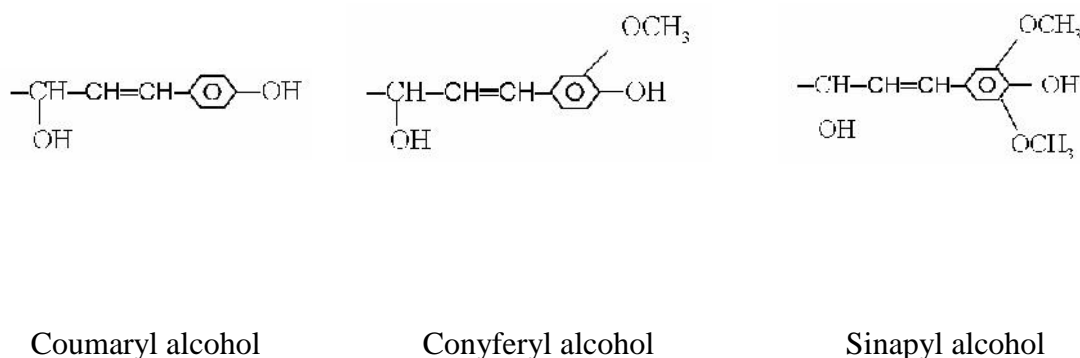


**Fig. 1.5** Lignin basic structural units

Although lignin only has three basic structures, the quantity proportions of these basic structures vary greatly in different families of plants. Lignin of hardwood includes large amounts of syringyl units whereas softwood lignin includes mainly guaiacyl-type units and a small amount of p-hydroxyphenyl-type. The prominent substructures of spruce lignin are collected in a scheme (Fig. 1.6) comprising 16 C<sub>9</sub> units. The sequence of the different units has been chosen arbitrarily (Adler, 1977).

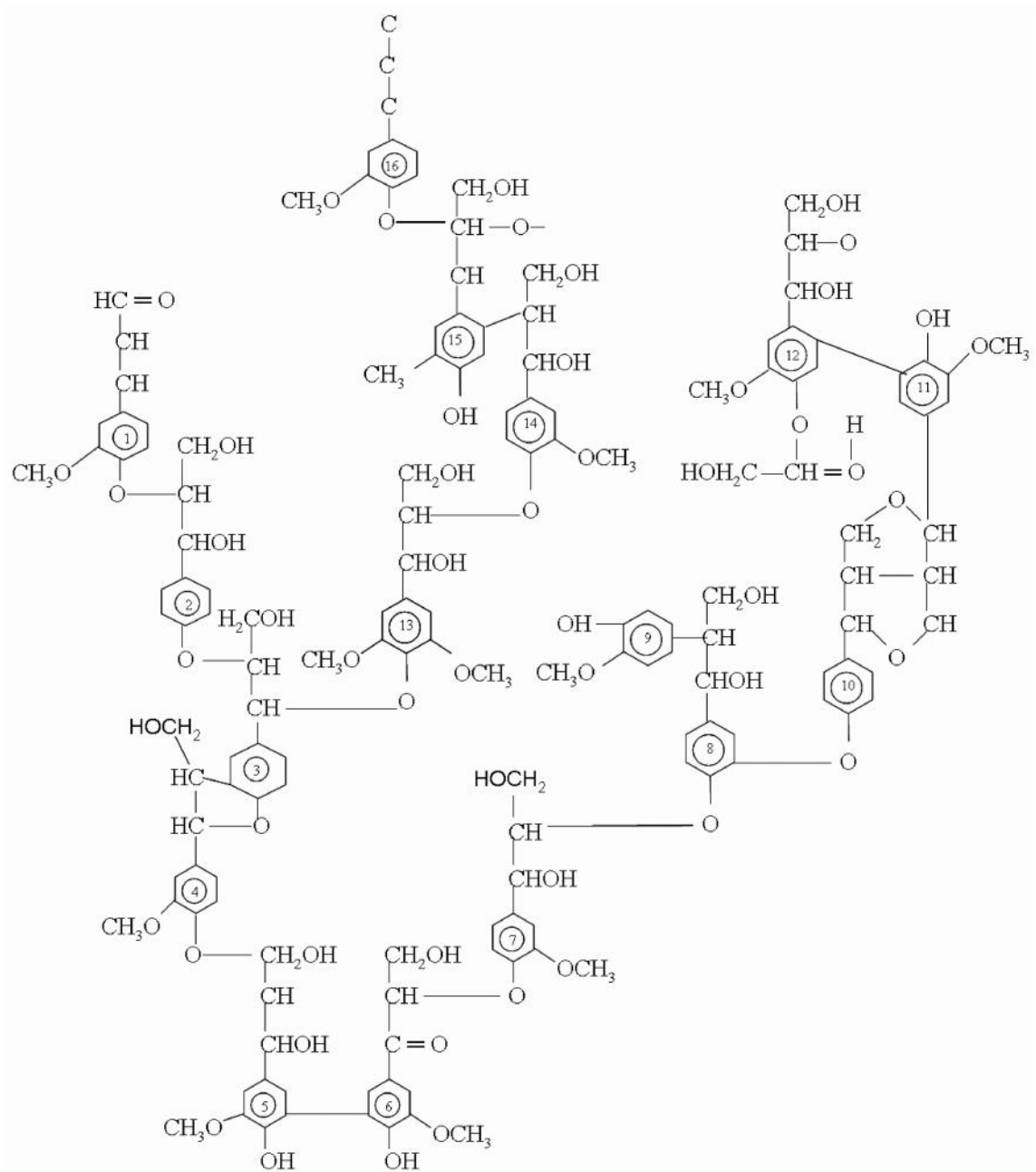


**Fig. 1.6** Schematic structural formula for lignin (Adler, 1977)

#### **1.1.4 Ash**

Nitrogen, sulfur, phosphorus, calcium, magnesium, iron, potassium, sodium, copper, zinc, manganese, chlorine are only some of the elements that are indispensable in plant cells except of carbon, hydrogen, oxygen, and other basic elements. When the sample is dried at 105 °C and further processed at 750 °C in a high temperature furnace, elements like carbon, hydrogen, oxygen, nitrogen, sulfur, etc. disappear in the form of gaseous compounds, and the residue is the ash which contains many types of mineral elements in the form of oxide. Different types of plants and growth environment would lead to different types and contents of elements. These elements are absorbed from soil and generally exist as ions. Additionally, as different parts of the plants have different functions in the process of plant growth, different distributions of metal ions is also observed. For example the metal elements and silicon content in the joints, leaves, and ears of wheat straw are significantly higher than in the internode stem (Yang, 2008). Moreover, when Gramineae was compared with other plant materials, SiO<sub>2</sub> was accounted for more than 60% of straw ash, even more than 80% in rice straw (Chen, 2014).

#### **1.1.5 Pectin**

Multiple lines of evidence indicate a role for pectin in plant growth, development, morphogenesis, defense, cell–cell adhesion, wall structure, signaling, cell expansion, wall porosity, binding of ions, growth factors and enzymes, pollen tube growth, seed hydration, leaf abscission, and fruit development (Ridley et al., 2001). Pectin is the most structurally complex family of polysaccharides in nature, making up ~35% of primary walls in dicots and non-graminaceous monocots, 2–10% of grass and other commelinoid primary walls, and up to 5% of walls in woody tissue (O'Neill et al., 1990; Ridley et al., 2001).

The structural classes of the pectic polysaccharides include homogalacturonan (HG), xylogalacturonan (XGA), apiogalacturonan (AGA), rhamnogalacturonan II (RG-II), and rhamnogalacturonan I (RG-I). It is generally believed that the pectic polysaccharides are covalently cross-linked since harsh chemical treatments or digestion by pectin-degrading enzymes are required to isolate HG, RG-I, and RG-II from each other and from walls. There is presently no consensus as to how the pectic polysaccharides are linked to each other, or to other polymers, in the wall; nevertheless, the available data (Ishii and Matsunaga, 2001; Nakamura et al., 2002, Coenen et al., 2007) support a model with HG,

RG-I, and RGII linked via their backbones (Fig. 1.7). There are also indications based on co-elution of pectins with other wall polymers and mutant phenotype studies that pectins may be covalently linked to, or tightly associated with, other types of wall polysaccharides including xyloglucans (Popper and Fry, 2007) and xylans (Nakamura et al., 2002b).

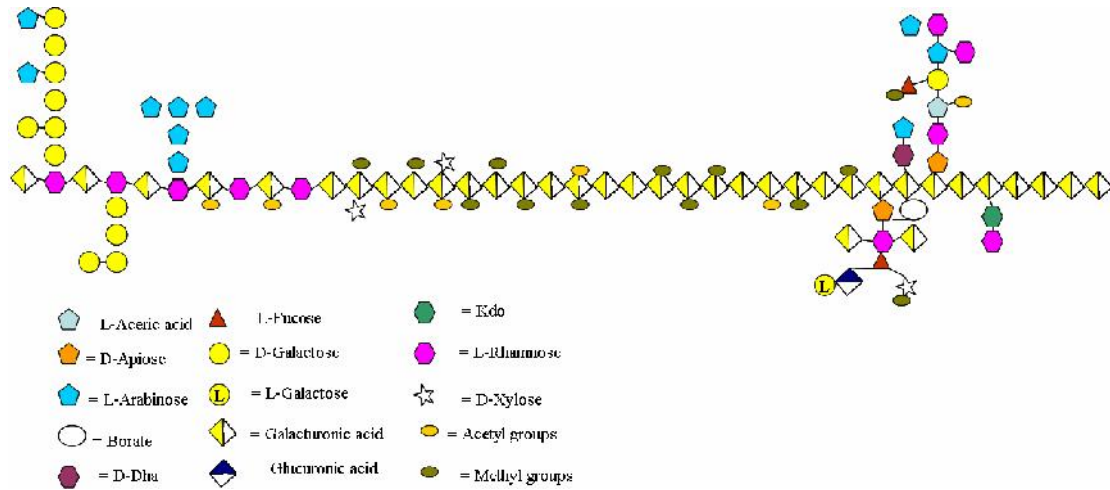


**Fig. 1.7** Schematic structure of pectin showing the four pectic polysaccharides homogalacturonan (HG), xylogalacturonan (XGA), rhamnogalacturonan I (RG-I) and rhamnogalacturonan II (RG-II) linked to each other. The representative pectin structure shown is not quantitatively accurate, HG should be increased 12.5-fold and RG-I increased 2.5-fold to approximate the amounts of these polysaccharides in walls (Mohnen, 2008).

## **1.2 The use of lignocellulosic biomass**

Globally large amount of agricultural residues are produced, most of which is burnt as waste disposal and thus underused. Over the years there have been several approaches on the subject and some of them will be presented herein.

A very appealing way to exploit the agricultural wastes is via pulping, refining and bleaching, of those residues, for papermaking. Several kinds of non-wood lignocellulosic agricultural remains have been investigated of which wheat, rice bagasse and barley straw were the most promising (Xu et al., 2013; Kaur et al., 2017). Other agricultural wastes like rapeseed straw (Mousavi et al., 2013), hemp core (Barberà et al., 2011) and olive tree trimmings (Díaz et al., 2005), orange tree trimmings (Moral et al., 2016) have been also studied.

Another approach suggests the use of lignocellulosic biomass as low cost alternative adsorbents for the removal of water pollutants like dyes. The term adsorption refers to a process wherein a material is concentrated at a solid surface from its liquid or gaseous surroundings. Some of the most commonly used, for dye wastewater treatment, adsorbents are: alumina, silica gel, zeolites and last but not least activated carbon (Gupta and Suhas, 2009). Various agricultural by-products like grapefruit peel (Saeed et al., 2010), banana peel (Annadurai et al., 2002), pineapple stem (Hameed et al., 2009), garlic peel (Hameed and Ahmad, 2009), rice husk (Vadivelan and Kumar, 2005) and others have been studied for their adsorption capacity.

Finally the most popular use is the production of energy and value-added materials. Fig. 1.8 presents the types of energy that can be produced from lignocellulosic residues.

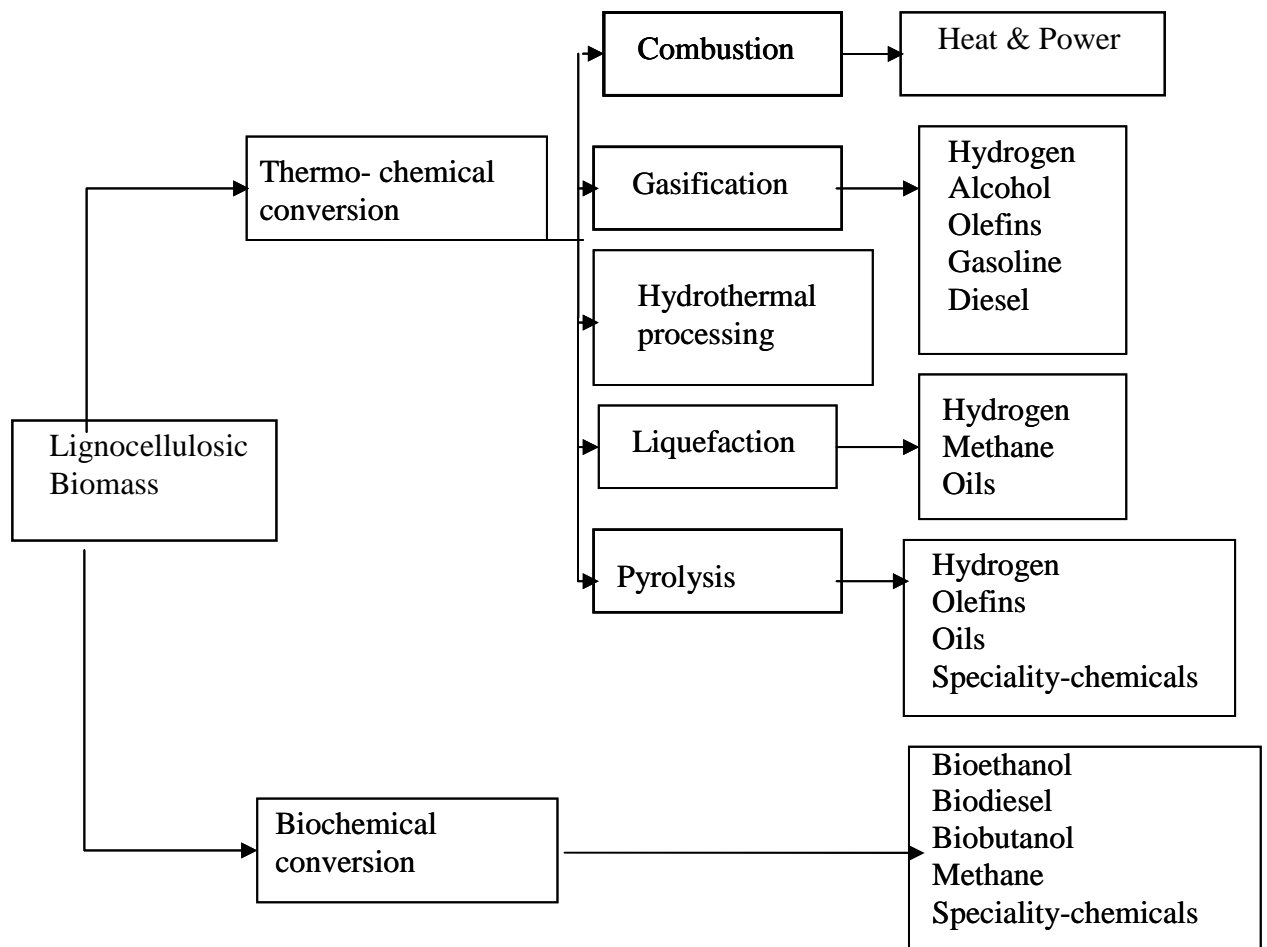


**Fig. 1.8** Thermochemical and biochemical processing of lignocellulosic biomass (Menon & Rao, 2012)

The production of biofuels along with value-added materials as well as the biorefinery concept will be analysed in greater detail in the following chapter.

## 2 Lignocellulosic biomass and the biorefinery concept

### 2.1 Biorefinery definition

Among the several definitions of biorefinery, the most complete was developed by the IEA Bioenergy Task 42 ‘‘Biorefineries’’:

‘‘Biorefining is the sustainable processing of biomass into a spectrum of marketable products and energy’’.

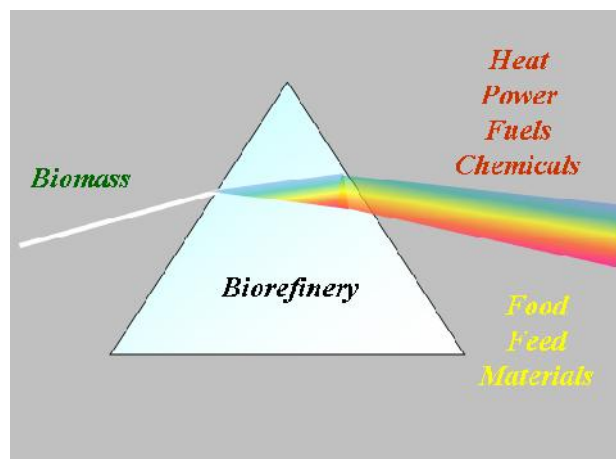


**Fig. 2.1** Biorefinery and its role in the transformation of biomass.

With this definition, biorefineries are expected to supply a wide range of bio-based products and energy in a socio-economically and environmentally sustainable manner. The products can be both intermediates and final products, and include food, feed, materials and chemicals; whereas energy includes fuels, power, and/or heat (Fig. 2.1). A biorefinery can exploit all kinds of biomass from forestry, agriculture, aquaculture, and residues from industry and households including wood, agricultural crops, organic residues (both plant and animal derived), forest residues, and aquatic biomass (algae and seaweeds).

Nevertheless, a biorefinery is not an utterly new concept. Many of the traditional biomass converting technologies such as the sugar, starch and pulp and paper industry can be (partly) considered as biorefineries (de Jong and Jungmeler, 2015).

## 2.2 Lignocellulosic biorefinery

Lignocellulosic feedstock (LCF) biorefinery scheme has shown significant promise as it has the potential to accommodate a wide range of low-cost feedstocks (straw, grass, wood, paper-waste, etc.) that could yield conversion products in both the existing petrochemical-dominated market and the future biobased product markets (FitzPatrick et al., 2010).

Fig. 2.2 is the schematic representation of the potential products of a lignocellulosic biorefinery facility (Kamm et al., 2006).

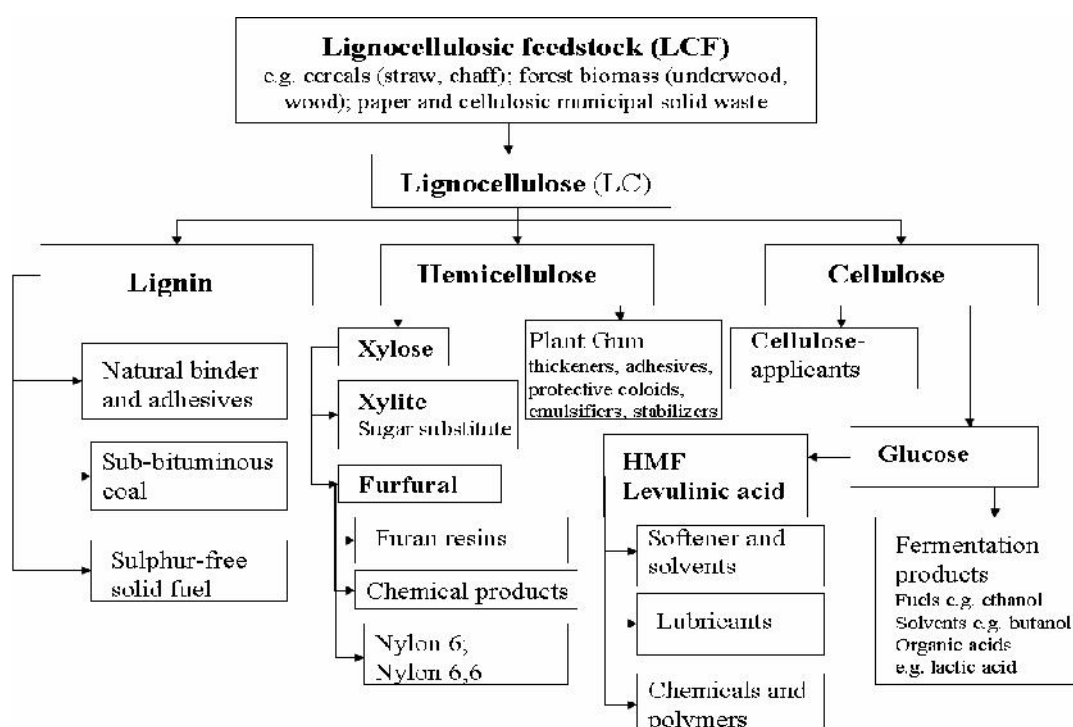


**Fig. 2.2** Lignocellulosic biomass potential products (Kamm et al., 2006)

In the last few years research efforts are underway to facilitate the transition from “oil-refinery” to “bio-refinery”, based on renewable lignocellulosic biomass (Barakat et al., 2013; Astner et al., 2015). The five major steps involved in biomass conversion into fuels and platform chemicals are: choice of suitable biomass, effective pretreatment, production of saccharolytic enzymes such as cellulases and hemicellulases along with the accessory enzymes, fermentation of hexoses and pentoses and the downstream processing (Menon and Rao, 2012).

However the economic feasibility of this transition depends on the capacity of establishing a strategy by which the key lignocellulosic components (cellulose, hemicelluloses and lignin) are totally utilized. Due to the highly intertwined nature of such

feedstock, gaining access to the native biomacromolecules for subsequent chemical transformation is foremost importance. Consequently, pretreatment as the second and very crucial step has come to denote processes by which cellulosic biomass is made amenable to the action of hydrolytic enzymes.

## **2.3 Pretreatment processes**

Typically a pretreatment involves the alteration of biomass so that (enzymatic) hydrolysis of cellulose and hemicellulose can be achieved more rapidly and with greater yields. Positive effects of the pretreatment processes are: a) Increase of surface area and porosity b) Modification of lignin structure c) Removal of lignin d) (Partial) depolymerization of hemicellulose e) Removal of hemicellulose f) Reducing the crystallinity of cellulose.

However several criteria must be met in order to characterize a pretreatment effective.

These criteria are:

- i. Avoiding size reduction
- ii. Preserving hemicellulose fractions
- iii. Limiting formation of inhibitors due to degradation products
- iv. Minimizing energy input
- v. Being cost effective
- vi. Catalyst recycling
- vii. Waste treatment

Pretreatment results must be balanced against their impact on the cost of the downstream processing steps and the trade-off between operating costs, capital costs, and biomass costs (Lynd et al., 1996; Agbor et al., 2011). As shown in Fig.2.3 the process utilizes pretreatment additives and/or energy to form solids that are more reactive than native material and/or generate soluble oligo- and monosaccharides (Mosier et al., 2005).

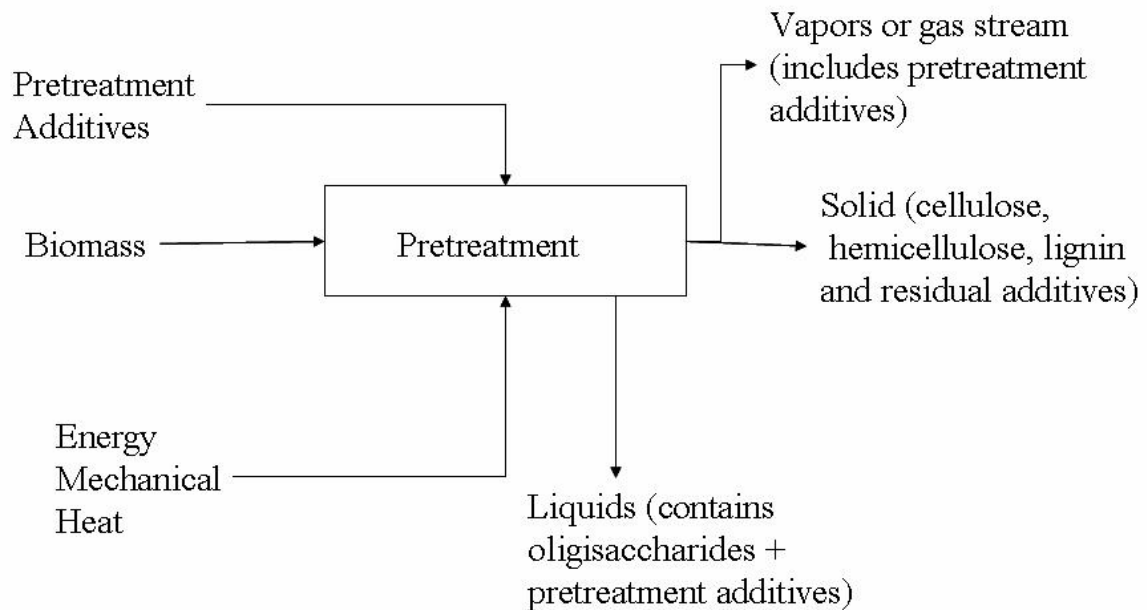


**Fig.2.3** Schematic of pretreatment process

The methods are generally categorized into “Physical pretreatment”, “Chemical pretreatment”, “Biological pretreatment” and their combinations (Menon and Rao, 2012; De Bhowmick et al., 2017).

### 2.3.1 Physical pretreatment

Changing the structure of biomass by increasing the enzyme surface area and reducing the degrees of polymerization of biomass in order to enhance digestibility can be partly achieved via mechanical processing such as size reduction. Different types of milling (e.g., ball milling, hammer milling, colloid milling, two-roll milling, and vibro energy milling), irradiations (e.g., by microwaves, gamma rays, electron beams, and ultrasonications), and extrusion (subjecting the biomass to heating, mixing, and shearing) are employed for this propose (Taherzadeh and Karimi 2008; Zheng et al. 2009).

Although studies have shown that milling increases biogas, bioethanol and biohydrogen yields, modification of biomass structure with a single physical treatment is typically not enough for efficient enzymatic hydrolysis. (Delgenes et al., 2002). Thus, the physical treatments are used prior to (or together with) chemical and biological treatments (Taherzadeh and Karimi, 2008; Yu et al. 2009).

## **2.3.2 Chemical pretreatment**

Treatment by using chemicals such as acids, alkali, organic solvents and ionic liquids has been reported to have significant effect on the native structure of lignocellulosic biomass (Swatloski et al. 2002). Subsequently is presented a short description of the most widely used chemical processes.

### **2.3.2.1 Acid pretreatment**

This chemical pretreatment method involves the use of concentrated or diluted acids to break the rigid structure of the lignocellulosic material. Although dilute acid hydrolysis presents the advantage of lower acid consumption, higher temperature is required and more severe conditions should be applied in order to achieve reasonable yield of glucose from crystalline cellulose, resulting in an extensive degradation of the amorphous hemicelluloses (Rabemanolontsoa and Saka, 2016). The most frequently used acid is dilute sulfuric acid ( $\text{H}_2\text{SO}_4$ ), which has been used for a wide variety of biomass types-sunflower straw (Antonopoulou et al., 2016), rice straw (Lee et al., 2015), soybean straw (Qing et al., 2017), corn stover (Qureshi et al., 2015; Chen et al., 2016), and oak spruce (Jeong et al., 2017). Other acids have also been studied, such as hydrochloric acid (HCl) (Wang et al., 2010; Antonopoulou et al., 2016), phosphoric acid ( $\text{H}_3\text{PO}_4$ ) (Zhang et al., 2007), formic acid ( $\text{CH}_2\text{O}_2$ ) (Dong et al., 2017) and nitric acid ( $\text{HNO}_3$ ) (Himmel et al., 1997).

### **2.3.2.2 Alkaline pretreatment**

Alkaline pretreatment refers to the use of bases, such as sodium hydroxide (Procentese et al., 2017), potassium hydroxide (Kassim and Bhattacharya, 2015) calcium hydroxide (or else lime) (Karr and Holtzapple, 2000; Kim and Holtzapple, 2005), and ammonium (Kim et al., 2003; Yoo et al., 2011), for the pretreatment of lignocellulosic biomass. The use of an alkali causes the degradation of ester and glycosidic side chains resulting in structural alteration of lignin, cellulose swelling, partial decrystallization of cellulose (Cheng et al., 2010; McIntosh and Vancov, 2010; Ibrahim et al., 2011), and partial solvation of hemicellulose (Sills and Gossett, 2011). Alkaline methods have the advantage to utilize mostly nonpolluting and non-corrosive chemicals. Moreover they are usually carried out under less severe conditions than those needed for acid pretreatment. Nevertheless, a neutralizing step is required in order to remove lignin and inhibitors (salts, phenolic acids, furfural, and aldehydes) before enzymatic hydrolysis.

### 2.3.2.3 Organosolv

Organosolv processes utilize an organic solvent or mixtures of organic solvents with water for removal of lignin before enzymatic hydrolysis of the cellulose fraction. The majority of organosolv pretreatments is conducted at high temperatures (100–250 °C) using low boiling point solvents (methanol and ethanol), high boiling point alcohols (ethylene glycol, glycerol, tetrahydrofurfuryl alcohol) and other classes of organic compounds including ethers, ketones, phenols, organic acids, and dimethyl sulfoxide (Thring et al. 1990). During the process, the hemicellulose is hydrolyzed, lignin is dissolved in the liquor and purified cellulose is produced as a pulp. The dissolved lignin can be separated by precipitation by water addition or solvent evaporation. The resulting products are (1) a pulp mainly consisting of cellulose, (2) solid lignin and (3) an aqueous stream containing hemicellulose sugars and derivatives such as furfural (Zhao et al., 2009). The organosolv pretreatment will be discussed in greater detail on the following chapter.

### 2.3.2.4 Ionic liquids (ILs) pretreatment

ILs are a new type of cellulose solvent, because of their high thermal stability and very low vapor pressure which enables processing plant operators to recover over 99% of the solvents and no toxic products during pretreatment, they are also known as “green solvents” (Fu and Mazza, 2011a,b). These solvents are organic salts mainly composed of organic cations (Liu et al., 2016), and organic/inorganic anion (Brandt et al., 2013; Wahlström and Suurnäkki, 2015; Dutta et al., 2016; Sun et al., 2016). Their key properties are: a) liquid below 100 °C or even at room temperature; b) high thermal stability; c) high polarity, and; d) very low vapor pressure (Zavrel, 2009). Pretreatment with ILs has been reported to reduce the lignin content of lignocellulosics as well as disrupting the crystalline structure of cellulose, thereby enhancing hydrolysis (Li et al., 2010; Uju et al., 2012). Compared to conventional processes using ionic liquids present several advantages (Nguyen et al., 2010; Ha et al., 2011):

- require mild conditions,
- possess low toxicity, and
- does not destroy the fermentable sugar

However, ionic liquids present the drawback of being expensive and require tedious recycling, since their toxicity and biodegradability are not yet well understood (Rabemanolontsoa and Saka, 2016).

### **2.3.3 Physico-chemical pretreatment**

Pretreatments that combine both chemical and physical processes in order to reduce reaction time and improve efficiency are referred as physico-chemical. Some of the most important processes are: steam explosion, liquid hot water, ammonia fiber explosion (AFEX) and microwave-chemical pretreatment. A brief introduction with these processes will take place at this section.

#### **2.3.3.1 Steam explosion**

Steam explosion involves exposing the lignocellulosic biomass to high pressure saturated steam for a short period of time, commonly starting in the range 160 °C to 260 °C (Sun and Cheng, 2002) followed by a sudden exposure to atmospheric pressure. The pretreatment is aiming at hemicellulose solubilization in order to increase the amenability of cellulose to enzymatic hydrolysis while also preventing the formation of inhibitors. Steam explosion has several advantages including: a) low energy requirement; b) minimal chemical use; c) minimal dilution of the released carbohydrate sugars; d) no recycling or environmental costs; e) low environmental impact; f) applicability to various feedstocks, specifically agricultural residues and hardwoods (Sun and Cheng, 2002; Mupondwa et al., 2017). However, it cannot achieve complete disruption of the lignin-carbohydrate matrix, and thus, products from hemicellulose are not completely recovered. Moreover due to the formation of inhibitors such as phenolic acids and dehydration by-products derived from pentoses (e.g., furfural) and hexoses (e.g., hydroxymethylfurfural) washing before enzymatic hydrolysis is needed (Palmqvist and Hahn-Hägerdal, 2000; Menon and Rao, 2012; Mupondwa et al., 2017).

#### **2.3.3.2 Liquid hot water**

Liquid hot water pretreatment is a hydrothermal process that involves exposure of lignocellulosic biomass to water at high temperature and pressure (Mupondwa et al., 2017). It was also variously referred as hydrothermolysis (Bobleter and Concin, 1979; Bobleter et al., 1981), aqueous or steam/aqueous fractionation (Bouchard et al., 1991), uncatalyzed solvolysis (Mok and Antal, 1992, 1994) and aquasolv (Allen et al., 1996). The difference between steam explosion and liquid hot water pretreatment lies in the state in which water is used (gaseous versus aqueous).

Liquid hot water pretreatment has been reported to have the potential to improve cellulose digestibility, sugar extraction, and pentose recovery, with the benefit of producing prehydrolyzates containing little or no inhibitor of sugar fermentation (Kim et al., 2009). Additional advantages are: a) removal up to 80% of hemicellulose; b) since water is the only pretreatment solvent there is no need for neutralization; c) no need for size reduction because the particles are broken apart during the pretreatment (Menon and Rao, 2012). On the other hand the disadvantages of the process are: a) long residence time; b) demands large volumes of water and equipments (that are expensive); c) high energy consumption for heating and evaporation of water; d) moderate formation of co products (Seidl and Goulart, 2016)

### **2.3.3.3 Ammonia fiber explosion (AFEX)**

Ammonia fiber explosion is a physico-chemical pretreatment process involving lignocellulosic biomass exposure to liquid ammonia at elevated temperature and pressure for a period of time followed by a sudden pressure release.

AFEX pretreatment results in the decrease of lignin content, partial depolymerization of hemicellulose, decrystallization of cellulose and increase in accessible surface area due to structural disruption (Teymouri et al., 2004; Kumar et al., 2009). Its advantages include: a) low formation of sugar degradation products; b) high lignin redistribution; c) no need for washing and neutralization; d) ammonia recovery-reuse possible (Menon and Rao, 2012, Seidl and Goulart, 2016; Mupondwa et al., 2017). The major drawbacks of the process are: the high cost of ammonia acquisition, recovery and recycle, as well as the fact that AFEX is not very efficient for biomass with higher lignin content (e.g. softwood) (Stephen et al., 2012).

### **2.3.3.4 Microwave-chemical pretreatment**

Microwaves are energy waves from the electromagnetic spectrum with frequencies ranging from 0.3 to 300 GHz, analogous to wavelengths varying from 1 m to 1 mm. The central idea of this process is exposing the biomass feedstock to microwaves of 2450 MHz in the range of 250–1000 W, with operating temperature ranging from 70 to 230 °C, heating time ranging from 5 to 12 (Mupondwa et al., 2017).

The pretreatment leads to: depolymerization and breakdown of the crystalline arrangement of cellulose molecules, fragmentation of lignocellulosic structure resulting in a

reduction in particle size and an increase in surface area and increase in hemicellulose hydrolysis and partial lignin depolymerization. In the case of lignocellulosic feedstocks, microwave pretreatment has been mainly used in combination with a chemical pretreatment technique with chemicals such as acids, alkalis, ionic liquids, oxidising agents and high boiling point liquids being commonly employed (Bundhoo, 2018). Microwave/chemical pretreatment has been used for a wide variety of cellulosic biomass including: sugarcane bagasse (Binod et al., 2012; Chen et al., 2011), palm fibers (Laghari et al., 2016), corn straw (Liu and Cheng, 2010), barley straw (Sapci, 2013), wheat straw (Xu et al., 2011) and many others.

#### **2.3.4 Biological pretreatment**

Biological pretreatment involves the use of microorganisms (including various bacteria and fungi) capable of deconstructing the cell wall of lignocellulosic biomass and modify the chemical composition and/or structure of the lignocellulosic biomass so as to improve the enzymatic saccharification rate. The specific mode of action or degradation characteristics of these microorganisms depends on which component of the biomass is targeted. In general, brown and soft rots mainly attack cellulose while imparting minor modifications to lignin, and white-rot fungi are more actively degrade the lignin component (Sánchez, 2009). There are several advantages of using microbial consortium which include increase adaptability, have the advantage of being safe, environmentally benign, and having low energy input relative to other pretreatment methods. However, large scale operation leads to high operational costs since pretreatment to be carried out in sterile conditions and this increases the cost of the process. Moreover, these selective pretreatments are not only slow, but they require a very large pretreatment space and great effort by processing plant managers to control growth conditions (Sindhu et al., 2016).

## **3 Organosolv fractionation**

### **3.1 Overview of organosolv fractionation**

The earliest report of organosolv treated lignocellulosic material can be traced back in 1893, when Klason used ethanol and hydrolytic acid to separate wood into its components so as to study the structure of lignin and carbohydrates. Subsequently Pauli et al. in 1918 applied formic acid and acetic acids to delignify wood so as to characterize its main components.

Over the following years several authors have investigated the potential of various organic solvents, e.g., various alcohols, phenol, acetone, prop ionic acid, dioxane, various amines, esters, formaldehyde, chloroethanol, whether pure or in aqueous solutions, and in the presence or absence of acids, bases or salts as catalysts mainly as alternatives to the classic pulping process (Johansson et al., 1987; Chum et al., 1990). This method of fractionation has been assessed also for the production of cellulosic substrates that can be easily hydrolyzed by enzymes (Holzapple and Humphrey, 1984; Chum et al., 1988) in biotechnological routes to fuels and chemicals.

At this point it should be cleared that even though organosolv pretreatment is similar to organosolv pulping, it does not require the equivalent degree of delignification as the latter. Furthermore, while slight degradation of the cellulose structure can promote enzymatic hydrolysis during the production of biofuels, preservation of fiber quality is of most importance during pulping.

### **3.2 Biorefinery and the organosolv fractionation process**

Within the biorefinery concept, organosolv pretreatment appears to be very promising among pretreatment methods due to its inherent advantages i.e. separation of high purity cellulose with only minor degradation, isolation of high quality lignin, higher efficiency of hemicellulose fractionation compared with conventional treatments and organic solvent recovery (Zhang et al., 2016; Goh et al., 2011). In Fig. 3.1, a possible lignocellulosic biorefinery scheme is depicted (Salapa et al., 2017 ).

As already mentioned, organosolv pretreatment can be performed using a number of organic or aqueous-organic solvents with or without addition of a catalyst (acid, base or salt). This mixture partially hydrolyzes lignin bonds and lignin-carbohydrate bonds, resulting in a solid residue composed mainly by cellulose and some hemicellulose. Ethanol appears to be the most popular organic solvent over the years (Toledano et al., 2013; Wildschut et al., 2013; Mesa et al., 2010; Sidiras and Koukios, 2004). However, other solvents like methanol (Gilarranz et al., 1999), acetone (Huijgen et al., 2010), formic acid, acetic acid (Snelders et al., 2014) and glycerol have been also studied (Sun et al., 2015). An analytical table including organosolv pretreatment with various solvents will be presented later on.

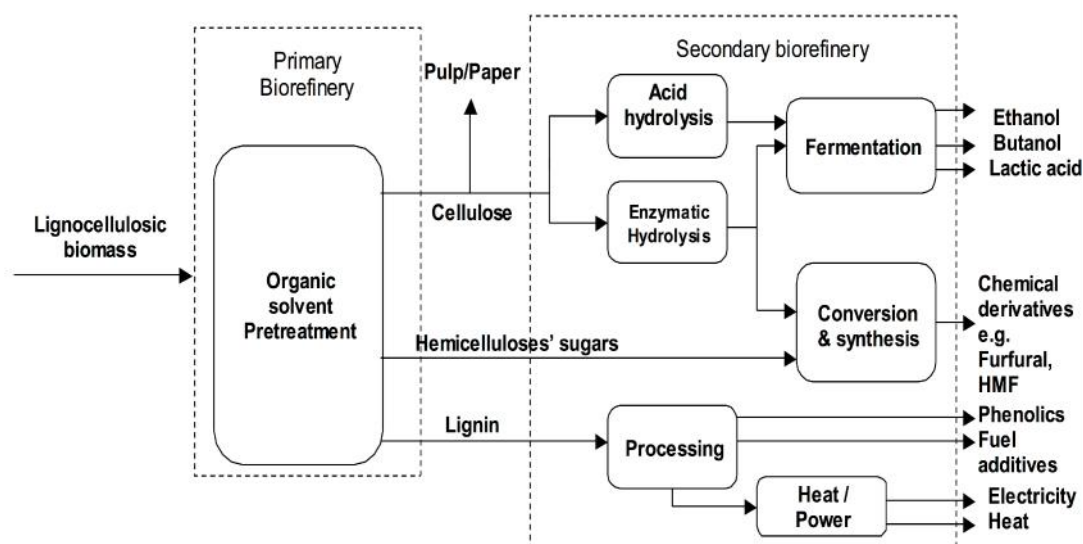


**Fig. 3.1** Organosolv-based lignocellulosic biorefinery (Salapa et al., 2017)

In Leuna, Germany at the Fraunhofer Center for Chemical-Biotechnological Processes (CBP) a pilot plant for the fractionation of wood into glucose, lignin and xylose was developed, built and is operating since 2012. The plant's estimated capacity is 50 t/h dry wood while operating 8000 h per year. The wood is pulped with ethanol/water mixture at selected conditions. As presented in Fig. 3.2 glucose is obtained by enzymatic hydrolysis of the pulp; lignin is precipitated from the pulping liquor via water dilution or thermal precipitation to receive organosolv lignin; liquid process streams are collected for solvent (ethanol) recovery and after ethanol recovery, a resulting fraction of C5-sugars (e.g. xylose) is obtained.

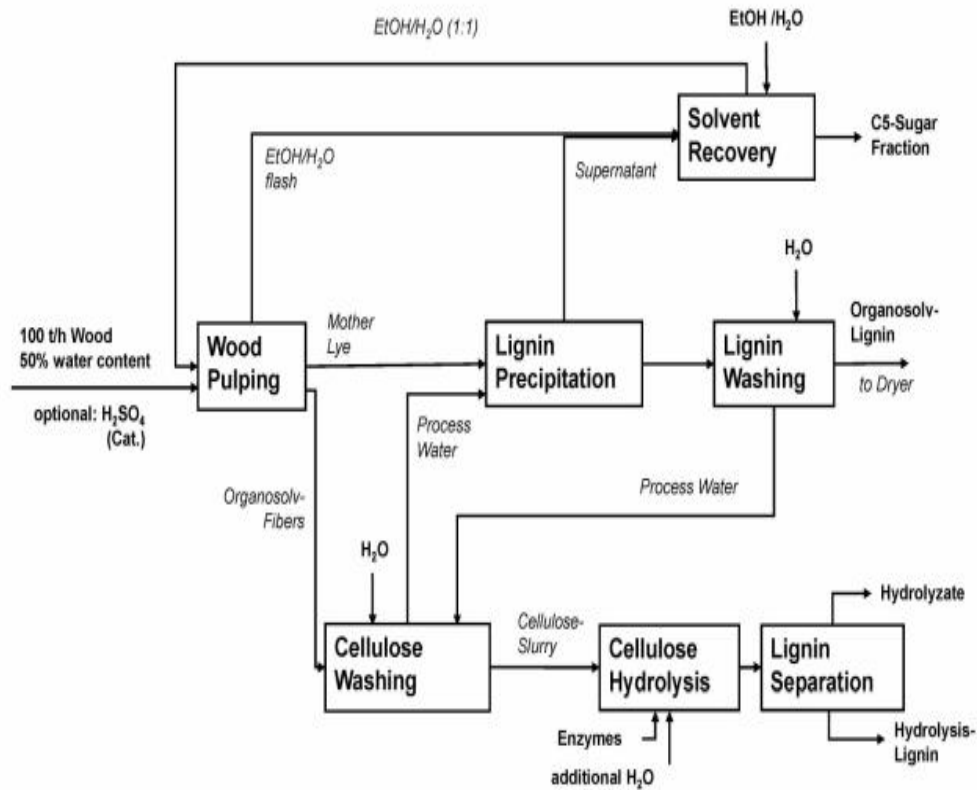


**Fig. 3.2** Process flow sheet of plant (Laure et al., 2014)

The economic and environmental assessment of the process revealed the potential competitiveness and benefits of a “lignocellulose biorefinery”. As a result the ethanol organosolv process appears to be a feasible and promising, from an economic and environmental point of view, integrated material utilization concept for lignocellulosic feedstock. Nevertheless, it is of most importance to valorize all the obtained fractions, including the C5 sugars, and to avoid effluent streams, which may burden the profitability (Laure et al., 2014).

### 3.3 Organosolv fractionation processes

In Table 3.1 are presented several organosolv fractionation processes by various solvent/water mixtures with or without catalyst. The choice of feedstock is very versatile depending on the availability. Moreover each raw material requires a different pretreatment strategy based on their composition.

**Table 3.1** Fractionation processes

Process	Feedstock	Fractionation conditions	Results	Ref.
Ethanol/H <sub>2</sub> SO <sub>4</sub>	Wheat straw	Ethanol 50% (w/v), H <sub>2</sub> SO <sub>4</sub> 0.02–2 N, liquid/solid ratio 20, 83–196 °C, 10–180 min	Maximum solubilized lignin 96%	Sidiras and Koukios, 2004
Ethanol/H <sub>2</sub> SO <sub>4</sub>	Hybrid poplar	Ethanol 50% (v/v), H <sub>2</sub> SO <sub>4</sub> dosage 1.25%, 180 °C, 60 min	Pulp: yield 52.72%, lignin content 6.19%; Solute lignin: yield 15.53%	Pan et al., 2006
Ethanol/H <sub>2</sub> SO <sub>4</sub>	Lodgepole pine	Ethanol 65% (v/v), H <sub>2</sub> SO <sub>4</sub> dosage 0.76–1.10%, liquid/solid ratio 5, 170-187 °C, 60 min	Solid fraction: yield 27–44%, solute lignin 16–23%	Pan et al., 2008
Acetone/H <sub>2</sub> SO <sub>4</sub>	Pinus radiata D. Don	Acetone 50% (v/v), H <sub>2</sub> SO <sub>4</sub> 0.9% (w/w), liquid/solid ratio 7, 183-197 °C, 4-46 min	Optimal conditions: 195 °C, 5 min, 99.5% ethanol yield	Araque et al., 2008
Acetic acid	Eucalyptus	Acetic acid 90%, HCl dosage 0.5%, Liquor/solid ratio 10, boiling point, 180 min	Pulp: yield 46%, kappa number 31	Ligero et al., 2008
Ethanol/H <sub>2</sub> SO <sub>4</sub>	Miscanthus x giganteus	Ethanol 44%, H <sub>2</sub> SO <sub>4</sub> dosage 0.5%, liquid/solid ratio 8, 170 °C, 60 min	Solid fraction: yield 62%, Klason lignin content 11.2%, cellulose cont. 81.5%	Brosse et al., 2010

Ethanol/NaOH	L.diversifolia	Ethanol 45% (v/v), alkali concentration 17%, liquid/solid ratio 8, 180 °C, 60 min	Pulp: yield 49.7%, brightness 41% ISO, Paper : tensile index 17.4 kNm/kg, burst index 0.68 MPam <sup>2</sup> /kg, tear index 1.03 Nm <sup>2</sup> /kg	Lopez et al., 2010
Ethanol/H <sub>2</sub> SO <sub>4</sub>	Sugar cane bagasse	Ethanol 50% (v/v), H <sub>2</sub> SO <sub>4</sub> dosage 1.25%, liquid to solid ratio 5, 175 °C, 60 min	Solid fraction: yield 87%, lignin content 28%	Mesa et al., 2010
Ethanol/NaOH	Carpolobia lutea	Ethanol 60% (v/v), alkali concentration 8%, liquid/solid ratio 7, 150 °C, 30 min	Pulp: yield 48.53%, lignin content 4.63%	Ogunsile & Quintana, 2010
Ethanol/H <sub>2</sub> SO <sub>4</sub> Ethanol/NaOH Ethanol/MgCl <sub>2</sub>	Pinus rigida	Ethanol 50% (v/v), liquid/solid ratio 10, 1% H <sub>2</sub> SO <sub>4</sub> (w/v), 1% MgCl <sub>2</sub> (w/v), 1-2% NaOH (w/v), 150-210 °C, 0-20 min	Maximum ethanol yield 70% obtained at 180 °C for 0 min with 1% H <sub>2</sub> SO <sub>4</sub> (w/v)	Park et al., 2010
Formic acid	Corn	Formic acid 88%, liquid/ solid ratio 10, 60 °C, 360 min	Hemicelluloses degradation 85%, delignification 70%	Zhang et al., 2010
Ethanol/NaOH	Sugar cane bagasse	Ethanol 50% (v/v), NaOH dosage 1.25%, liquid/solid ratio 5, 175 °C, 60 min	Solid fraction: yield 90%, lignin content 27%	Lopez et al., 2011
Ethanol/H <sub>2</sub> SO <sub>4</sub>	Empty palm fruit bunch	Ethanol 65% (v/v), liquid/solid ratio 8, H <sub>2</sub> SO <sub>4</sub> 0.5-2%, 160-200 °C, 45-90 min	Optimal conditions: 160 °C, 78 min, 2.0% H <sub>2</sub> SO <sub>4</sub> resulted in 96.03% glucose recovery	Goh et al., 2011
Ethanol/H <sub>2</sub> SO <sub>4</sub>	Wheat straw	Ethanol 50-80% (w/w),	Optimal conditions:	Wildschut et

		H <sub>2</sub> SO <sub>4</sub> 0-30 mM, liquid/solid ratio 10, 160-210 °C, 60-120min	210 °C, 50% (w/w) aqueous ethanol, no catalyst or 190 °C, 60% (w/w), 30 mM H <sub>2</sub> SO <sub>4</sub> resulted in 86% glucose yield, 84% lignin yield Solid fraction: 71.9 g L <sup>-1</sup> glucose, 17.1 g ethanol/ 100g	al., 2013
Ethanol	Olea europea pruning	Ethanol 70% (w/w) liquid/solid ratio 6, 200 °C, 90 min	olive tree pruning Liquid fraction: lignin depolymerized into catechol and 4-methylcatechol Maximum glucose yield 75%, xylose yield 45%, arabinose yield 43% achieved at 180 °C, 30 min with 30% ethanol At 180 °C for 30 min achieved highest glucose yield 46.2%	Toledano et al., 2013
Ethanol	Wheat bran	Ethanol 30-60% (w/w), liquid/solid ratio 4, 160-200 °C, 30 min	fermented to 80.3 g butanol, 21.1 g acetone, 22.5 g ethanol After 40 d anaerobic digestion acetic acid and ethanol led to highest methane yield i.e. over 0.30 m <sup>3</sup> CH <sub>4</sub> /kg volatile solids	Reisinger et al., 2014
Ethanol/H <sub>2</sub> SO <sub>4</sub>	Rice straw	Ethanol 75% (v/v), liquid/solid ratio 8, H <sub>2</sub> SO <sub>4</sub> 1% (w/w), 150 or 180 °C, 30 or 60 min		Amiri et al., 2014
Ethanol, Methanol, Acetic acid	Forest residues	Solvent 50% (v/v), liquid/solid ratio 10, 190 °C, 60 min		Kabir et al., 2015

Formic acid/H <sub>2</sub> SO <sub>4</sub> , Acetic acid/H <sub>2</sub> SO <sub>4</sub> , Ethanol, Ethanol/H <sub>2</sub> SO <sub>4</sub>	Wheat straw (WS)	Acetic or formic acid 68-88% (w/w), liquid/solid ratio 10, 0-0.1% (w/w) H <sub>2</sub> SO <sub>4</sub> , boiling point, 0.5-1.5h Ethanol 60% (w/w), H <sub>2</sub> SO <sub>4</sub> 30 mM, 190 °C, 1h Ethanol 65% (v/v), 220 °C, 20min	Highest ethanol yield obtained by formiline pretreatment 12.2 g ethanol/100 g WS Lowest by acetiline 7.5 g ethanol/100 g WS Ethanol + H <sub>2</sub> SO <sub>4</sub> 11.4 g ethanol/100 g WS Ethanol no catalyst 11.8 g ethanol/100 g WS	Chen et al., 2015
Ethanol	Eucalyptus chips	Ethanol 60% (w/w), liquid/solid ratio 6, 160 °C, 90min	Maximum glucose yield after 72h 47.9%	Mou and Wu, 2016

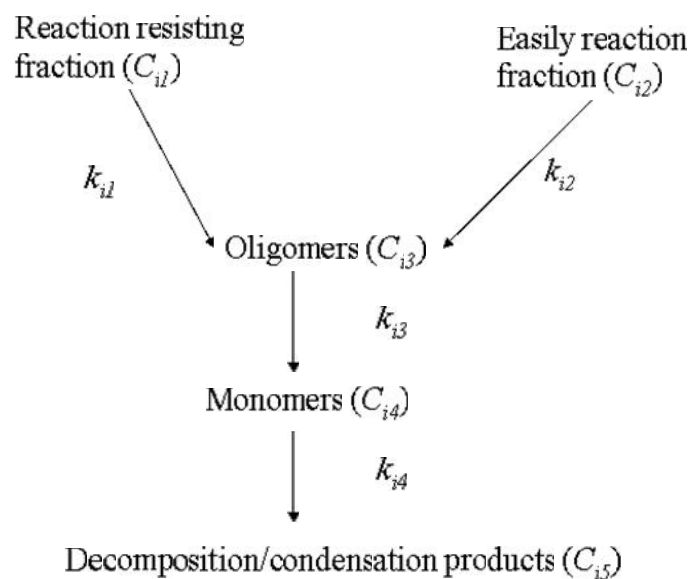
## 4 Process simulation and mathematical models

### 4.1 Organosolv fractionation

Organosolv is based on the treatment of biomass with an organic solvent at elevated temperatures (Zhao et al., 2009; Wildschut et al., 2013). Organosolv processes primarily delignify lignocellulose, with the organic solvent working as lignin extractant. At the same time, the hemicellulose fraction is depolymerized through acid-catalyzed hydrolysis. In general, organosolv processes aim to fractionate the lignocellulosic biomass as much as possible and in contrast to other pretreatment technologies produces a fraction of high purity lignin. Over the years several approaches were employed so as to describe the fractionation process. The generalized pseudo-first kinetic model (Sdiras and Koukios, 2003), the combined severity factor (Chum et al., 1990), the response surface methodology (Jiménez et al., 1997; Goh et al., 2011) are the approaches described in detail herein.

#### 4.1.1 Generalized pseudo-first-order kinetic model

Sdiras and Koukios (2003) described the kinetics of the organosolv fractionation concerning the cases of lignin solubilization and acid hydrolysis of the polysaccharides as follows:



where  $i = L$  corresponds to lignin solubilization,  $i = C$  to cellulose acid hydrolysis and  $i = H$  to hemicelluloses acid hydrolysis, respectively.

The following equations simulated organosolv fractionation of lignocellulosic materials based on a generalized pseudo-first-order kinetic model:

$$-dC_{i1} / dt = k_{i1} \cdot C_{i1} \quad (4.1)$$

$$-dC_{i2} / dt = k_{i2} \cdot C_{i2} \quad (4.2)$$

$$dC_{i3} / dt = k_{i1} \cdot C_{i1} + k_{i2} \cdot C_{i2} - k_{i3} \cdot C_{i3} \quad (4.3)$$

$$dC_{i4} / dt = k_{i3} \cdot C_{i3} - k_{i4} \cdot C_{i4} \quad (4.4)$$

$$k_{ij} = p_{ij} \cdot C_{acid}^n \cdot e^{\frac{-E_{ij}}{RT}} \quad (4.5)$$

where  $i = C, H, L$  and  $j = 1, 2, 3, 4$ ,  $p_{ij}$  ( $\text{min}^{-1}$ ) is the pre-exponential factor,  $n$  the acid concentration exponent,  $E_{ij}$  (kJ/mol) the activation energy,  $k_{ij}$  ( $\text{min}^{-1}$ ) the rate constants,  $t$  (min) the reaction time and  $T$  (K) the reaction temperature. All concentrations  $C_{ij}$  were expressed in w/w units based on initial quantity of dry component in the reacting system.

#### 4.1.2 Severity factor

The modeling of complex reaction systems is possible only when the sequence of all of the elementary steps is established. However, few complex reactions have a known and clearly determined set of elementary steps. Thus the severity factors which try to combine the effect of different operational variables were introduced.

Overend and Chornet (1987) defined the severity parameter as a function of treatment time (min) and temperature ( $^{\circ}\text{C}$ ), as

$$R_o = t \exp\left(\frac{(T - T_{ref})}{14.75}\right) \quad (4.6)$$

where  $T$  is the reaction temperature ( $^{\circ}\text{C}$ )  $T_{ref}$  is the reference temperature (usually  $100^{\circ}\text{C}$ ) and  $t$  is the time at  $T_{ref}$ . This factor has been derived assuming that the overall kinetics follows a first-order law concentration dependence on key reaction components with an Arrhenius-type rate constant dependence on temperature; the apparent activation energy may be a function of the temperature.

Chum et al. (1990) introduced the combined severity factor, which included also the effect of pH, as shown in Eq. (4.7):

$$R'_o = 10^{-pH} t \exp\left(\frac{(T - T_{ref})}{14.75}\right) \quad (4.7)$$

Based on previous work (Sdiras et al., 2011; Weinwurm et al., 2017), the following CSF for non-isothermal reaction conditions is proposed

$$R_o^* = 10^{-pH} \int_0^t \exp\left(\frac{T - T_{ref}}{14.75}\right) dt \quad (4.8)$$

where pH is the acidity of the liqueur after the organosolv pretreatment,  $T_{Ref} = 100$  °C.

### 4.1.3 Design of experiments and Response surface methodology

The multivariate design of experiments (DOE) is an important issue because it facilitates the gathering of large quantities of information while minimizing the number of experiments, thus taking less time efforts and resources than the univariate procedures (Brereton, 2003). DOE and response surface methodology have been proved valuable for developing improving and optimizing processes (Myers and Montgomery, 2009). However, little literature has been traced concerning organosolv fractionation process and RSM.

RSM is a collection of mathematical and statistical techniques useful for defining the relationships between the response and the independent variables. RSM defines the effect of the independent variables, alone or in combination, on the processes. Other than analyzing the effects of the independent variables, this experimental methodology, also generates a mathematical model. The graphical perspective of the mathematical model has led to the term Response Surface Methodology (Myers and Montgomery, 1995; Anjum et al., 1997; Baş and Boyacı, 2007).

The stages in the application of RSM as an optimization technique are the following:

- (1) selection of the response variables
- (2) selection of factors and their levels
- (3) the selection of the experimental design
- (4) execution of the experiments and determination of the responses
- (5) the mathematic-statistical treatment of the obtained experimental data through the fit of a polynomial function
- (6) the evaluation of the model's fitness
- (7) obtaining the optimum values for each variable.

Some of the basic stages are described below.

#### ➤ Selection of response variables

A variable which can give the necessary information in the evaluation of the performance of a process must be selected to be subjected to the optimization procedure.

This variable is referred as response and according to the objective it may be needed to observe more than one response (Candiotti et al., 2014).

➤ **Selection of factors and their levels**

Numerous factors may affect the response of the system studied, and it is practically impossible to identify and control the small contributions from each other. Since the number of factors can be important, it is necessary to perform screening experiments to determine which of the several experimental variables and their interactions present more significant effects. Full factorial, fractional factorial and Plackett-Burman designs are the most widely used designs for this objective (Bezerra et al., 2008; Candiotti et al., 2014).

➤ **Choice of the experimental design**

The linear function is the simplest model which can be used in RSM. However, for its application it is necessary that the responses obtained are well fitted to the following equation:

$$y = S_0 + \sum_{i=1}^k S_i x_i + V \quad (4.9)$$

where  $k$  is the number of variables,  $S_0$  is the constant term,  $S_i$  represents the coefficients of the linear parameters,  $x_i$  are the variables and  $V$  is the residual associated to the experiments.

Although two-level factorial designs can estimate the first-order effects, in the case of significant additional effects, such as second-order, are inadequate. Hence a central point in two-level factorial designs can be used for evaluating curvature. The next level of the polynomial model should contain additional terms, in order to describe the interaction between the different experimental variables. Thus a model for a second-order interaction presents the following terms:

$$y = S_0 + \sum_{i=1}^k S_i x_i + \sum_{1 \leq i < j \leq k} S_{ij} x_i x_j + V \quad (4.10)$$

where  $S_{ij}$  represents the coefficients of the interaction parameters.

So as to determine a critical point (minimum, maximum, saddle), it is necessary for the polynomial function to include quadratic terms according to the equation presented below:

$$y = S_0 + \sum_{i=1}^k S_i x_i + \sum_{i=1}^k S_{ii} x_i^2 + \sum_{1 \leq i < j \leq k} S_{ij} x_i x_j + V \quad (4.11)$$

To estimate the parameters in Eq.4.11 , the experimental design needs to assure that all studied variables are carried out in at least three factor levels. Therefore, two modelling symmetrical response surface designs are available. Among the more known second-order symmetrical designs are the three-factorial design, Box-Behnken design (Box and Behnken, 1960), central composite design (Box and Wilson, 1951) and Doehlert design (Doehlert, 1970). The designs differ from one another with respect to experimental point selection, number of levels for variables and numbers of runs and blocks. Their main features are presented in Table 4.1

**Table 4.1** Response-surface designs

Design	Factor levels	Number of experiments
Central composite	5	$2^k + 2k + C_p$
Box-Behnken	3	$2k(k-1) + C_p$
Full three level factorial	3	$3k$
Doehlert Matrix	Different for each factor	$k^2 + k + C_p$

$C_p$  is the number of center points;  $k$  is the number of factors

Although little literature has been traced concerning fractionation processes and RSM. The full factorial design has been used for optimizing the conversion of sawdust after wet oxidation (Ayeni et al., 2013) and the central composite design for optimizing the organosolv pretreatment of empty palm fruit (Goh et al., 2011).

➤ **Evaluation of the fitted model**

The mathematical model found after fitting the function to the data may sometimes not satisfactorily describe the experimental domain studied. The more reliable way to evaluate the quality of the model fitted is through the analysis of variance (ANOVA). The basic idea of ANOVA is to compare the variation due to the treatment (change in the combination of variable levels) with the variation due to the measurements of the generated responses (Vieira and Hoffman, 1989). From this comparison, it is possible to evaluate the

significance of the regression used to predict responses considering the sources of experimental variables.

➤ **Optimal location**

The graphical representation of the model is a suitable way to find the optimal location. Two types of graphs may prove helpful: (a) the response surface in the three dimensional space and (b) the graph of the contours which is the projection of the surface in plane, represented as lines of constant response. In these graphics the response is represented as a function of two factors. Based on the established optimization criterion, the optimal value sought may correspond to a minimum, a maximum or a specific value, that can be found by visual assessment of the graph. If there are three or more variables, the plot visualization is possible if one or more variables are set to a constant value (Bezerra et al., 2008; Candiotti et al., 2014).

## 4.2 Adsorption kinetic-study

The controlling mechanisms of adsorption process such as chemical reaction, diffusion control or mass transfer coefficient are employed to determine kinetic models. The adsorption kinetics study illustrates the rate of the solute uptake which controls the residence time of the adsorbate at the solution interface. Thus, information on the solute uptake is prerequisite for choosing the best operating conditions for the full-scale batch (Yagub et al., 2014; Calvete et al., 2009; Vaghetti et al., 2009). Over the years, many models have been proposed to elucidate the mechanism of adsorption. Three of the most popular are the pseudo-first-order model (Lagergren, 1898), the pseudo-second-order model (Ho and McKay, 1999) and the intra-particle kinetic model (Weber and Morris, 1963).

### 4.2.1 Pseudo-first-order model

The pseudo-first-order model was proposed by Lagergren (1898) and it is based on solid capacity. This model considers the rate of occupation of sorption proportional to the number of unoccupied sites and is generally expressed as follows:

$$\frac{dq}{dt} = k_1 (q_e - q) \quad (4.12)$$

After integrating and applying the boundary conditions, for  $q = 0$  at  $t = 0$  and  $q = q$  at  $t = t$ , the integrated form of Eq. becomes:

$$q_t = q_e (1 - e^{-k_1 t}) \quad (4.13)$$

where  $q_e$  and  $q_t$  (both in mg/g) are respectively the amounts of dye adsorbed at equilibrium and at any time 't',  $k_1$  ( $\text{min}^{-1}$ ) is the rate constant of sorption.

### 4.2.2 Pseudo-second-order model

The pseudo-second-order model was proposed by Ho and McKay (1999) and is based on the assumption that the adsorption follows second order chemisorption. The pseudo-second-order model can be expressed as:

$$\frac{dq}{dt} = k_2 (q_e - q)^2 \quad (4.14)$$

after integrating for the same boundary conditions, the following equation can be obtained:

$$q_t = \frac{k_2 q_e^2 t}{1 + k_2 q_e t} \quad (4.15)$$

where  $k_2$  ( $\text{g mg}^{-1} \text{min}^{-1}$ ) is the rate constant of pseudo-second-order adsorption.

### 4.2.3 Intra-particle diffusion model

The adsorption occurs in several steps involving transport of solute molecules from the bulk aqueous phase to the surface of the adsorbent particles followed by molecules into the interior of the solid pores. According to Weber and Morris (1963) for most adsorption processes the amount of adsorption has a linear relationship with the  $t^{0.5}$  rather than with the contact time and it can be expressed as:

$$q_t = k_p t^{0.5} + C \quad (4.16)$$

where  $q_t$  ( $\text{mg/g}$ ) is the adsorption capacity at time  $t$ ,  $k_p$  ( $\text{mg/g min}^{0.5}$ ) is the rate constant of intra-particle diffusion and  $C$  ( $\text{mg/g}$ ) is a constant providing information about the thickness of boundary layer.

In order to determine the initial adsorption behavior Wu et al. (2009) introduced the initial adsorption factor of the intra-particle diffusion model ( $R_i$ ) expressed as:

$$R_i = 1 - \left( \frac{C}{q_{ref}} \right) \quad (4.17)$$

indicating that  $R_i$  can be represented in terms of the ratio of the initial adsorption amount ( $C$ ) to the final adsorption amount ( $q_e$ ). When  $C = 0$  (i.e., there is no initial adsorption behavior),  $R_i = 1$ . In this case, Eq. passes through the origin. Additionally, when  $C = q_{ref}$  (i.e. adsorption occurs right at the beginning of the process)  $R_i = 0$ .

The  $R_i$  value is divided into four zones:  $1 > R_i > 0.9$  is called weak initial adsorption (zone 1);  $0.9 > R_i > 0.5$ , intermediate initial adsorption (zone 2);  $0.5 > R_i > 0.1$ , strong initial adsorption (zone 3);  $R_i < 0.1$ , approaching total initial adsorption (zone 4) (Wu et al., 2009).

## 4.3 Applicability of various adsorption isotherm models on adsorption

The adsorption isotherms are important for the explanation of how the adsorbent will interact with the adsorbate and give an idea of adsorption capacity. They play a vital role in understanding the mechanism of adsorption. The surface phase may be considered as a monolayer or multilayer. Several isotherm models are presented in literature (Srinivasan and Viraraghavan, 2010) but Langmuir and Freundlich models are the most widely used.

### 4.3.1 Freundlich model

Freundlich isotherm (Freundlich, 1906) is the earliest known empirical equation describing the non-ideal and reversible adsorption, not restricted to the formation of monolayer. The model endorses the heterogeneity of the surface and assumes that the adsorption takes place at sites with different energy of adsorption. The equation of this model is given by:

$$q_e = K_F C_e^{1/n} \quad (4.18)$$

The linearised form of Freundlich can be expressed as:

$$\ln q_e = \ln K_F + \frac{1}{n} \ln C_e \quad (4.19)$$

where  $q_e$  (mg/g) is adsorbed amount at equilibrium time,  $C_e$  is the equilibrium concentration of dye in solution (mg/L),  $K_F$  ( $\text{mg g}^{-1} (\text{L mg})^{1/n}$ ) and  $n$  (-) are Freundlich isotherm constants related to adsorption capacity and intensity, respectively. The plot of  $\ln q_e$  versus  $\ln C_e$  is employed to determine the  $K_F$  and  $n$  from intercept and slope respectively.

### 4.3.2 Langmuir model

The most popular equation for modeling equilibrium is the Langmuir adsorption model (Langmuir, 1918) and was based on three hypotheses: a) uniformly energetic adsorption sites, b) monolayer coverage, and c) no lateral interaction between adsorbed molecules. The basic assumption is that the sorption occurs at specific homogeneous sites within the

adsorbent. Once a dye molecule occupies a site no further adsorption can take place. A mathematical expression of the model is given by Eq. (4.20)

$$q_e = \frac{q_m K_L C_e}{1 + K_L C_e} \quad (4.20)$$

where  $q_e$  (mg/g) is the adsorbed amount at equilibrium time,  $C_e$  is the equilibrium concentration of dye in solution (mg/L),  $K_L$  is the Langmuir equilibrium constant (L/mg) and  $q_m$  the maximum adsorption capacity (mg/g).

The essential characteristics of Langmuir equation can be expressed in terms of dimensionless separation factor,  $R_L$  which was defined by McKay et al., (1983) as:

$$R_L = \frac{1}{1 + K_L C_0} \quad (4.21)$$

$C_0$  is the initial dye concentration. There are four possibilities for  $R_L$  value:

- $R_L > 1$  unfavourable
- $R_L = 1$  linear
- $0 < R_L < 1$  favourable
- $R_L = 0$  irreversible

### 4.3.3 Sips model

The three-parameter Sips isotherm (Sips, 1948) inherently includes the features of Freundlich and Langmuir models and has more capability in describing adsorption equilibrium. This model is shown by:

$$q_e = \frac{q_m (K_S C_e)^{1/n_S}}{1 + (K_S C_e)^{1/n_S}} \quad (4.22)$$

where  $q_m$  is the maximum adsorption capacity (mg/g),  $q_e$  (mg/g) is the adsorbed amount at equilibrium time,  $K_S$  ( $L \text{ mg}^{-1}$ )<sup>1/n<sub>S</sub></sup> is Sips equilibrium constant and  $n_S$  is the isotherm model exponent.

The heterogeneity factor of  $n_S$  close to or even 1 indicates adsorbent with comparatively homogeneous binding sites, while  $n_S$  close to 0 shows heterogeneous adsorbent (Chatterjee et al., 2010; Bera et al., 2013).

#### 4.3.4 Redlich-Peterson model

Another combination of Freundlich and Langmuir systems was proposed by Redlich and Peterson (1959). The empirical equation may be used to represent adsorption equilibrium over a wide concentration range.

$$q_e = \frac{K_R C_e}{1 + a_R C_e^s} \quad (4.23)$$

where  $s > 1$ .

The equation reduces to a linear isotherm at low surface coverage, to Freundlich isotherm at high adsorbate concentration and to Langmuir isotherm when  $s = 1$  (Barka et al., 2013).

#### 4.3.5 Temkin model

Temkin and Pyzhev (1940) suggested that the heat of adsorption of all the molecules in the layer would decrease linearly with coverage due to the effect of some indirect adsorbate / adsorbate interactions. The Temkin isotherm has been used in the following form:

$$q_e = \frac{RT}{b} \ln(AC_e) \quad (4.24)$$

where  $q_e$  (mg/g) is the adsorbed amount at equilibrium time,  $C_e$  is the equilibrium concentration of the adsorbate (mg/L),  $A$  and  $b$  are Temkin parameters. The constant  $b$  is related to the heat adsorption.

#### 4.3.6 Dubinin-Radushkevich model

Dubinin and Radushkevich (1947) proposed the following isotherm model:

$$q_e = q_m e^{-BV^2} \quad (4.25)$$

where  $B$  ( $\text{mol}^2 \text{kJ}^{-2}$ ) is a constant related to the mean free energy of adsorption,  $V$  is the Polanyi potential which is equal to  $RT \ln(1 + (1/C_e))$ .  $R$  ( $\text{J mol}^{-1} \text{K}^{-1}$ ) is the universal gas constant and  $T$  (K) is the absolute temperature. The mean free energy,  $E$  ( $\text{kJ mol}^{-1}$ ) written as  $E = 1/(2B)^{1/2}$ , obtained from this model, provides information about the adsorption mechanism, more specifically its physical or chemical nature. If the value of  $E < 0.8 \text{ kJ mol}^{-1}$ , the process is governed by physical adsorption (Sharma et al., 2014; Deniz and Ersanli, 2016).

### 4.3.7 Toth model

The Toth isotherm (Toth, 1971) is derived from the potential theory and is applicable to heterogeneous adsorption. It assumes a quasi-Gaussian energy distribution. Most sites have an adsorption energy lower than the peak or maximum adsorption energy. The application of this equation is best fit to multilayer adsorption. The Toth correlation is expressed as:

$$q_e = \frac{q_m C_e}{(1/K_T + C_e^t)^{1/t}} \quad (4.26)$$

where  $q_e$  is the adsorbed amount at equilibrium (mg/g),  $C_e$  the equilibrium concentration of the adsorbate (mg/L),  $q_m$  the Toth maximum adsorption capacity (mg/g),  $K_T$  the Toth equilibrium constant, and  $t$  is the Toth model exponent. When the exponent  $t$  is equal to unity the model of Toth is reduced to the Langmuir model.

### 4.3.8 Unilan model

The Unilan isotherm (Do, 1998) is based on the following model:

$$q = \frac{q_m}{2s} \ln \left( \frac{1 + K_L C_e e^s}{1 + K_L C_e e^{-s}} \right) \quad (4.27)$$

where  $K_L$  is the Langmuir equilibrium constant (L/mg),  $q_m$  is the maximum adsorption capacity (mg/g) and  $S$  is Unilan constant.

## 5 Materials and Methods

### 5.1 Materials

Modification experiments were performed using barley (*Hordeum Vulgare L.*) and wheat straw (*Triticum durum Desf.*). In both cases, the feedstock was received ambient-dried from Kapareli Village of Thebes, Greece, (38°14'8"N 23°12'59"E). It was chopped in small pieces with hedge shears and the fraction with sizes 1–2 cm was collected by sieving. The moisture mass fraction, in the case of barley straw was ~8%, whereas in the case of wheat straw ~9%. Their composition is presented in Table 5.1

**Table 5.1** Composition of untreated barley and wheat straw (mass fraction (%) on dry solid).

Component	Barley straw	Wheat straw
Cellulose	34.9	31.6
Hemicelluloses	21	28.1
• Xylan	19.4	24.4
• Arabinan	1.6	3.7
Acid insoluble lignin	19.2	19.1
Acid soluble lignin	1.2	1
Ash	5.03	5.7

The NREL standard biomass laboratory analytical procedure “Determination of Structural Carbohydrates and Lignin in Biomass” was used to analyze the summative composition (Sluiter et al., 2008). The ash content was measured by combustion at 550 °C according to the NREL/TP-510-42622 protocol (National Renewable Energy Laboratory (NREL), 2009).

## 5.2 Modification processes

All processes were performed in a 3.75-L batch reactor PARR 4550 made of alloy 600 (8% Fe, 76% Ni, 16% Cr) Fig.5.1



**Fig .5.1** The 3.75-L batch reactor PARR 455

## **5.3 Organosolv pretreatment**

### **5.3.1 Wheat straw organosolv pretreatment with various catalysts**

The organosolv fractionation was conducted in the same 3.75-L batch reactor PARR 4550 made of alloy 600 (8% Fe, 76% Ni, 16% Cr). The reactor was loaded with 100 g of wheat straw and 2 L of a 50 % volume fraction of the organosolv solvent in acidified water with a final concentration of  $23 \text{ mol m}^{-3} \text{ H}_2\text{SO}_4$ . Ethanol, methanol, butanol, acetone and 2,2 Oxydi(ethan-1-ol) (Diethylene glycol) were used as organic solvents.

Reaction temperatures were 160 °C and 180 °C, whereas the reaction was carried out for 20 min and 40 min (Table 1). The reactor was heated for approximately 40 and 50 min respectively, while stirring was occurred at 150 rpm. Residence time was counted from the moment the desired temperature was achieved. The reactor was kept isothermal ( $\pm 2 \text{ }^\circ\text{C}$ ) during the reaction time and subsequently cooled down (temperature halved after around 30 min) to below 30 °C. After filtration through a Whatman type 3 paper filter, the solid residue was washed with distilled water (7 times using 1 L each time to achieve pH 5.5), oven dried at 105 °C and weighed to determine the solid residue yield.

### **5.3.2 Acetone organosolv pretreatment process of barley straw**

The same batch reactor, as mentioned previously PARR 4550, was used for the pretreatment. The Box-Behnken experimental design was employed with the key variables selected being temperature (140-180 °C), residence time (0-40 min) and sulfuric acid concentration ( $10\text{-}35 \text{ mol m}^{-3}$ ). A hundred grams of barley straw were treated with acetone/water mixture in a volume ratio of 50:50 with sulfuric acid as a catalyst. The solid-to-liquid rate used was 1:20. Residence time was counted from the moment the desired temperature was achieved. The reactor was kept isothermal ( $\pm 2 \text{ }^\circ\text{C}$ ) during the reaction time and subsequently cooled down to below 30 °C, while stirring was occurred at 150 rpm. After filtration through a Whatman type 3 paper filter, the pretreated biomass was washed with distilled water (7 times using 1 L each time to achieve pH 5.5), oven dried at 105 °C and weighed to determine the solid residue yield. Furthermore, the organosolv liquor was stored in a refrigerator for analysis.

## 5.4 Analyses

### 5.4.1 Organosolv liquors

Organosolv liquors were analyzed for their pH and content of monomeric and oligomeric sugars. Analysis of monomeric sugars was performed with high-performance liquid chromatography (HPLC, Agilent 1260) with Aminex Hi-Plex Column, refractive index detector and Millipore water as the mobile phase Fig. 5.2.



**Fig. 5.2** The HPLC, Agilent 1260

The sugar analyses were performed both directly and after post-hydrolysis of the sample (post-hydrolysis conditions  $1.8 \text{ mol m}^{-3}$  sulfuric acid,  $100 \text{ }^\circ\text{C}$ , 4.5 h). The concentration of oligomeric sugars in the liquors was calculated from the difference between the two analyses.

### **5.4.2 Composition of fractionated solids**

The summative composition of solids was analyzed, as already mentioned using the NREL /TP-510-42618 standard biomass analytical procedure (Sluiter et al., 2008). In brief, the content of lignin, hemicelluloses and cellulose was determined in duplicate by hydrolysis. The sample was milled with a ball mill and hydrolyzed in two steps: (1) sulfuric acid concentration 72% w/w at  $30 \pm 3$  °C for  $60 \pm 5$  min and (2) 4% w/w at 121 °C for 60 min. The acid-insoluble lignin was determined gravimetrically and its ash content was measured. Finally, the hydrolysate was analyzed for monomeric sugars (with HPLC, after being neutralized first with  $\text{CaCO}_3$ ) and acid-soluble lignin (UV-VIS adsorption at 205 nm).

### **5.4.3 Enzymatic digestibility**

Enzymatic saccharification was carried out in 100 cm<sup>3</sup> Erlenmeyer flasks in an orbital shaker (Zhicheng, Sanghai, China). Straw loading was 13% mass fraction in 100 mmol L<sup>-1</sup> citrate–phosphate buffer at pH 5.0 and an enzyme load of 9 mg g<sup>-1</sup> dry matter (DM) of the commercial enzyme solution Cellic® CTec2 was used. Saccharification duration was 72 h at 50 °C and 200 rpm. The addition of sodium azide (0.2g kg<sup>-1</sup>) was included to prevent microbial contaminations. To estimate cellulose hydrolysis samples were taken at different time intervals and soluble sugars were measured. Total reducing sugars concentration was determined according to dinitro-3,5-salicylic acid (DNS) method (Miller, 1959) and glucose was measured according to commercial enzyme preparation of glucose oxidase/peroxidase (GOD/PAP) assay.

## **5.5 Pretreatment effect on lignocellulosic feedstock adsorptivity**

Since dyes are an important class of pollutants their disposal in valuable water resources must be avoided. Various treatment technologies are in use and among them adsorption occupies a prominent place in dye removal. The growing demand for efficient and low-cost treatment methods as well as the importance of adsorption has given rise to low-cost alternative adsorbents like lignocellulosic residues. The dye used herein, was Methylene Blue (MB) with a chemical formula of  $\text{C}_{16}\text{H}_{18}\text{ClN}_3\text{S}\cdot x\text{H}_2\text{O}$  and 373.9 10<sup>-3</sup> kg mol<sup>-1</sup> molecular weight. A stock solution was prepared by dissolving 5 g of MB in 25 L distilled water. Working solutions were 1.6-156 mg L<sup>-1</sup>. MB concentrations were analyzed

by measuring the absorbent values in each experiment with a HACH DR6000 UV-VIS spectrophotometer at  $\lambda = 664$  nm.

### **5.5.1 Kinetic experiments**

Adsorption rate batch experiments were conducted in a 2-L glass totally mixed reactor equipped with a twisted blade agitator type, operating at 450 rpm, for maintaining the lignocellulosic material in suspension. The reactor, containing  $V = 1$  L aqueous solution of dye was placed in a water bath to maintain constant temperature at the desired level. The adsorbent mass was  $m = 1$  g, the temperature was  $23$  °C, the initial concentration of MB was  $C_0 = 14$  mg L<sup>-1</sup>. Every 10 or 5 min, 10 mL samples were taken from the reactor using a pipette and the adsorbent was separated from MB solution using a 0.1 mm nylon filter. Then, MB concentration was measured as described above.

### **5.5.2 Isothermal experiments**

Isotherms were obtained from batch experiments. After the batch process, weigh accurately the quantities of sample were transferred to 0.8-L bottles, where  $V = 0.5$  L adsorbate solution were added. The adsorbent weight was 0.5 g, the temperature was  $T = 23$  °C, the original MB (Merck, CI 52015) concentration ranged from  $C_0 = 1.6$  mg L<sup>-1</sup> to 156 mg L<sup>-1</sup>. The bottles were sealed and mechanically filled for a period of 7 days. This time period was chosen after pilot studies (the time varies from 4 hours to 14 days) to ensure that nearly equilibrium conditions are achieved. The resulting solution was determined concentrations and balance data from each bottle represented one point on the adsorption isotherm plots. The values of solution pH were near 8.

## **6 Results and discussion**

### **6.1 Organosolv pretreatment with various solvents**

The organosolv pretreatment process is studied with regard to the biorefinery concept. Wheat straw was selected because it is the most abundant among agricultural residues in Europe and thus considered to be very interesting for the production of second generation bioethanol and biorefinery in general. Ethanol, methanol and acetone were the organic solvents chosen as the most commonly used in literature, whereas butanol due to its rarity. A new solvent, diethylene glycol (2,2'-Oxydi(ethan-1-ol)), is introduced with respect to its polarity, environmental impact, cost and overall physicochemical properties. Sulfuric acid served as catalyst for the pretreatments. With regard to the effectiveness of the process, in terms of delignification, xylan hydrolysis and enzymatic digestibility, organic solvent type as well as reaction temperature and time, were investigated. The potential of the pretreated feedstock for the production of ethanol was also evaluated in simultaneous saccharification and fermentation (SSF) process with the implementation of an enzymatic prehydrolysis step. Finally the adsorption capacity of the derived pretreated material was examined.

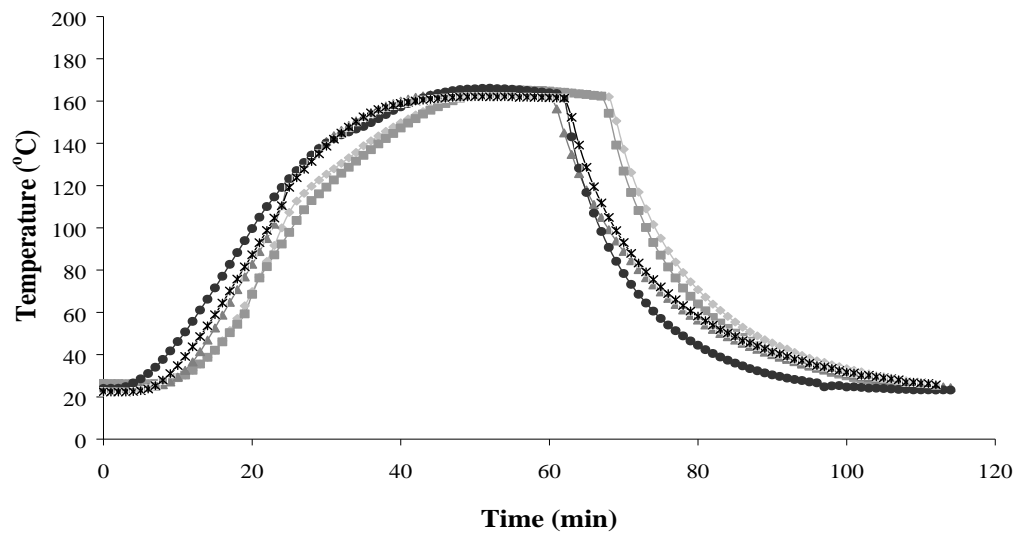
### 6.1.1 Compositional analysis

An overview of the conducted fractionation experiments is presented in Table 6.1

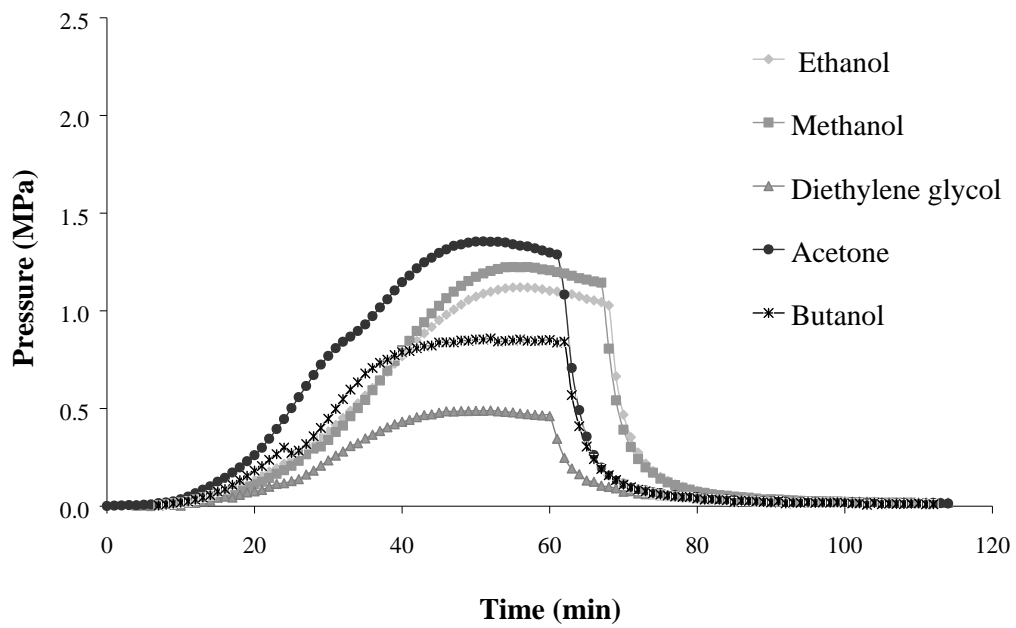
**Table 6.1** Organosolv pretreatment of wheat straw at varying temperature, reaction time and solvent.

Experiment	Solvent	Temperature (°C)	Time (min)
1	Ethanol	160	20
2	Ethanol	160	40
3	Ethanol	180	20
4	Ethanol	180	40
5	Methanol	160	20
6	Methanol	160	40
7	Methanol	180	20
8	Methanol	180	40
9	Butanol	160	20
10	Butanol	160	40
11	Butanol	180	20
12	Butanol	180	40
13	Acetone	160	20
14	Acetone	160	40
15	Acetone	180	20
16	Acetone	180	40
17	Diethylene glycol	160	20
18	Diethylene glycol	160	40
19	Diethylene glycol	180	20
20	Diethylene glycol	180	40
21	Untreated	(-)	(-)

The temperature and pressure profiles of two selected pretreatment conditions (160 and 180 °C for 20 min) are presented in Figures 6.1 and 6.2. The final pretreatments' pressures varied among the different organic solvents between 4.9 bar for diethylene glycol (2,2'-Oxydi(ethan-1-ol)) and 13.6 bar for acetone at 160 °C (Fig. 6.1b). Similarly, the final pretreatments' pressures varied among the different organic solvents between 8.5 bar for diethylene glycol and 19.6 bar for acetone at 180 °C (see Fig. 6.2b).

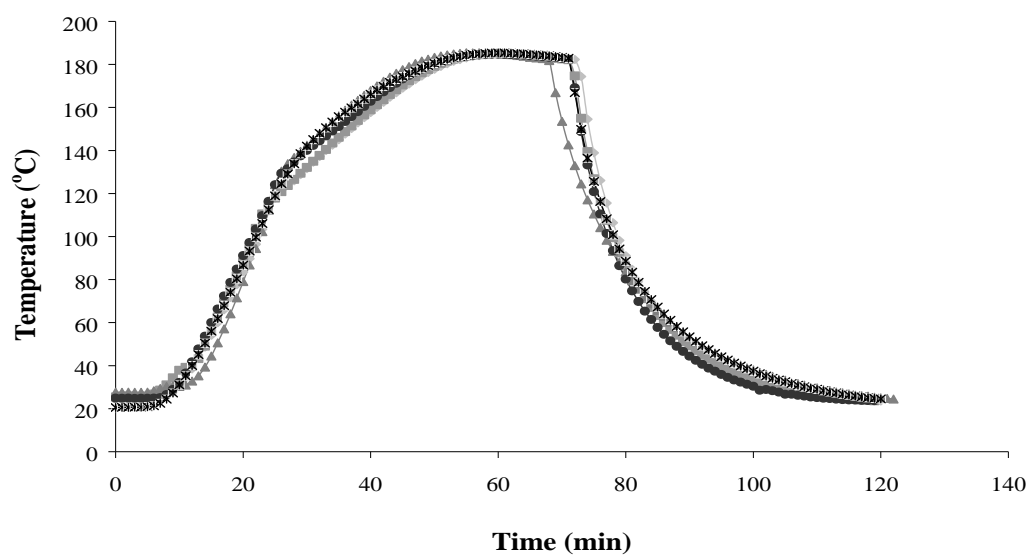


(a)

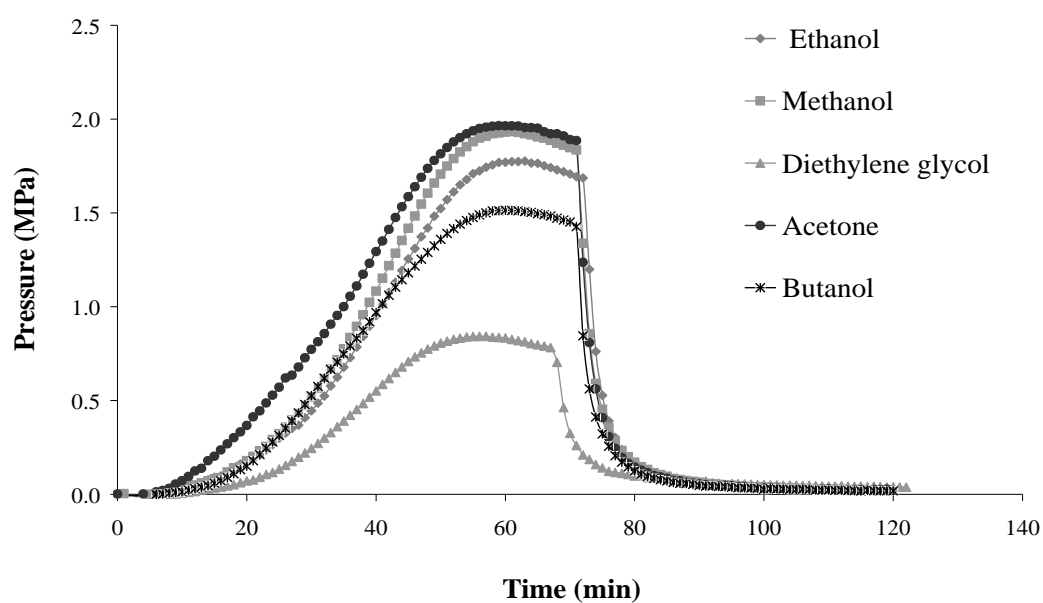


(b)

**Fig. 6.1** Organosolv pretreatment temperature (a) and pressure (b) profiles vs. time at 160 °C for 20 min.



(a)



(b)

**Fig. 6.2** Organosolv pretreatment temperature (a) and pressure (b) profiles vs. time at 180 °C for 20 min.

In Table 6.2, the yield of the resulting pulps for the five organic solvents, studied herein, is presented. Diethylene glycol pretreatment, at any case, resulted in higher pulp yields than the other four solvents. As expected, a temperature increase, as well as an extension of the

reaction time resulted in a pulp yield decrease due to increased delignification and xylan hydrolysis (Wildschut et al., 2013).

**Table 6.2** Composition of pulps and raw wheat straw (mass fraction (%) on dry solid).

<b>Experiment</b>	<b>Pulp yield (%)</b>	<b>Lignin</b>	<b>Cellulose</b>	<b>Xylan</b>
1	45.8	22.8 (0.3) <sup>a</sup>	59.0 (0.9)	4.9 (0.2)
2	42.5	20.3 (1.3)	59.8 (1.7)	3.2 (0.1)
3	39.1	20.9 (0.6)	66.6 (1.8)	1.2 (0.3)
4	38.9	17.9 (0.3)	57.8 (0.7)	2.8 (0.8)
5	47.9	23.7 (1.0)	59.1 (1.3)	5.0 (0.2)
6	44.3	24.3 (0.8)	59.6 (0.7)	3.5 (0.3)
7	42.5	23.4 (0.5)	62.7 (2.6)	1.3 (0.3)
8	40.6	24.1 (0.4)	64.3 (2.0)	1.7 (0.3)
9	41.1	23.2 (0.7)	69.3 (1.2)	3.3 (0.4)
10	38.7	21.3 (1.8)	70.5 (1.4)	1.2 (0.5)
11	31.9	18.3 (1.1)	67.1 (0.1)	0.4 (0.1)
12	27.7	17.9 (0.2)	71.0 (0.7)	0.5 (0.2)
13	41.3	18.6 (0.2)	68.5 (1.9)	2.6 (0.1)
14	41.3	16.3 (1.0)	66.1 (0.4)	1.5 (0.1)
15	34.7	19.9 (1.0)	60.0 (1.7)	0.7 (0.2)
16	25.5	17.7 (0.1)	67.2 (0.8)	0.6 (0.4)
17	50.8	23.5 (1.3)	56.6 (1.7)	8.3 (1.4)
18	51.1	20.9 (2.2)	51.3 (2.1)	7.0 (0.4)
19	43.7	19.9 (1.8)	63.5 (1.2)	1.6 (0.3)
20	41.7	19.8 (0.3)	60.3 (1.0)	1.4 (0.4)
21	(-)	19.1 (0.4)	31.6 (1.1)	20.7 (1.8)

<sup>a</sup> Numbers in parentheses are the estimates of the standard errors

According to the lignin contents as presented in Table 6.2, minimum lignin percentage of 16.0% w/w was achieved in the case of acetone at 160 °C for 40 min (exp14). However lignin content in the case of acetone pretreatment at 160 °C for 20 min (exp13) is only slightly higher (16.8% w/w). Very close to the above compositions is the lignin percentages

of the butanol organic solvent processes at 160 °C for 20 min (exp9) and 180 °C for 20 min (exp11) (16.3 and 17.0% w/w respectively).

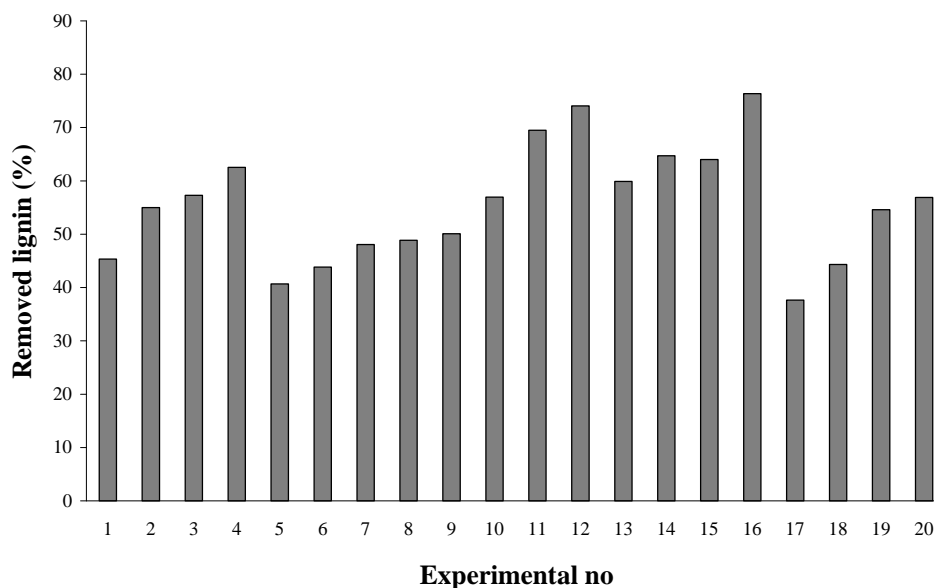


**Fig. 6.3** Effects of organic solvent, temperature and time on lignin removal; organosolv pretreatments catalyzed by 23 mol m<sup>-3</sup> H<sub>2</sub>SO<sub>4</sub>; organic solvents: ethanol (1-4), methanol (5-8), butanol (9-12), acetone (13-16), diethylene glycol (17-20).

The comparison of the five organic solvents delignification degree is presented in Fig. 6.3. Among the organic solvents, methanol and diethylene glycol appear to have the poorest results especially in the mildest conditions whereas in the case of acetone organosolv pretreatment at 180 °C for 40 min delignification reaches 76.4% (exp16). As far as ethanol is concerned, delignification varies between 45.2% and 62.5%, which is in agreement with previous studies (Wildschut et al., 2013). Cellulose content of the untreated wheat straw was 31.6%, which was in all cases increased and at some cases more than doubled. More specifically, for butanol based process at 180 °C for 40 min (exp12) increased up to 71.0% (see Table 6.2).

**Table 6.3** Mass balance (expressed as mass fraction of the initial dry cellulose).

<b>Experiment</b>	<b>Cellulose in pulp (%)</b>	<b>Glucose (%)</b>	<b>Glucose after post-hydrolysis (%)</b>	<b>Sum</b>
1	85.5	6.0	6.6	92.1
2	80.4	5.7	6.8	87.2
3	82.4	8.4	10.6	93.0
4	73.2	17.6	20.0	93.2
5	89.5	3.8	4.0	93.5
6	83.5	3.3	4.4	87.9
7	84.3	5.7	6.0	90.3
8	82.6	6.2	6.5	89.1
9	90.2	8.4	9.6	99.8
10	86.4	9.9	10.6	97.0
11	67.7	17.1	19.9	87.6
12	62.3	17.3	19.9	82.2
13	89.5	10.3	10.4	99.9
14	86.4	10.7	11.1	97.5
15	65.9	18.7	19.4	85.3
16	54.2	22.3	22.6	76.8
17	91.0	5.1	6.5	97.5
18	83.0	9.9	11.4	94.4
19	87.9	9.1	9.3	97.2
20	79.5	8.4	10.3	89.8

Tables 6.3 and 6.4 list the mass balances expressed as the mass fraction of the initial dry polysaccharide i.e. cellulose and xylan.

**Table 6.4** Mass balance (expressed as mass fraction of the initial dry xylan).

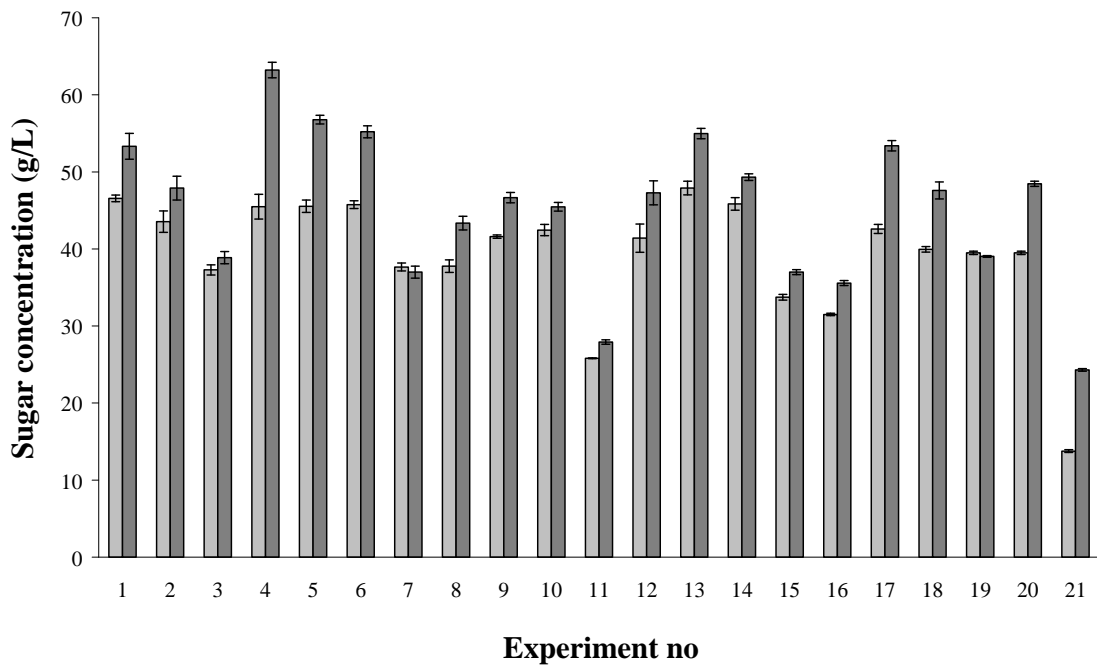
<b>Experiment</b>	<b>Xylan in pulp (%)</b>	<b>Xylose (%)</b>	<b>Xylose after post-hydrolysis (%)</b>	<b>Sum</b>
1	10.8	43.1	53.7	64.5
2	6.6	46.8	49.5	56.1
3	2.2	45.2	47.4	49.6
4	5.3	41.2	42.2	47.5
5	11.7	36.7	41.7	53.4
6	7.4	38.9	40.6	48.0
7	2.6	38.3	39.6	42.2
8	3.3	34.5	36.2	39.5
9	6.5	70.7	71.2	77.7
10	2.3	67.5	73.3	75.6
11	0.6	35.3	38.0	38.6
12	0.7	34.9	36.8	37.5
13	5.1	83.8	88.0	93.1
14	3.0	85.3	85.5	88.5
15	1.2	40.1	40.4	41.6
16	0.7	26.9	28.1	28.8
17	20.5	53.8	55.6	76.1
18	17.3	46.2	48.9	66.2
19	3.3	42.5	45.1	48.4
20	2.9	32.0	33.3	36.2

Hemicellulose fraction, as derived from Table 6.4, appears to be the most reactive major biomass constituent with very small amounts of xylan traced after pretreatment. Additionally, the more severe pretreatment conditions enhance the formation of degradation products such as 5-HMF in the case of hexose sugars and furfural in the case of pentose sugars.

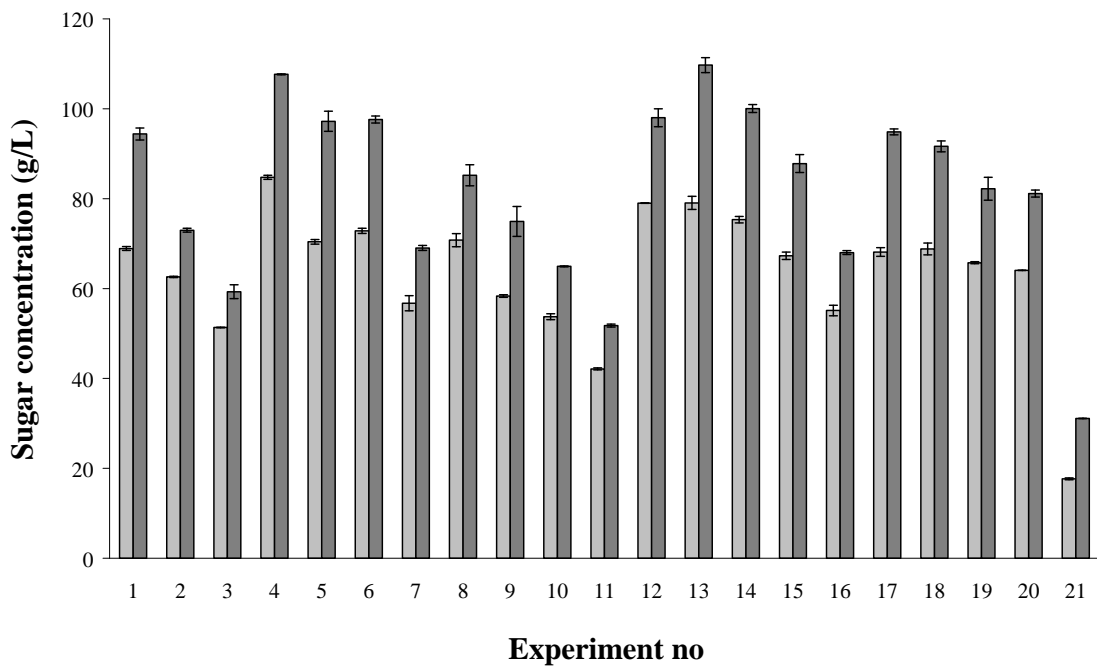
### **6.1.2 Enzymatic digestibility**

The pretreated and untreated straws were subjected to enzymatic hydrolysis at 50 °C for 72 h using an enzyme load of 9 mg/g DM Cellic<sup>®</sup> CTec2 with 13% solid loadings. The experiments were conducted in the Biotechnology Laboratory, School of Chemical Engineering, National Technical University of Athens. Concentrations of glucose and total reducing sugars, after 8h and 72 h enzymatic hydrolysis, are presented in Fig. 6.4. After the pretreatment in all applied conditions, both total reducing sugars as well as glucose concentration were increased.

In the case of ethanol-based organosolv pretreatment, maximum glucose (84.8 g/L) was released from the straw at 180 °C for 40 min (exp4), which corresponds to 89.2% conversion of cellulose towards glucose (Table 4). The enzymatic release of glucose from the ethanol pretreated wheat straw was found 151% higher than that of the untreated material. Wildschut et al. (2013) optimized the process, towards enzymatic cellulose hydrolysis to glucose, achieving maximum cellulose conversion very close to the values obtained herein. Regarding the other three experimental conditions, despite of the higher lignin content (21.5%), straw pretreated at 160 °C for 20 min (exp1) shows the best cellulose conversion 71.5%. Whereas a 33.8% increase in cellulose conversion, pretreated straw at 180 °C for 20 min (exp3) gives the poorest results with just 47.8%.



(a)



(b)

**Fig. 6.4** Glucose and total reducing sugars (TRS) concentration after (a) 8 and (b) 72 h of enzymatic hydrolysis of pretreated samples using an enzyme load of 9 g kg<sup>-1</sup> of dry matter DM Cellic® CTec2 at 130 g kg<sup>-1</sup> dry solids in the total liquid mass.

Glucose concentration obtained after 72 h enzymatic hydrolysis, when methanol is used as organic solvent, does not provide as clear results as ethanol. Maximum cellulose to glucose conversion was almost 105% higher than that of the untreated wheat straw (Table 6.5).

**Table 6.5** Cellulose conversion (%) achieved after 72 h of enzymatic hydrolysis of organosolv pretreated wheat straw samples using an enzyme load of 9 g kg<sup>-1</sup> of dry matterDM Cellic® CTec2 at 130 g kg<sup>-1</sup> dry solids in the total liquid mass.

Experiment	Cellulose conversion (%)
1	71.54 (0.41) <sup>a</sup>
2	65.66 (0.15)
3	47.76 (0.07)
4	89.23 (0.46)
5	74.38 (0.54)
6	74.21 (0.60)
7	57.50 (1.71)
8	68.72 (1.42)
9	52.33 (0.26)
10	46.59 (0.57)
11	37.61 (0.20)
12	67.54 (0.06)
13	72.21 (1.34)
14	67.97 (0.66)
15	65.14 (0.78)
16	49.97 (1.06)
17	76.70 (1.07)
18	77.02 (1.48)
19	64.36 (0.22)
20	65.13 (0.00)
21	35.70 (0.44)

<sup>a</sup> Numbers in parentheses are the estimates of the standard errors.

Maximum glucose concentration (79.0 g/L) was achieved in the case of butanol at 180 °C for 40 min (exp12). In the same conditions 67.5% cellulose was converted to glucose; this being 87.6% higher than that of the untreated wheat straw. The poorest improvement

was at 180 °C for 20 min (exp11), only 37.6% cellulose conversion was achieved and the glucose concentration was 42.1 g/L.

Regarding acetone based organosolv pretreatment, after 72 h enzymatic hydrolysis, maximum glucose (79.1 g/L) was obtained from the straw at 160 °C for 20 min (exp13). Put differently, 72.2% cellulose was converted to glucose (Table 3), which was 100% higher than that of the untreated wheat straw. With a 39%, increase in cellulose conversion, pretreated straw at 180 °C for 40 min (exp16) gives the poorest results just 50%. Despite their different nature, *Pinus radiata* D. Don wood pretreated with a 50:50 (v/v) acetone: water mixture, containing sulfuric acid as catalyst (9 g kg<sup>-1</sup> on dry wood dry wood), gave relatively similar results to the values obtained herein. More specifically, the obtained enzymatic hydrolysis yields ranged between 38.2 and 71.8%, depending on the process's severity (Araque et al., 2008).

Finally, diethylene glycol pretreated, in the selected conditions, straw show no significant differences as regards the glucose concentration after enzymatic hydrolysis. Yet cellulose conversion of the pretreated wheat straw at 160 °C for 20 and 40 min (experiments 17 and 18) was significantly higher (76.7% and 77.0%, respectively) compared to the other two (experiments 19 and 20). Maximum cellulose to glucose conversion was almost 113% higher than that of the untreated wheat straw.

A number of parameters could affect enzymatic hydrolysis. The most effective are believed to be cellulose crystallinity, lignin and cellulose protection, degree of polymerization of cellulose, accessible surface area, biomass swelling capacity and cellulase adsorption and desorption (Taherzadeh and Karimi, 2007; Hendriks and Zeeman, 2009).

### **6.1.3 Fermentability of pretreated solids for ethanol production**

The experiments were conducted in the Biotechnology Laboratory, School of Chemical Engineering, National Technical University of Athens. The effect of organosolv pretreatment with different organic solvents at selected conditions on ethanol yield is shown in Table 6.6. The concentration of ethanol has been increased significantly, by the pretreatments, regardless the organic solvent. Ethanol pretreatment at 180 °C for 40 min (exp4) resulted in the maximum production of 35.59 g/L. The ethanol yield was increased

from 27.81% to 67.24% of maximum theoretical when the material is subjected organosolv pretreatment with ethanol at the previously mentioned conditions.

In the same conditions (exp8), methanol also exhibits the highest ethanol concentration (compared to the other three) of 29.52 g/L. However, relative ethanol yield reached only the 56.19%. It should be noted, that pretreatment at 160 °C for 20 min provided also very good results. More specifically, 26.51 g/L of ethanol were produced whereas ethanol yield reached 54.90% of theoretical yield. Only limited data was found for methanol pretreatment for enzymatic hydrolysis and fermentation. Hörmeyer et al. (1988) pretreated poplar wood and wheat straw with methanol at 175–235 °C and then used wild type and mutant *Clostridium thermocellum* to ferment the wood and straw. As a result, for every 100 g of raw wheat straw with the wild type *C. thermocellum* maximum ethanol yield of 18 g was achieved whereas with the mutant 23.1 g. Although methanol is an effective solvent with easy recovery from boiling point, toxicity and inflammability should be taken into consideration.

Butanol similarly to the previously mentioned solvents resulted in a maximum ethanol concentration at 180 °C for 40 min (exp12). Nevertheless, all four pretreatment conditions provided relatively close results. Relative ethanol yield varied from 42.32% (at 180 °C for 20 min, exp11) to 48.80% (at 180 °C for 40 min, exp12) of theoretical yield.

In the case of acetone pretreatment, except of the one at 180 °C for 20 min (exp15) which was rather low (14.32 g/L), the remaining three resulted in similar ethanol concentrations. Translated into ethanol yield, the minimum of 27.18% of theoretical is met at 180 °C for 20 min (exp15); whereas the maximum of 43.69% of theoretical yield at 160 °C for 20 min (exp13).

Treatment with diethylene glycol resulted in the production of close amounts of relative ethanol in all experimental conditions. However, ethanol yield is considerably higher when the pretreatment takes place at 160 °C for 40 min (exp18). Particularly it resulted to an ethanol yield of 65.28% of theoretical yield, whereas the best of the remaining three only reaches 51.42% (exp20).

**Table 6.6** Effect of different organosolv pretreatment conditions on maximum ethanol production, ethanol productivity, and relative ethanol yield (calculated as percentage of maximum theoretical yield).

<b>Experiment</b>	<b>Ethanol concentration (g L<sup>-1</sup>)</b>	<b>Ethanol productivity (g L<sup>-1</sup> h<sup>-1</sup>)</b>	<b>Ethanol mass yield (%)</b>
1	26.74 (0.03) <sup>a</sup>	0.56	54.46 (0.06)
2	21.74 (1.12)	0.45	44.76 (2.31)
3	17.54 (0.60)	0.37	31.99 (1.09)
4	32.59 (0.42)	0.68	67.24 (0.87)
5	26.51 (0.69)	0.22	54.90 (1.43)
6	23.35 (1.21)	0.49	46.68 (2.42)
7	20.26 (0.52)	0.42	40.29 (1.03)
8	29.52 (2.23)	0.62	56.19 (4.24)
9	27.11 (0.11)	0.56	47.65 (0.19)
10	26.16 (0.78)	0.36	44.49 (1.33)
11	24.17 (1.28)	0.34	42.32 (2.24)
12	29.12 (1.17)	0.61	48.80 (1.96)
13	24.40 (0.29)	0.42	43.69 (0.52)
14	23.36 (0.93)	0.49	41.32 (1.64)
15	14.32 (2.78)	0.60	27.18 (5.28)
16	23.91 (1.19)	0.50	42.50 (2.12)
17	21.58 (0.54)	0.45	47.67 (1.19)
18	29.75 (0.88)	0.62	65.28 (1.93)
19	25.98 (0.27)	0.36	49.89 (0.52)
20	25.79 (0.80)	0.54	51.42 (1.60)
21	7.03 (0.08)	0.29	27.84 (0.32)

<sup>a</sup> Numbers in parentheses are the estimates of the standard errors.

A simple linear regression was used in order to describe the relationship between cellulose conversion (%) and ethanol yield (%) (Fig. 6.5). Thus derived the linear Eq(6.1)

with a correlation coefficient of 0.680, which is only relatively good. This observation is in accordance with literature, suggesting that overall ethanol yield and ethanol production rate depend not only on the sugar yield, but also on the fermentability of the solution (Galbe and Zacchi, 2002).

$$Y(\%) = 0.506X + 14.51 \quad (6.1)$$

Where X is cellulose conversion (%) and Y is relative ethanol yield.

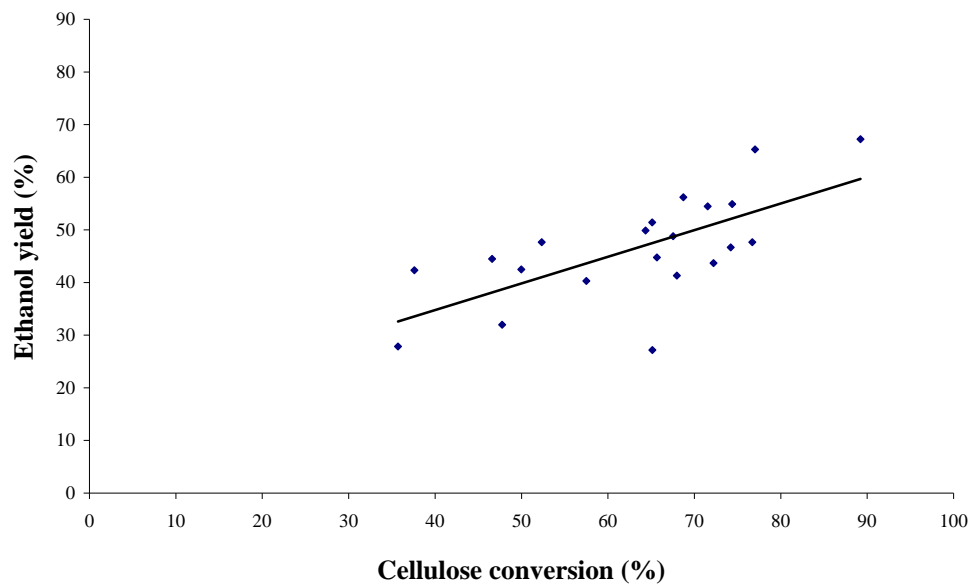


**Fig. 6.5** Cellulose conversion (%) achieved after 72 h of enzymatic hydrolysis and relative ethanol yield (%).

Compared to literature, the ethanol yields obtained by the organosolv process in the present manuscript are in the range of reported data for wheat straw after various pretreatments (Talebnia et al., 2010). In the case of organosolv processes, when formiline, acetoline, sulfuric acid-catalyzed ethanol and auto-catalyzed ethanol pretreatments were performed, at 15% solid loading, resulted in 65.0%, 46.3%, 62.5% and 60.1% ethanol yield respectively (Chen et al., 2015).

## 6.1.4 Adsorption capacity

At this point the potentiality of modified, via organosolv pretreatment, wheat straw for the adsorptive removal of Methylene Blue (MB), a representative basic dye, from aqueous solutions, will be examined.

### 6.1.4.1 Kinetic of adsorption

Adsorption kinetic studies are important in the treatment of aqueous effluents as they provide valuable information on the mechanism of the adsorption process (Calvete et al., 2009, 2010; Vaghetti et al., 2009). Thus, the experimental data of the kinetics of MB adsorption onto untreated and pretreated wheat straw were interpreted with the pseudo-first-order, pseudo-second-order and intra-particle diffusion models.

The models were evaluated by the coefficient of determination factor ( $R^2$ ) and the Standard Error of Estimate (SEE), which measures the differences in the amount of dye taken up by the adsorbent predicted by the models and the actual  $q$  measured experimentally.

$$SEE = \sqrt{\left(\frac{1}{n-p}\right) \cdot \sum_i^n (q_{i,\text{exp}} - q_{i,\text{mod}})^2} \quad (6.2)$$

where  $q_{i,\text{mod}}$  is the value of  $q$  predicted by the fitted model,  $q_{i,\text{exp}}$  is the value of  $q$  measured experimentally,  $n$  is the number of experiments performed and  $p$  is the number of parameter of the fitted model.

Parameters of the pseudo-first-order, pseudo-second-order and intra-particle kinetic models were estimated with the aid of the non-linear regression. The obtained data along with the correlation coefficients  $R^2$  and SEE are given in Tables 6.7 and 6.8.

**Table 6.7** Pseudo-first-order kinetic model parameters.

<b>Experiment</b>	<b><math>k_1</math> (<math>min^{-1}</math>)</b>	<b><math>q_e</math> (mg/g)</b>	<b><math>R^2</math></b>	<b><math>SEE</math></b>
1	0.042	8.23	0.956	0.471
2	0.03	8.31	0.978	0.368
3	0.007	11.76	0.994	0.211
4	0.03	6.63	0.965	0.365
5	0.035	7.06	0.946	0.479
6	0.024	7.65	0.975	0.378
7	0.033	6.82	0.954	0.428
8	0.027	8.16	0.984	0.314
9	0.014	8.69	0.999	0.106
10	0.034	9.02	0.968	0.462
11	0.025	9.12	0.990	0.272
12	0.011	11.62	0.996	0.193
13	0.032	8.19	0.951	0.523
14	0.047	10.46	0.943	0.672
15	0.052	9.36	0.939	0.617
Untreated	0.018	4.8	0.967	0.270

**Table 6.8** Pseudo-second-order kinetic model parameters.

Experiment	$k_2$ ( $g\ mg^{-1}\ min^{-1}$ )	$q_e$ (mg/g)	$R^2$	SEE
1	0.006	9.31	0.991	0.215
2	0.004	9.79	0.996	0.147
3	0.0003	18.57	0.995	0.226
4	0.005	7.75	0.986	0.214
5	0.006	8.09	0.979	0.276
6	0.003	9.24	0.988	0.234
7	0.006	7.87	0.983	0.241
8	0.003	9.8	0.996	0.159
9	0.001	12.08	0.997	0.164
10	0.004	10.41	0.992	0.225
11	0.003	11.13	0.995	0.192
12	0.0005	16.98	0.995	0.242
13	0.004	9.51	0.983	0.302
14	0.006	11.65	0.985	0.338
15	0.008	10.35	0.984	0.298
Untreated	0.003	6.04	0.981	0.199

Since the identification of the mechanisms involved in the adsorption process could not be performed using the pseudo-first and pseudo-second kinetic models the experimental data were further tested by the intra-particle. It has been reported that the initial adsorption behaviour can be explained based on the intra-particle diffusion model. As already mentioned, based on the  $R_i$  value, it is divided into four zones:  $0 < R_i < 0.9$ , which is called weak initial adsorption (zone 1);  $0.5 < R_i < 0.9$ , intermediately initial adsorption (zone 2);  $0.1 < R_i < 0.5$ , strong initial adsorption (zone 3); and  $R_i < 0.1$ , approaching complete initial adsorption (zone 4). As shown in Table 6.9 the majority of the  $R_i$  values for the modified wheat straw belongs to zone 2 (intermediate initial adsorption). The results are in accordance with literature references of 86 adsorption systems reporting also, that the main two zones were the intermediate (48%) and the strong (31%) initial adsorption (Wu et al., 2009).

**Table 6.9** Initial adsorption factor  $R_i$  and kinetic behavior based on the intra-particle diffusion model.

Experiment	$C$ (mg/g)	$k_p$ (mg g <sup>-1</sup> min <sup>-0.5</sup> )	$R_i$	$R^2$	$SEE$
1	2.28	0.529	0.743	0.882	0.743
2	1.54	0.575	0.821	0.931	0.598
3	1.23	0.726	1.0	0.975	0.448
4	1.32	0.452	0.806	0.930	0.477
5	1.68	0.467	0.776	0.919	0.533
6	1.05	0.54	0.865	0.962	0.411
7	1.53	0.457	0.787	0.921	0.512
8	1.24	0.577	0.855	0.947	0.525
9	0	0.652	1.0	0.975	0.398
10	2.07	0.603	0.781	0.911	0.721
11	1.10	0.665	0.882	0.933	0.682
12	0	0.827	1.0	0.980	0.458
13	1.72	0.555	0.804	0.974	0.558
14	3.28	0.647	0.707	0.856	1.018
15	3.13	0.567	0.683	0.835	0.967
Untreated	0.347	0.344	0.931	0.990	0.132

Tables 6.7, 6.8 and 6.9 show that all three models give a good correlation to experimental data. However, based on the SEE values, it was observed that the pseudo-second-order kinetic model provides the best fit to the data for all modified wheat straw adsorbents, because its SEE values were at least 20% lower, than the values obtained for pseudo-first-order and intra-particle kinetic models. The lower the SEE, the lower the difference of the  $q$  calculated by the model from the experimentally measured  $q$  (Royer et al., 2009; Calvete et al., 2010). Also, it was verified that the  $q_e$  values found in the pseudo-second-order were closer to the experimental  $q_e$  values, when compared with the presented kinetic models. These results indicate that the pseudo-second-order kinetic model should explain the adsorption process. The adsorption capacity of the wheat straw increased by the pretreatment, regardless the organic solvent. The effect of pretreatment temperature and reaction time on the adsorption capacity of modified wheat straw, according to the pseudo-second order kinetic model for each solvent separately, was investigated and presented in

Figures 6.6, 6.7, 6.8, 6.9 and 6.10. In the cases of ethanol, methanol and acetone an increase in the pretreatment temperature had more positive impact on the adsorption capacity of wheat straw, whereas in the cases of butanol and diethylene glycol organosolv reaction time increase was more significant.

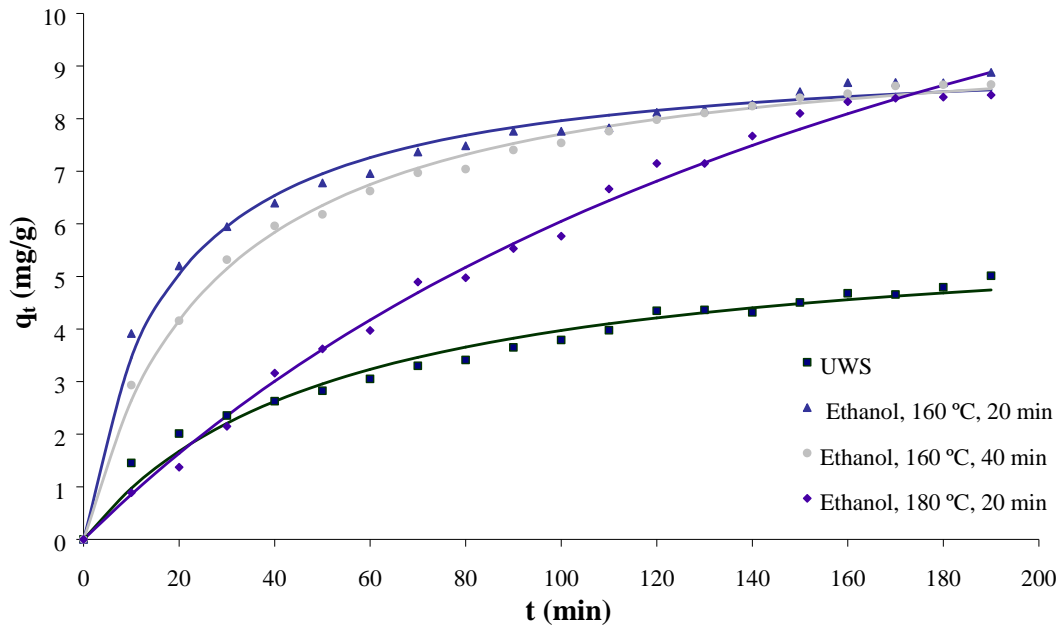


**Fig. 6.6** Curves according to the Pseudo-second-order kinetic model for untreated and organosolv pretreated with ethanol wheat straw.

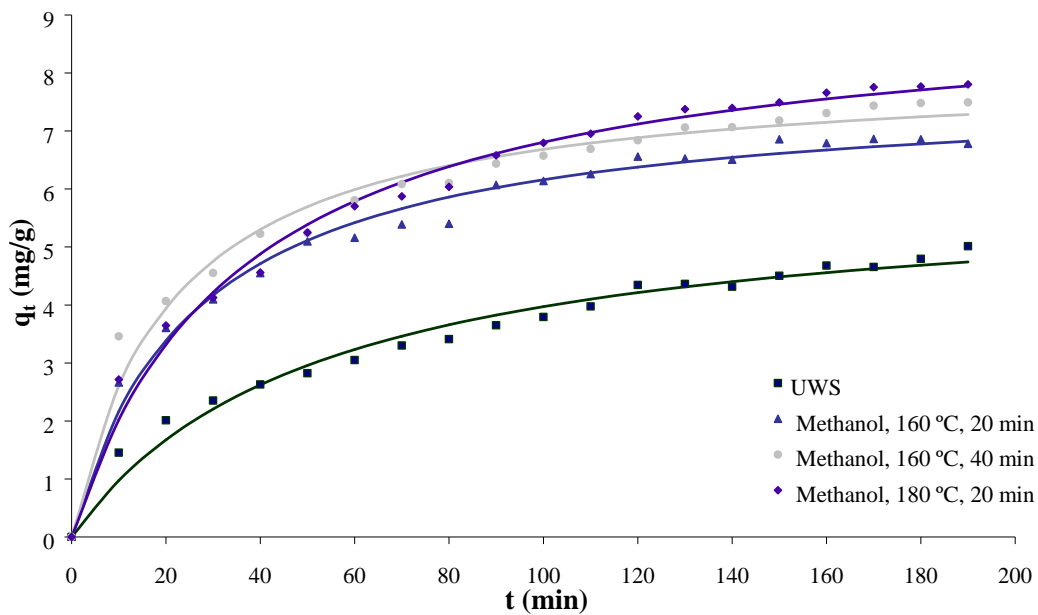


**Fig. 6.7** Curves according to the Pseudo-second-order kinetic model for untreated and organosolv pretreated with methanol wheat straw.

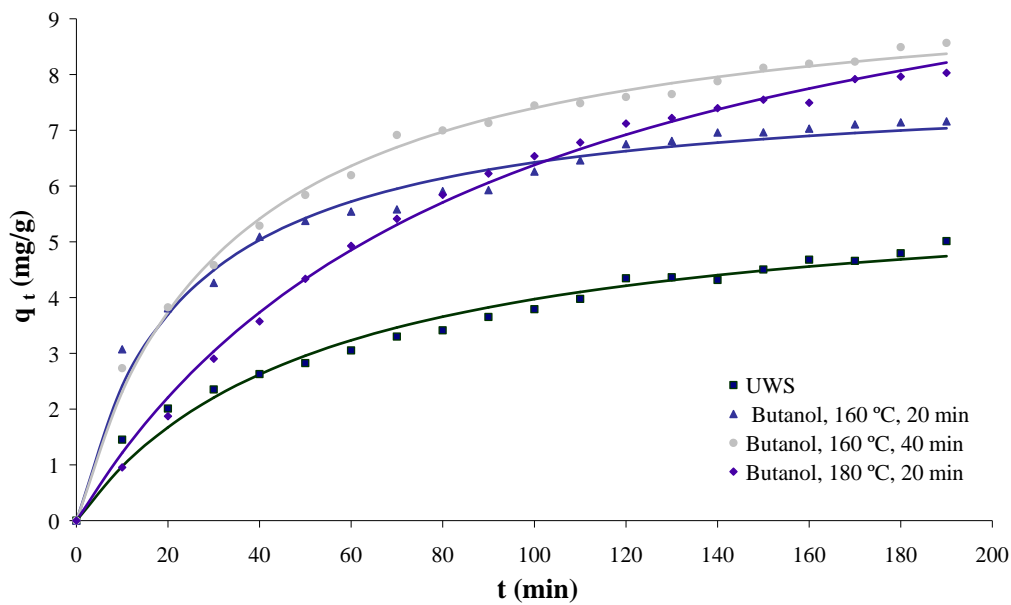


**Fig. 6.8** Curves according to the Pseudo-second-order kinetic model for untreated and organosolv pretreated with butanol wheat straw.

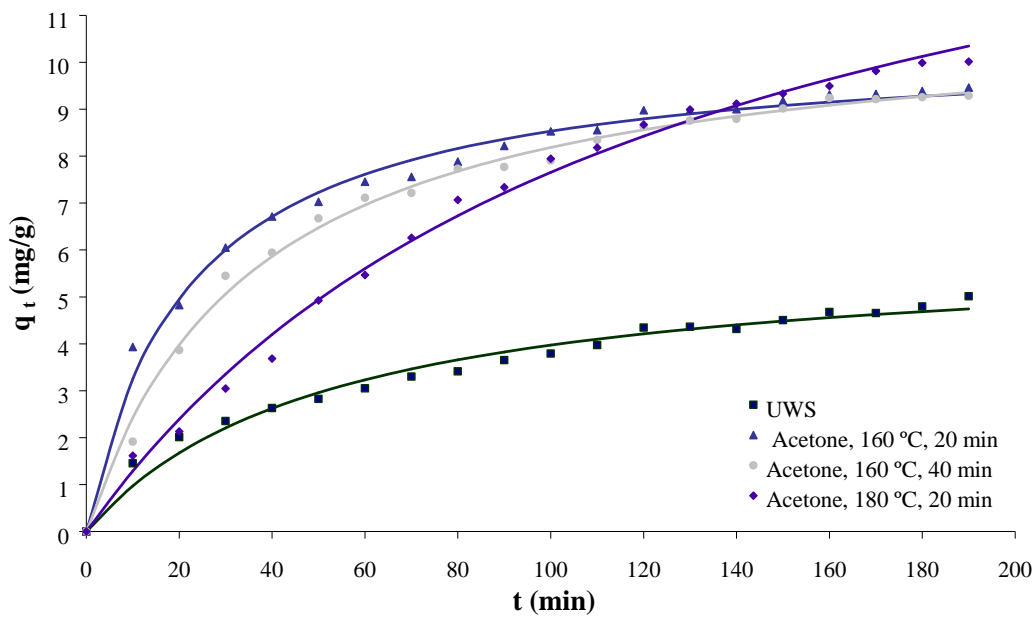


**Fig. 6.9** Curves according to the Pseudo-second-order kinetic model for untreated and organosolv pretreated with acetone wheat straw.

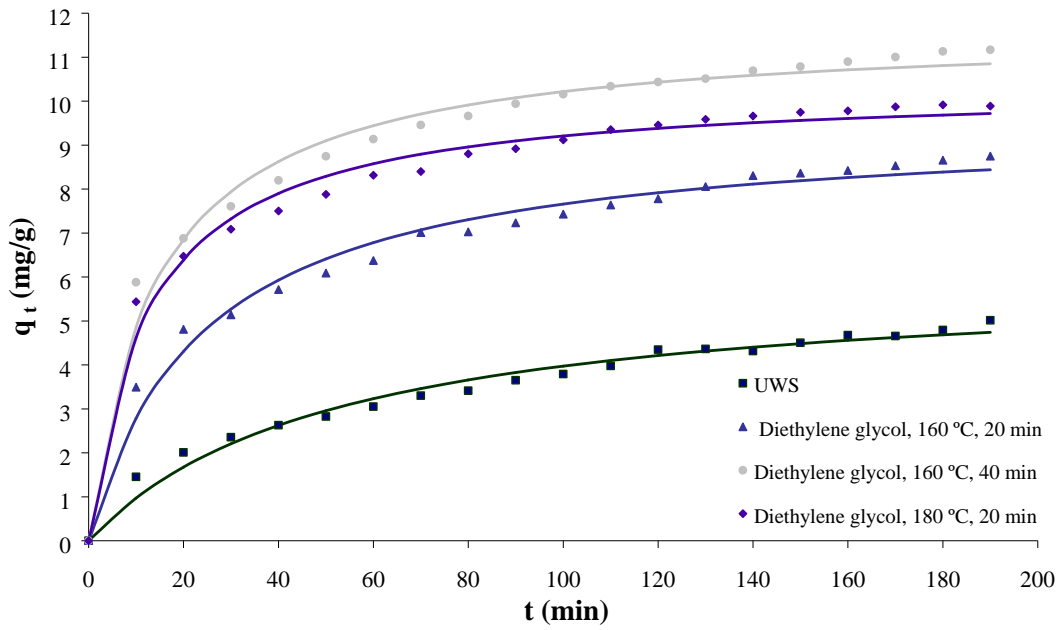


**Fig. 6.10** Curves according to the Pseudo-second-order kinetic model for untreated and organosolv pretreated diethylene glycol wheat straw.

The effect of organosolv pretreatment, with different organic solvents at selected conditions, on the amount of dye adsorbed at equilibrium time ( $q_e$ ) is shown in Fig. 6.11. The two organosolv pretreatments that stand out are ethanol at 180 °C for 20 min (exp3) and acetone at the same conditions (exp12). Nevertheless, when taking into account the intra-particle diffusion model, the acetone based process at 180 °C for 20 min exhibits the highest (compared to all others) adsorption rate constant ( $k_p$ ).

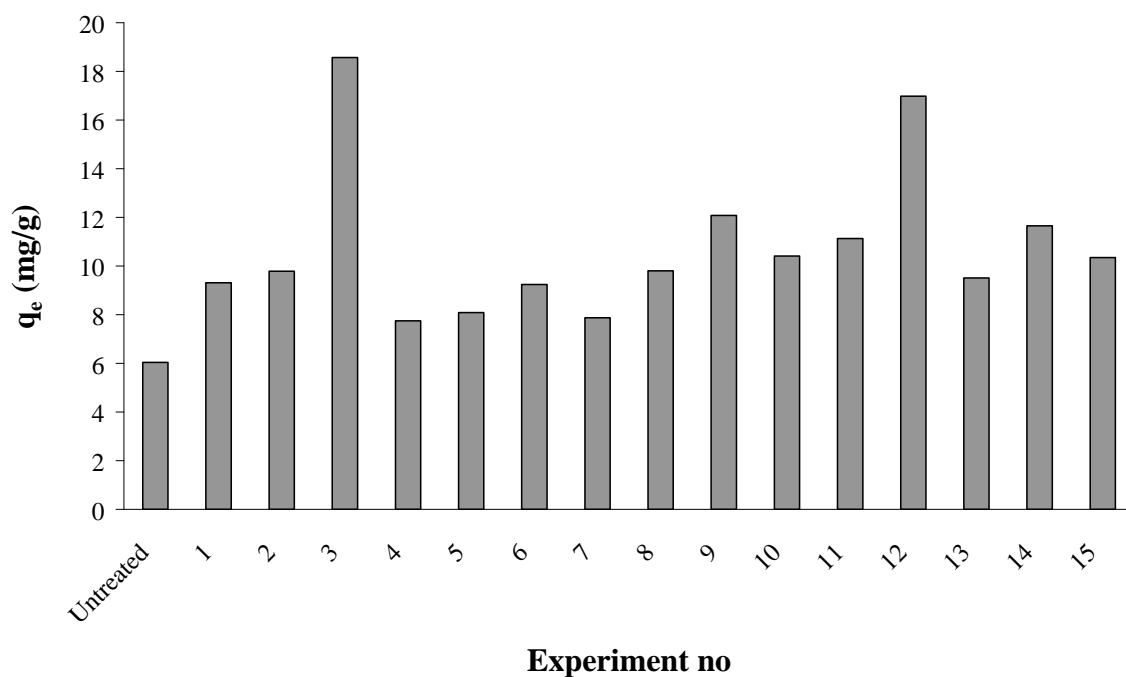


**Fig. 6.11** Kinetic parameter  $q_e$  according to the pseudo-second order model; organosolv pretreatments catalyzed by  $23 \text{ mol m}^{-3} \text{ H}_2\text{SO}_4$ ; organic solvents: ethanol (1-3), methanol (4-6), butanol (7-9), acetone (10-12), diethylene glycol (13-15).

#### 6.1.4.2 Adsorption isotherm

The adsorption isotherm is important in describing the relationship between the amount of adsorbate taken up by the adsorbent ( $q_e$ ) and the adsorbate concentration remaining in the solution after the system attained the equilibrium ( $C_e$ ). Different two and three-parameter models have been widely considered for the description of the adsorption isotherms. From them the Freundlich model, the Langmuir model and the Sips model were used to fit the experimental data. The models were also evaluated, as previously stated in the adsorption kinetic, by the coefficient of determination factor ( $R^2$ ) and the Standard Error of Estimate ( $SEE$ ).

As formerly mentioned (section 4.3.1) the Freundlich isotherm assumes that the surfactant adsorption occurs on a heterogeneous surface by multilayer sorption. In the model's equation two constants are introduced  $K_F$  and  $n$  related to adsorption capacity and intensity respectively. When,  $0.1 < 1/n < 0.5$ , adsorption is favourable;  $0.5 < 1/n < 1$ , it is easy to adsorb;  $1/n > 1$ , it is difficulty to adsorb (Samiey and Dargahi, 2010). According to Table 6.10 the  $1/n$  values in all experiments range from 0.23 to 0.50, thus indicating the adsorption as favourable, except from exp19 where it is easy to adsorb. It should also be

mentioned, based on  $K_F$  values, that adsorption capacity was improved after organosolv pretreatment in all cases as compared with the untreated material.

**Table 6.10** Parameters of Freundlich isotherm model of MB adsorption on modified and untreated wheat straw.

Experiment	$K_F ((\text{mg g}^{-1})(\text{L mg}^{-1})^{1/n})$	$n$	$R^2$	$SEE$
1	3.98	2.71	0.949	1.80
2	2.86	3.31	0.869	1.42
3	3.43	3.74	0.783	1.95
4	4.82	3.45	0.880	2.28
5	3.14	4.37	0.826	1.17
6	2.12	3.85	0.741	1.23
7	3.28	3.31	0.823	2.01
8	2.95	3.19	0.910	1.34
9	1.45	1.97	0.924	1.66
10	3.38	2.92	0.885	2.01
11	4.52	3.94	0.740	2.72
12	2.74	2.27	0.942	1.85
13	5.14	2.60	0.947	2.58
14	8.02	3.47	0.836	4.63
15	4.26	2.92	0.907	2.31
Untreated	2.53	2.22	0.925	2.09

As shown in Table 6.11 the Langmuir isotherm model fitted relatively well to the experimental data for both organosolv pretreated adsorbents and untreated material  $R^2 > 0.8$ . The monolayer saturation capacities of pretreated wheat straw were found to vary significantly based on the organic solvent, but also the pretreatment's conditions (reaction time and temperature). The nature of the sorption was determined by the dimensionless separation factor  $R_L$ . As previously stated (ch.), there are four possibilities for the  $R_L$  value:

- $0 < R_L < 1$ , adsorption is favourable
- $R_L > 1$ , adsorption is unfavourable
- $R_L = 1$  indicates linearity of adsorption,
- $R_L = 0$ , adsorption is irreversible

The values of  $R_L$  obtained in this study were between 0 and 1, indicating that the adsorption of MB onto modified but also untreated wheat straw is favourable.

**Table 6.11** Parameters of Langmuir isotherm model of MB adsorption on modified and untreated wheat straw.

<b>Experiment</b>	$q_m$ (mg/g)	$K_L$ (L/mg)	$R^2$	$SEE$
1	22.3	0.099	0.917	2.32
2	11.3	0.159	0.877	1.37
3	11.8	0.182	0.920	1.19
4	18.1	0.173	0.962	1.27
5	8.24	0.407	0.803	1.25
6	6.86	0.202	0.796	1.09
7	13.3	0.148	0.941	1.17
8	12.9	0.121	0.984	0.55
9	20.2	0.027	0.892	2.01
10	16.9	0.105	0.962	1.15
11	14.5	0.211	0.932	1.41
12	23.5	0.053	0.911	2.32
13	31.7	0.084	0.942	2.71
14	30.1	0.178	0.973	1.86
15	20.7	0.120	0.900	2.39
Untreated	23.0	0.050	0.956	1.67

The results obtained for fitting the Langmuir and Freundlich models to the experimental data of MB adsorption were similar, so it could not be determined the type of interaction among the molecules and the sorbents using these models. In this regard, the three-parameter Sips isotherm comes into prominence. As known, Sips isotherm is a combination of Langmuir and Freundlich models. The heterogeneity factor of  $n_s$  close to 0 displays heterogeneous sorbent (the Sips isotherm becomes Freundlich), while  $n_s$  close to or even 1 the Sips isotherm equation reduces to the Langmuir equation; that is, adsorption takes place on homogeneous surface. As before the results vary significantly among the organic solvents but also the pretreatment's conditions (Table 6.12). In the case of untreated wheat

straw and several pretreated materials (exp4, exp6, exp7, exp8, exp10) the  $n_s$  factor revealed that adsorption takes place on homogeneous surface (Chatterjee et al., 2010).

**Table 6.12** Parameters of Sips isotherm model of MB adsorption on modified and untreated wheat straw.

Experiment	$q_m$ (mg/g)	$K_S$ (L/mg)	$n_s$	$R^2$	$SEE$
1	56.2	0.004	2.09	0.951	1.86
2	14.1	0.073	1.52	0.894	1.34
3	10.9	0.213	0.65	0.935	1.12
4	18.3	0.168	1.04	0.961	1.34
5	16.0	0.018	2.73	0.829	1.23
6	7.09	0.183	1.11	0.797	1.14
7	12.3	0.178	0.86	0.952	1.10
8	12.9	0.120	1.00	0.984	0.58
9	162	0.0001	1.87	0.923	1.75
10	16.1	0.121	0.86	0.963	1.18
11	13.5	0.240	0.59	0.961	1.11
12	120	0.0004	2.05	0.942	1.95
13	47.1	0.023	1.61	0.955	2.48
14	27.8	0.214	0.68	0.829	1.23
15	29.5	0.035	1.66	0.919	2.26
Untreated	24.2	0.043	1.08	0.951	1.76

Based on the  $R^2$  and  $SEE$  values, the Sips model is the best isotherm model for the adsorbents derived from the experimental processes presented herein. The Sips model showed in Table 6.12 presents the lowest  $SEE$  along with the highest  $R^2$  values, which means that the  $q$  fit by this isotherm model was closer to the  $q$  measured experimentally when compared with the other isotherm models. In Figures 6.12, 6.13, 6.14, 6.15 and 6.16 is presented the effect of pretreatment reaction temperature and time on the adsorption of MB by organosolv pretreated wheat straw, based on the Sips isotherm model, for each organic solvent separately.

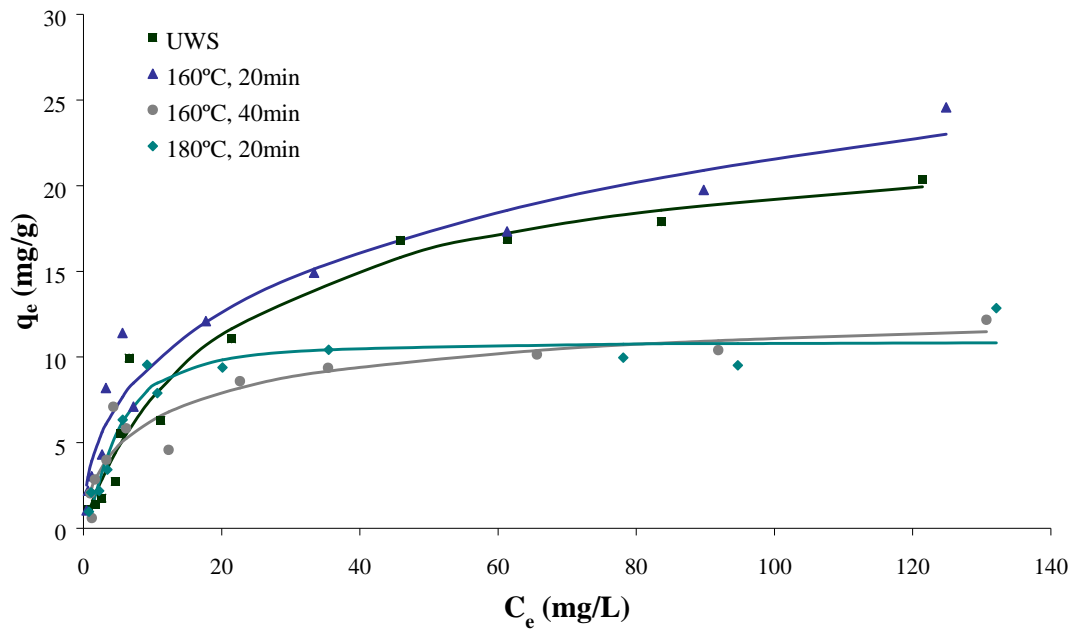


**Fig. 6.12** Sips plots for the adsorption of MB by untreated and organosolv pretreated with ethanol wheat straw.

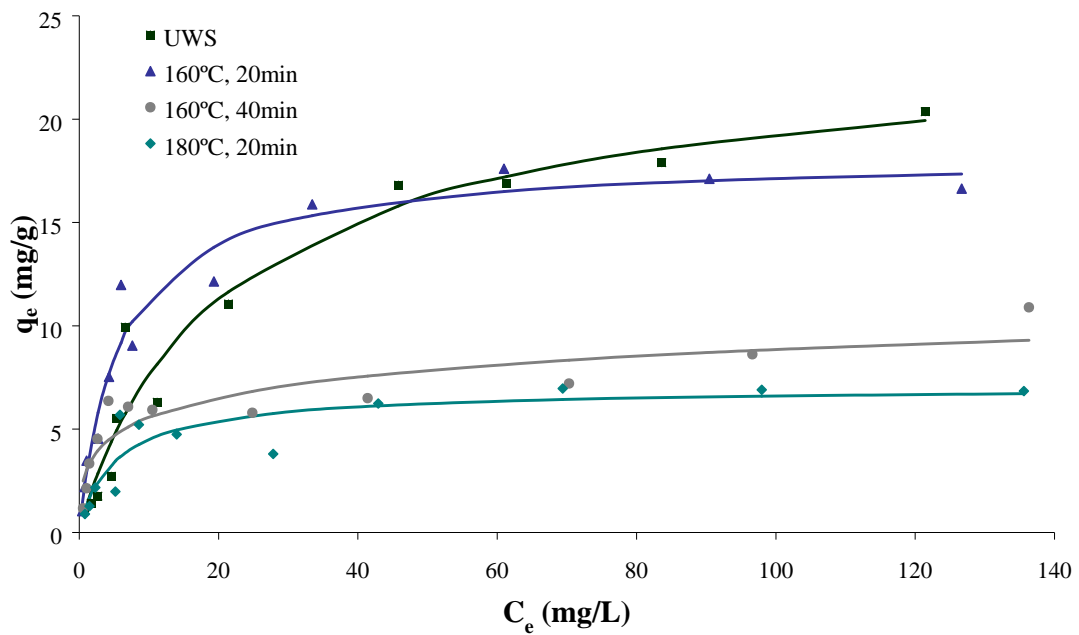


**Fig. 6.13** Sips plots for the adsorption of MB by untreated and organosolv pretreated with methanol wheat straw.

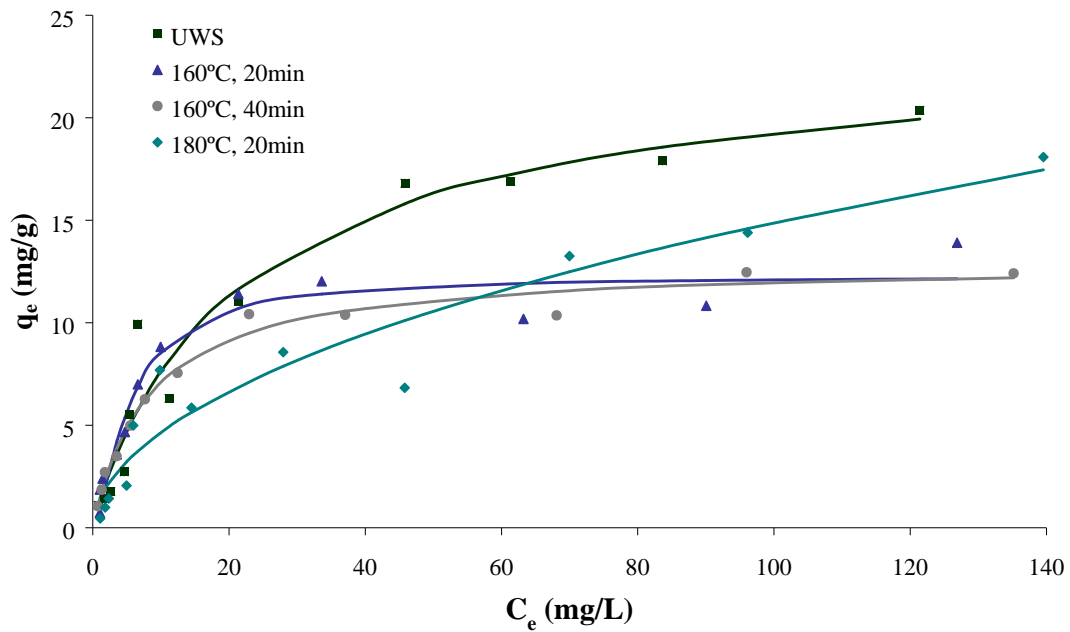


**Fig. 6.14** Sips plots for the adsorption of MB by untreated and organosolv pretreated with butanol wheat straw.

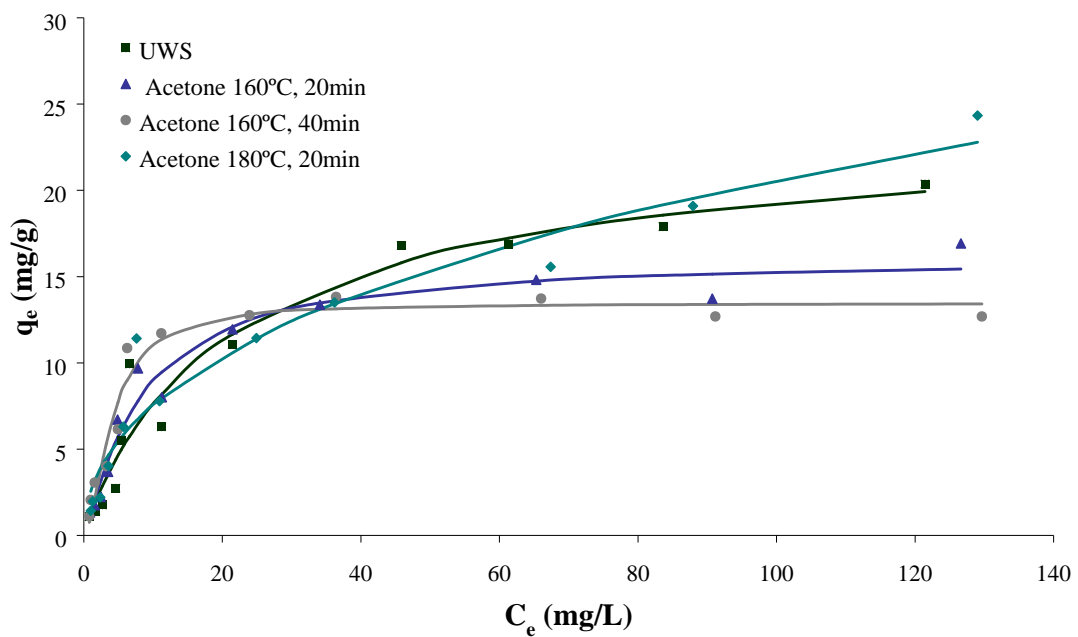


**Fig. 6.15** Sips plots for the adsorption of MB by untreated and organosolv pretreated with acetone wheat straw.

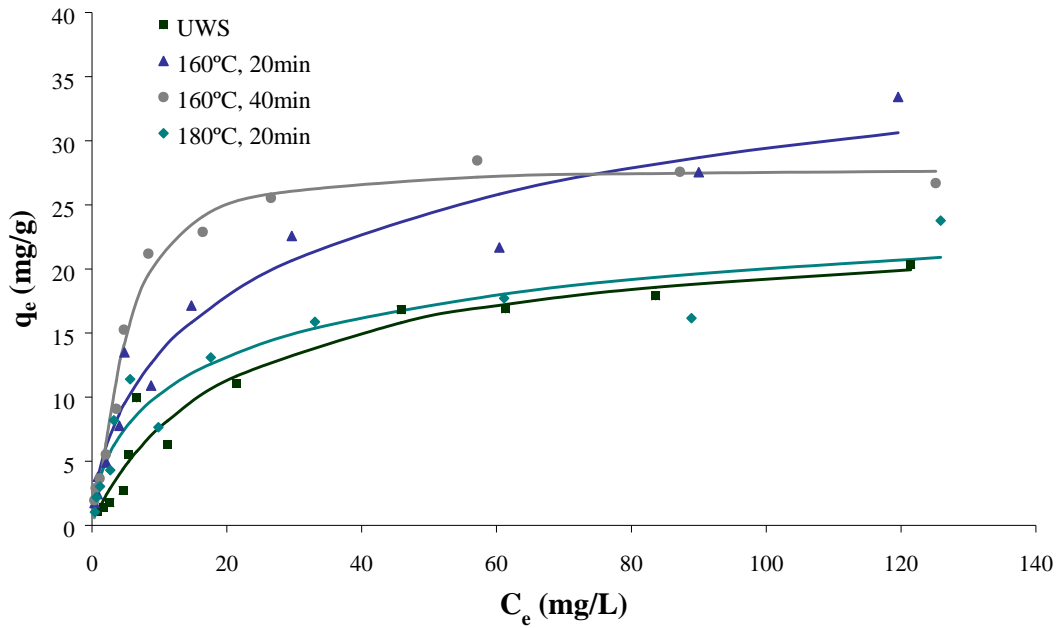


**Fig. 6.16** Sips plots for the adsorption of MB by untreated and organosolv pretreated with diethylene glycol wheat straw.

Regarding the organosolv treated materials with ethanol and diethylene glycol higher values were achieved at the mildest pretreatment conditions whereas in the cases of acetone increasing the reaction's temperature led to better results. An overall comparison of the maximum adsorption capacity, according to the Sips model, is presented in Fig. 6.17. The maximum adsorption potentials of sorbent for MB were found after butanol and acetone organosolv pretreatment of wheat straw at 180 °C for 20 min. It should be noted that only some pretreatments have enhanced the adsorption capacity of wheat straw.

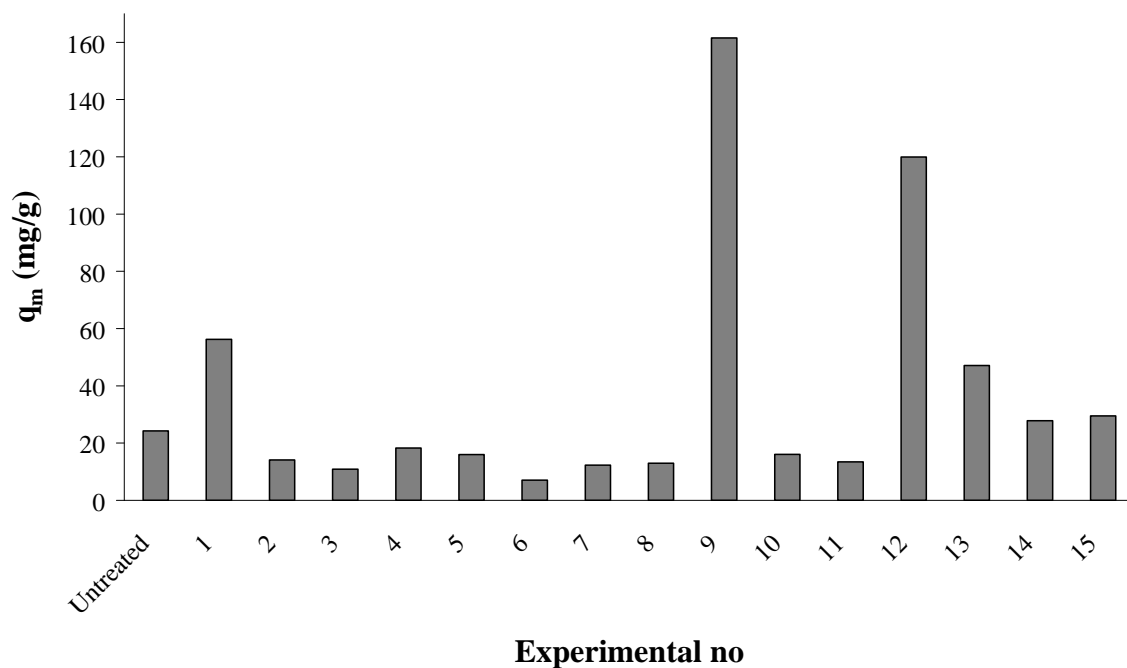


**Fig. 6.17** Effect of organosolv pretreatment based on Sips maximum adsorption capacity ( $q_m$ ); organosolv pretreatments catalyzed by  $23 \text{ mol m}^{-3} \text{H}_2\text{SO}_4$ ; organic solvents: ethanol (1-3), methanol (4-6), butanol (7-9), acetone (10-12), diethylene glycol (13-15).

## 6.2 Acetone organosolv pretreatment of barley straw

Acetone organosolv pretreatment conditions (catalyst concentration, reaction temperature and time) were simulated and optimized for the pretreatment of barley straw. The Response Surface Methodology (RSM) based on Box-Behnken experimental design and the Combined Severity Factor (CSF) were the two approaches evaluated, for the organosolv fractionation of barley straw and the enzymatic hydrolysis of the cellulosic residues data correlation. The experimental matrix along with the CSF logarithm is presented in Table 6.13.

**Table 6.13** Box-Behnken experimental design and the combined severity factor.

Conditions				
Run	T (°C)	t (min)	SA (mol/m <sup>3</sup> )	logR <sub>o</sub> *
1	140	20	10	-1.97
2	160	0	10	-1.37
3	160	40	10	-1.31
4	140	0	22.5	-0.82
5	180	20	10	-0.78
6	140	40	22.5	0.08
7	160	20	22.5	0.42
8	160	20	22.5	0.45
9	160	20	22.5	0.45
10	160	0	35	0.60
11	140	20	35	0.61
12	180	0	22.5	0.68
13	160	40	35	1.25
14	180	40	22.5	1.28
15	180	20	35	1.63

Abbreviations: T = temperature (°C); t = time (min); SA = sulfuric acid

## 6.2.1 Compositional analysis

Table 6.14 shows the effect of pretreatment conditions on the composition of the liquors. Monomeric sugars expressed as the mass fraction of the initial polysaccharides i.e. cellulose and xylan, were determined after a post-hydrolysis step.

**Table 6.14** Liquor composition (% on initial polysaccharides).

Run	Glucose	Xylose	Total Glucose	Total Xylose
1	0.67 (0.01) <sup>b</sup>	1.2 (0.07)	1.3 (0.11)	3.4 (0.14)
2	0.76 (0.02)	1.4 (0.18)	1.3 (0.36)	3.3 (0.25)
3	0.87 (0.04)	7.9 (0.56)	1.4 (0.06)	12.9 (0.59)
4	0.69 (0.02)	4.1 (0.54)	1.4 (0.40)	10.3 (0.10)
5	0.34 (0.07)	12.2 (1.10)	0.9 (0.13)	21.6 (0.69)
6	0.85 (0.06)	12.9 (0.28)	1.9 (0.13)	24.6 (1.03)
7	1.22 (0.02)	32.5 (0.63)	1.9 (0.13)	48.5 (0.93)
8	1.25 (0.04)	30.8 (1.05)	2.0 (0.06)	44.0 (0.81)
9	1.02 (0.09)	34.9 (1.85)	1.9 (0.11)	49.2 (0.35)
10	3.16 (0.14)	46.0 (1.13)	4.2 (0.08)	59.0 (0.97)
11	3.42 (0.40)	65.3 (0.96)	4.3 (0.16)	76.8 (1.32)
12	5.19 (0.19)	49.6 (0.97)	6.0 (0.03)	60.5 (1.38)
13	7.24 (0.24)	53.2 (1.85)	7.8 (0.07)	61.9 (1.22)
14	6.53 (0.32)	46.6 (1.05)	7.1 (0.10)	58.3 (1.17)
15	7.07 (0.68)	42.7 (0.65)	7.6 (0.05)	52.8 (0.83)

<sup>a</sup> Measured after post-hydrolysis

<sup>b</sup> Numbers in parentheses are the estimates of the standard errors.

Moreover, the composition of the pretreated and untreated barley straw is given in Table 6.15. The results show that acetone organosolv pretreatment, using sulfuric acid as catalyst, had a moderate effect in lignin removal. However, this observation agrees with previous works on organosolv pretreatment (Pan et al., 2007; Kabir et al., 2015).

**Table 6.15** Composition of pulps and untreated barley straw (mass fraction (%) on dry pulp).

Run	Pulp yield (%)	Pulp composition (%)		
		Lignin	Cellulose	Xylan
1	77.0	19.4 (0.3)	41.7 (1.7)	23.0 (0.4)
2	80.6	21.7 (1.6)	36.4 (0.5)	17.2 (0.9)
3	70.9	19.8 (0.6)	41.8 (1.2)	21.3 (1.4)
4	78.1	21.4 (1.1)	33.1 (0.9)	15.1 (0.8)
5	59.9	20.5 (0.9)	51.4 (1.1)	13.6 (0.4)
6	65.0	21.1 (0.8)	48.8 (0.6)	17.3 (0.9)
7	52.3	20.6 (1.0)	57.3 (0.4)	11.3 (0.5)
8	53.5	19.8 (0.6)	58.8 (1.3)	12.2 (0.8)
9	54.6	19.1 (0.4)	59.1 (0.6)	13.1 (1.1)
10	48.0	21.4 (1.2)	61.3 (2.1)	4.7 (0.6)
11	48.5	19.0 (0.3)	50.8 (1.8)	7.0 (0.8)
12	46.7	20.0 (0.5)	63.7 (0.8)	12.6 (1.2)
13	40.6	21.0 (1.1)	70.6 (1.1)	4.1 (0.4)
14	43.7	21.1 (0.9)	64.2 (0.6)	2.7 (0.3)
15	35.7	19.4 (0.5)	64.4 (1.2)	5.9 (0.9)
Untreated	(-)	19.2 (1.8)	34.8 (1.1)	19.4 (0.4)

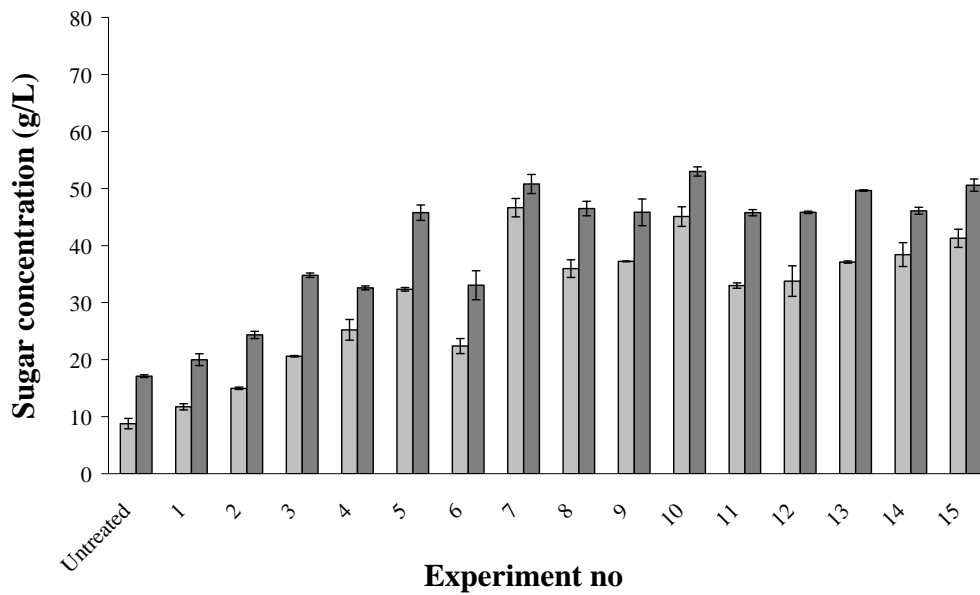
Numbers in parentheses are the estimates of the standard errors.

As expected, cellulose content of pulp was significantly increased by the treatment conditions due to little degradation of cellulose, high degradation of hemicellulose and moderate lignin removal.

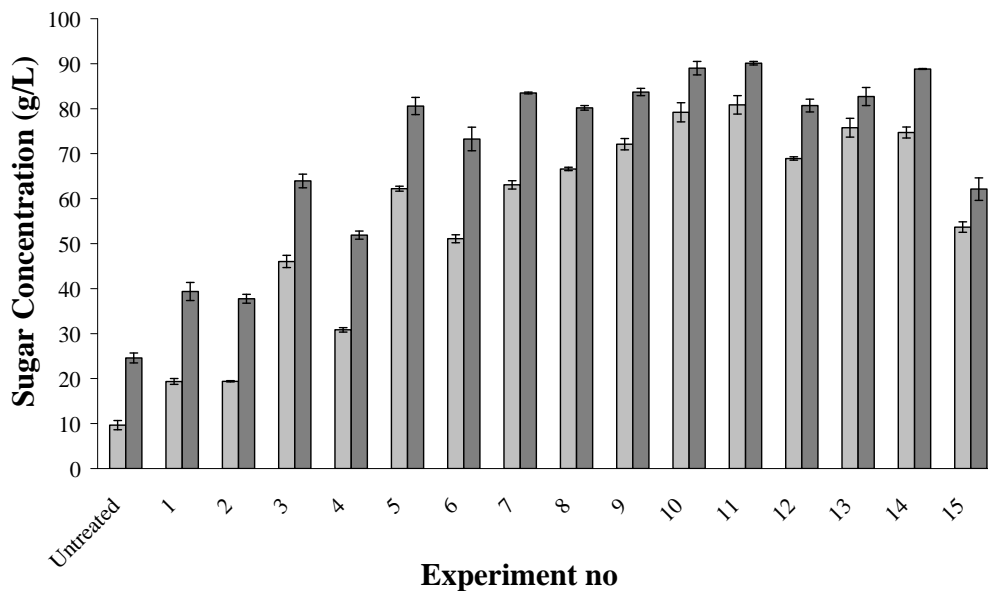
## 6.2.2 Enzymatic digestibility

The pretreated and untreated straws were subjected to enzymatic hydrolysis at 50 °C for 72 h using an enzyme load of 9 mg/g DM Cellic<sup>®</sup> CTec2 with 13% solid loadings. In Fig. 6.18 the concentrations of glucose and total reducing sugars, after 8h and 72 h enzymatic

hydrolysis, are presented. As expected, the pretreated materials' concentration of both total reducing sugars and glucose was increased in all cases.



(a)



(b)

**Fig. 6.18** Glucose and total reducing sugars (TRS) concentration after (a) 8 and (b) 72 h of enzymatic hydrolysis of pretreated samples using an enzyme load of  $9 \text{ g kg}^{-1}$  of dry matter DM Cellic® CTec2 at  $130 \text{ g kg}^{-1}$  dry solids in the total liquid mass.

### 6.2.3 Simulation based on CSF

In Fig. 6.19 pulp's delignification rate as a function of  $\log R_o^*$  is presented. It appears that an increase in treatment severity resulted in an increase of the removed lignin percentage, which is in accordance to literature (Goh et al., 2011).

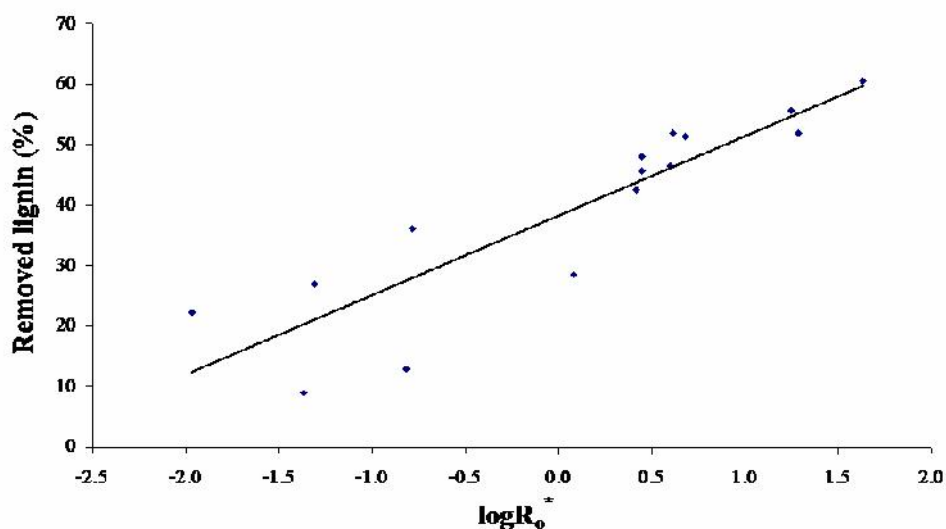


**Fig. 6.19** Removed lignin (%) as a function of the combined severity factor logarithm.

A simple linear regression was used to describe the relationship between lignin removal (%) and  $\log R_o^*$ . Thus, derived the linear Eq. (6.3)

$$\text{Removed lignin (\%)} = 36.27 + 13.15 \log R_o^* \quad (6.3)$$

Fig. 6.20 shows the recovery of sugars (xylose and glucose) in the hydrolyzates obtained after post-hydrolysis as a function of the CSF logarithm ( $\log R_o^*$ ). Severe pretreatment conditions enhance the formation of degradation products such as 5-HMF in the case of hexose sugars and furfural in the case of pentose sugars.

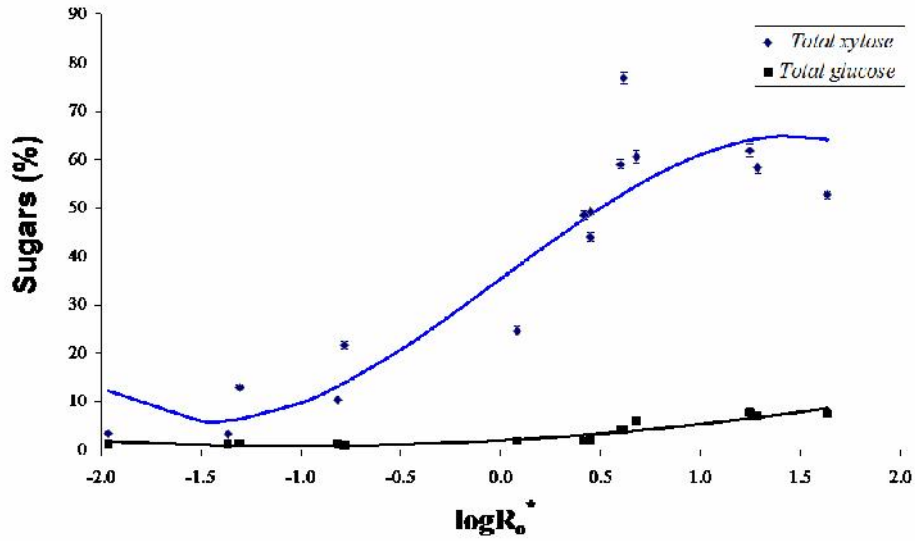


**Fig. 6.20** Total glucose and total xylose as a function of the combined severity factor logarithm.

Thus, a decrease in total xylose can be observed when  $\log R_o^* > 1$ . Literature data agree that at higher severity factors a part of the released xylose is converted to furfural (Kabel et al., 2007). The empirical polynomials used to describe the relationship between total xylose, total glucose and  $\log R_o^*$  are as follows:

$$\text{Total xylose} = 35.40 + 30.48 \log R_o^* - 4.85 (\log R_o^*)^3 \quad (6.4)$$

$$\text{Total glucose} = 2.01 + 2.26 \log R_o^* + 1.10 (\log R_o^*)^2 \quad (6.5)$$

Cellulose-to- glucose conversion yields after 72 h of enzymatic hydrolysis as a function of  $\log R_o^*$  of the treatment used for the pulp extraction are given in Fig. 6.21.

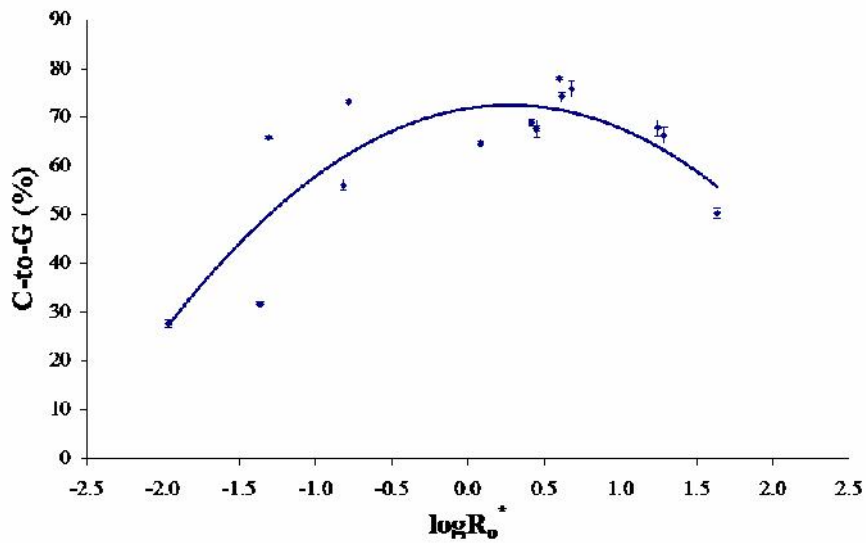


**Fig. 6.21** Enzymatic cellulose to glucose conversion(%) after 72 h, as a function the combined severity factor logarithm.

It was observed that cellulose conversion reached higher values when  $-0.5 < \log R_o^* < 0.5$ . Whereas harsher conditions  $\log R_o^* > 1$  had negative impact. Eq. (6.6) was used to describe the relationship among cellulose conversion (%) and  $\log R_o^*$

$$C - to - G = 71.84 + 4.92 \log R_o^* - 9.04 (\log R_o^*)^2 \quad (6.6)$$

Statistical analysis of variance (ANOVA) was required to test the significance and adequacy of the empirical models presented above. The estimated t-values and p-values are summarized in Table 6.16. P- values lower than 0.05 (95% confidence interval) are widely considered as the threshold of significance for the coefficients. On the contrary, larger t-values indicate significance as t equals Coefficient/Standard error.

**Table 6.16** Estimated t-values and p-values for the regression coefficients obtained from the combined severity factor.

	<b>t-value</b>	<b>p-value</b>
<b><i>Removed lignin</i></b>		
Constant	19.63	$4.81 \cdot 10^{-11}$
$\log R_o^*$	7.04	$8.74 \cdot 10^{-6}$
<b><i>Total xylose</i></b>		
Constant	12.70	$2.57 \cdot 10^{-8}$
$\log R_o^*$	5.50	$1.36 \cdot 10^{-4}$
$(\log R_o^*)^3$	-2.13	0.05
<b><i>C-to-G</i></b>		
Constant	21.42	$6.24 \cdot 10^{-11}$
$\log R_o^*$	2.16	0.05
$(\log R_o^*)^2$	-4.07	$1.55 \cdot 10^{-3}$

In Table 6.17 the analysis of variance for the models is given. More specifically, the Fisher's variance ratio (F-value) along with the significance of F (SigF) is provided as indications of the models' adequacy.

**Table 6.17** Analysis of variance for polynomial models derived from the combined severity factor.

Source	R <sup>2</sup>	SEE	SS	DF	MS	F	SigF
<b><i>Removed lignin</i></b>							
Regression	0.79	7.53	2812.9	1	2812.9	49.6	8.74·10 <sup>-6</sup>
Residual			736.8	13	56.7		
Total			3549.7	14			
<b><i>Total xylose</i></b>							
Regression	0.90	8.99	7340.8	4	1835.2	22.7	5.26·10 <sup>-5</sup>
Residual			807.6	10	80.8		
Total			8148.4	14			
<b><i>C-to-G</i></b>							
Regression	0.71	14.30	2266.7	2	1133.3	14.9	5.55·10 <sup>-4</sup>
Residual			911.0	12	75.9		
Total			3177.7	14			
SS = Sum of squares; DF = Degrees of Freedom; MS = Mean Square; F = the Fisher's variance ratio; SigF = Significance of F							

## 6.2.4 Simulation based on RSM

The significance of the model, individual terms, and their interaction on the responses (removed lignin, total xylose, and cellulose-to-glucose conversion) were evaluated through ANOVA and the results are presented in Tables 6.18 and 6.19.

**Table 6.18** Estimated t-values and p-values for the regression coefficients.

	t-value			p-value		
	<i>Removed lignin</i>	<i>Total xylose</i>	<i>C-to-G</i>	<i>Removed lignin</i>	<i>Total xylose</i>	<i>C-to-G</i>
Constant	11.30	5.72	20.05	$9 \cdot 10^{-5}$	$2.29 \cdot 10^{-3}$	$5.70 \cdot 10^{-6}$
A	4.28	1.93	3.54	0.01	0.11	0.017
B	2.20	0.61	1.52	0.08	0.57	0.188
C	6.11	5.17	4.33	$1.70 \cdot 10^{-3}$	$3.55 \cdot 10^{-3}$	$7.49 \cdot 10^{-3}$
AB	-1.08	-0.57	-0.20	0.33	0.59	0.852
AC	-0.38	-1.48	-5.90	0.72	0.20	$1.99 \cdot 10^{-3}$
BC	-0.65	-0.23	-3.76	0.55	0.82	0.013
AA	-0.14	-0.30	-1.02	0.89	0.78	0.353
BB	-2.40	-0.89	0.42	0.06	0.42	0.689
CC	-0.60	-0.85	-2.81	0.57	0.43	0.038

Abbreviations: Normalized variables A = temperature (°C); B = time (min); C = sulfuric acid concentration (mol/m<sup>3</sup>)

**Table 6.19** Analysis of variance for polynomial models.

Source	R <sup>2</sup>	SEE	SS	DF	MS	F	SigF
<i>Removed lignin</i>							
Regression	0.93	6.96	3305.8	9	367.3	7.58	0.02
Residual			242.4	5	48.5		
Total			3548.2	14			
<i>Total xylose</i>							
Regression	0.85	10.04	6938.9	2	3469.5	34.42	1.07·10 <sup>-5</sup>
Residual			1209.5	12	100.8		
Total			8148.4	14			
<i>C-to-G</i>							
Regression	0.95	5.88	3170.3	9	352.3	10.2	0.009
Residual			172.9	5	34.6		
Total			3343.3	14			
SS =Sum of squares; MS = Adjusted Mean Square; F = the Fisher's variance ratio; SigF = Significance of F							

Antagonistic effects in the equations are shown with the negative sign while synergetic with the positive one. The second order polynomial obtained in the case of lignin removal was as follows:

$$\begin{aligned} \text{Removed lignin (\%)} = & 45.42 + 7.96A + 4.10B + 11.37C - 2.15AB - 0.76AC \\ & - 1.29BC - 0.30A^2 - 4.98B^2 - 1.25C^2 \end{aligned} \quad (6.7)$$

The RSM plots regarding the removed lignin as a function of the three variables studied herein are given in Figures 6.22, 6.23 and 6.24. Sulfuric acid concentration has significant effects on lignin removal when reaction time (Fig.6.22) or temperature (Fig.6.23) is at central level. Its significance can also be verified from Table 6.12 (p-value =1.70·10<sup>-3</sup>). On the other hand, when sulfuric acid is maintained constant at central concentration both temperature and time reaction factors have significant effects (Fig.6.24).

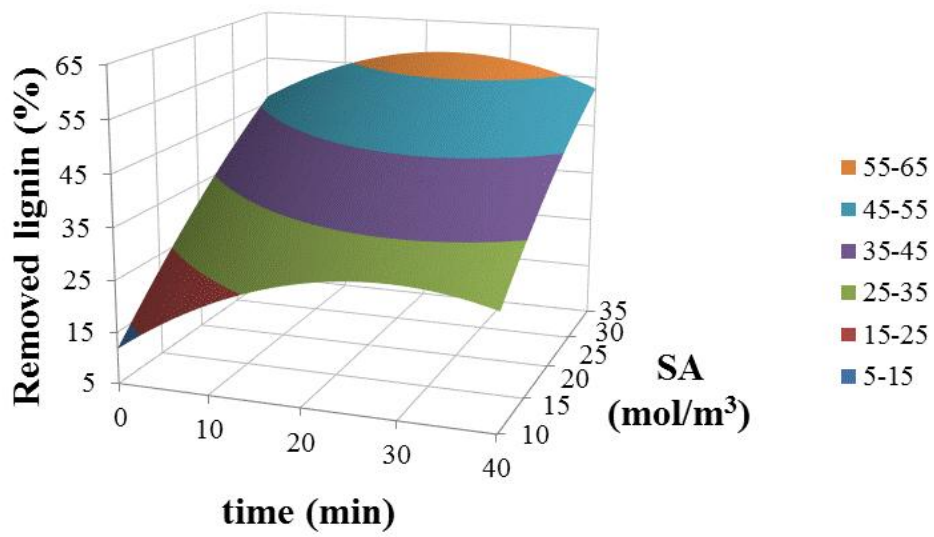


**Fig. 6.22** Response surface graphs for the effect of sulfuric acid concentration and reaction time on lignin removal.

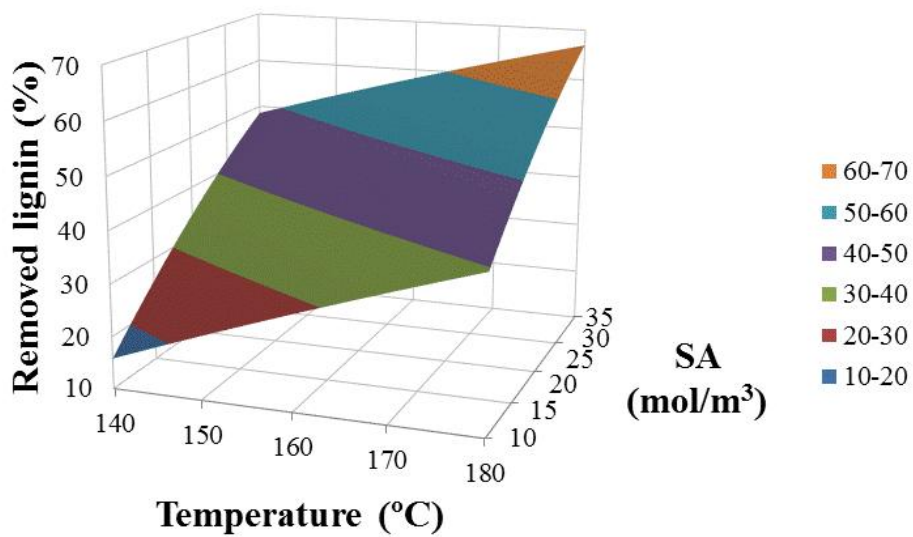


**Fig. 6.23** Response surface graphs for the effect of sulfuric acid concentration and reaction temperature on lignin removal.

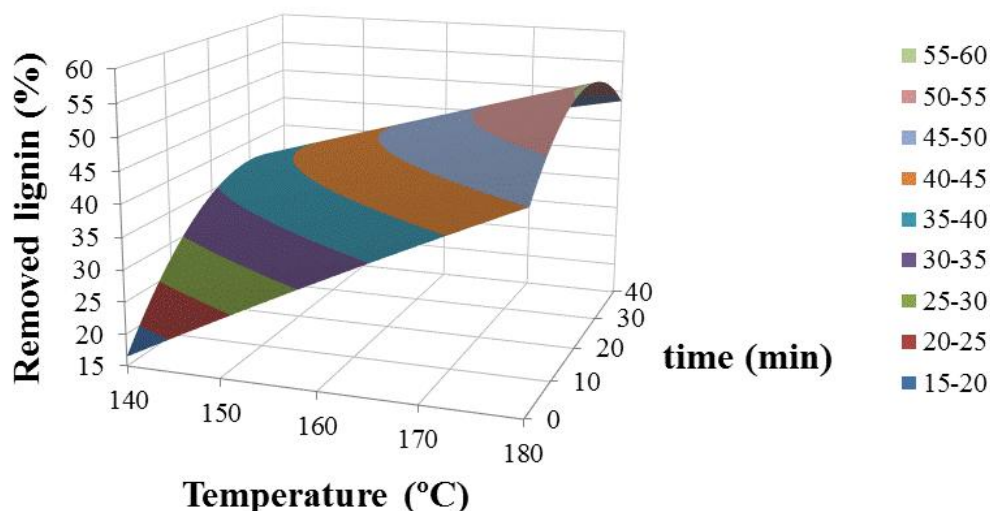


**Fig. 6.24** Response surface graphs for the effect of reaction time and temperature on lignin removal.

For the experimental design data and its corresponding total xylose (%), in the liquor after post-hydrolysis, a quadratic polynomial was also determined Eq. (6.8)

$$\begin{aligned}
 \text{Total Xylose (\%)} = & 47.21 + 7.37A + 2.32B + 19.77C - 2.34AB - 6.04AC \\
 & - 0.96BC - 1.26A^2 - 3.76B^2 - 3.62C^2
 \end{aligned}
 \tag{6.8}$$

Figures 6.25, 6.26 and 6.27 show the surface plots of the interaction effect of sulfuric acid concentration, reaction temperature and time on total xylose concentration in the liquid phase. As shown in the graphs, besides Table 6.18 ( $p\text{-value}=3.55 \cdot 10^{-3}$ ), sulfuric acid concentration value is the most important factor for overall xylose recovery. However, both temperature and time have noteworthy effects when sulfuric acid concentration is kept at central level.

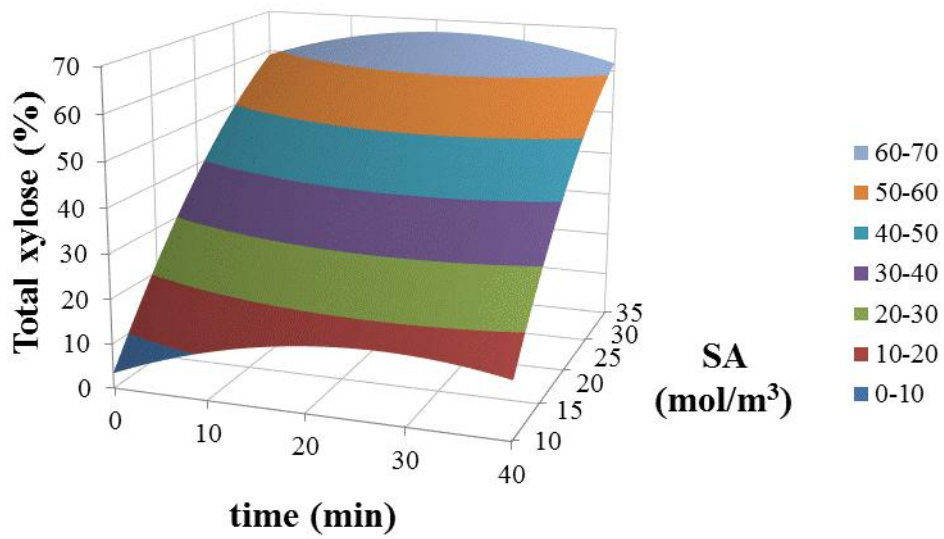


**Fig. 6.25** Response surface graphs for the effect of sulfuric acid concentration and reaction time temperature on total xylan concentration.

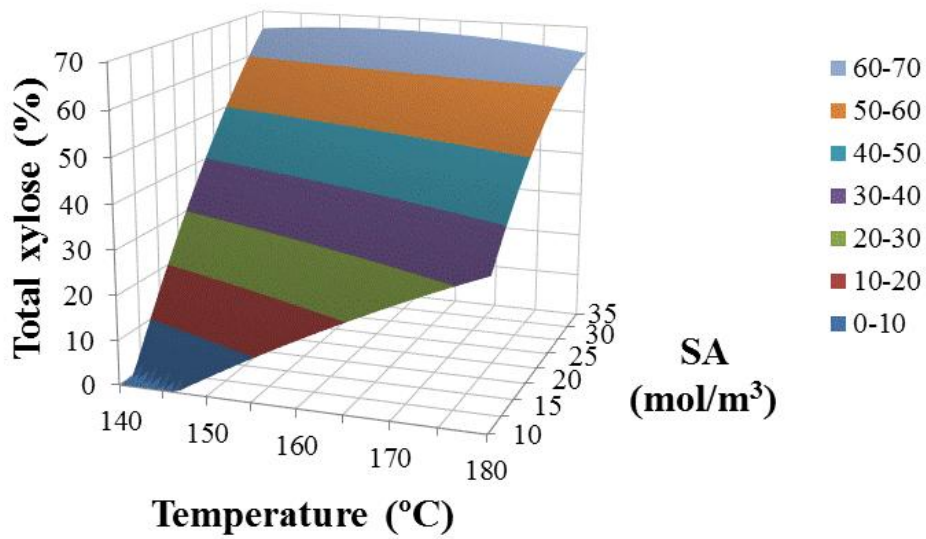


**Fig. 6.26** Response surface graphs for the effect of sulfuric acid concentration and reaction temperature on total xylan concentration.

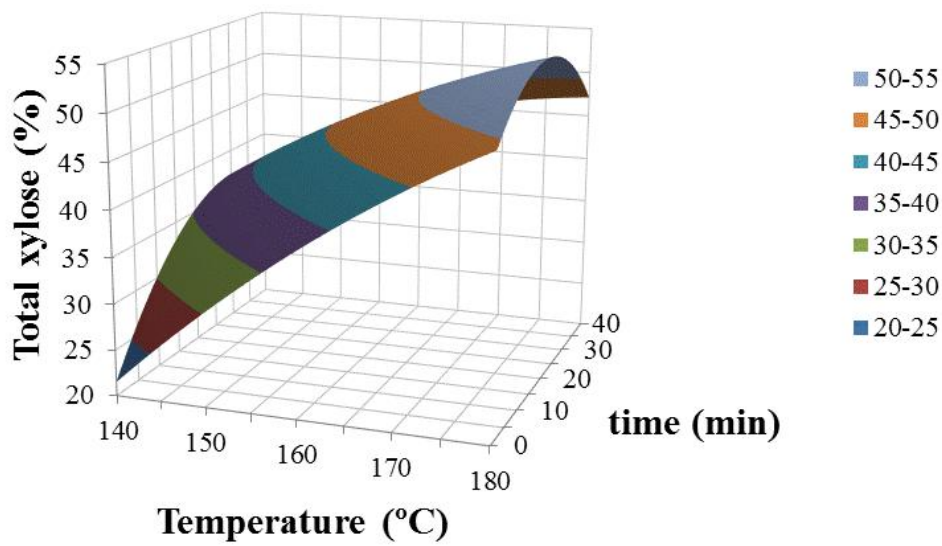


**Fig. 6.27** Response surface graphs for the effect reaction time and temperature on total xylan concentration.

The quadratic function corresponding to cellulose conversion (%) is described as follows in Eq. (6.9)

$$C - to - G (\%) = 68.09 + 5.56A + 2.39B + 6.81C - 0.33AB - 9.92AC - 6.32BC - 1.79A^2 + 0.74B^2 - 4.91C^2 \quad (6.9)$$

Fig. 6.28 provides a three-dimensional representation of the interaction of sulfuric acid concentration and reaction time. Organosolv pretreated barley straw in presence of sulfuric acid ( $35 \text{ mol/m}^3$ ) favors the glucose release from cellulose by enzymatic hydrolysis when residence time was at its low level. Similarly, in Fig.6.29 maximum cellulose conversion can be found at low temperature and again high sulfuric acid concentration. Fig.6.30 reveals that cellulose-to-glucose conversion is more dependent on acid loading than on temperature and residence time.

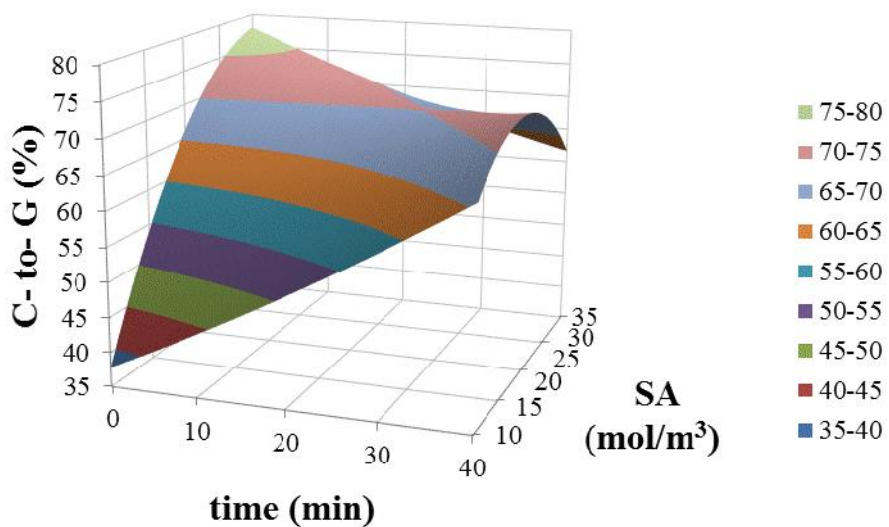


**Fig. 6.28** Response surface graphs for the effect of sulfuric acid concentration and reaction time.

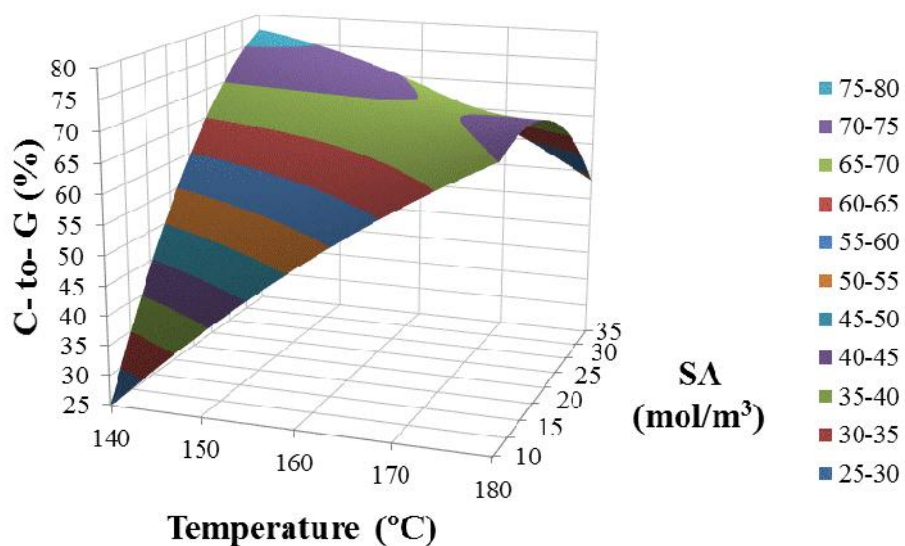


**Fig. 6.29** Response surface graphs for the effect of sulfuric acid concentration and reaction temperature on cellulose to glucose conversion.

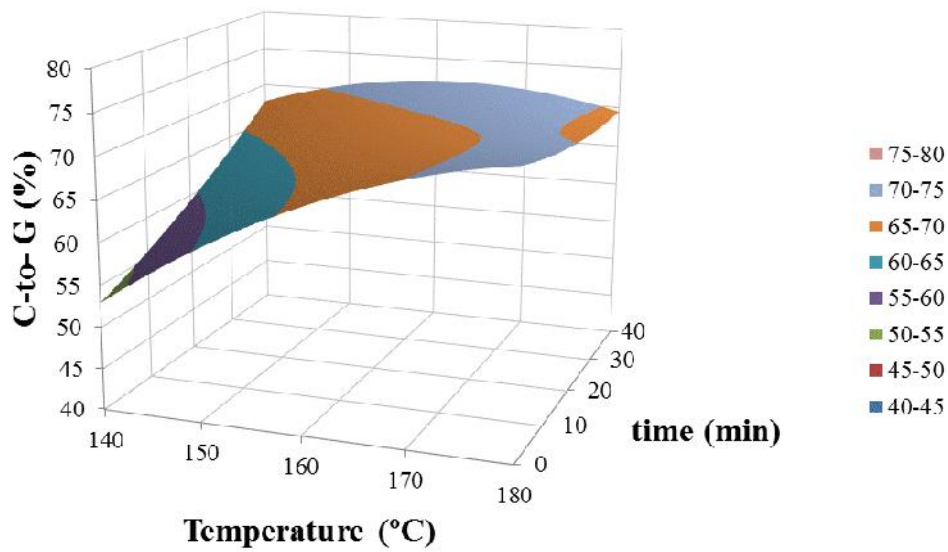


**Fig. 6.30** Response surface graphs for the effect of reaction time and temperature on cellulose to glucose conversion.

It should be noted, that the response models were mapped against two experimental factors while the third factor was set constant at its central value. Overall, RSM plots revealed the large impact of sulfuric acid concentration on lignin removal, xylan hydrolysis and enzymatic digestibility, which is in agreement with literature (Wildschut et al., 2013).

### 6.2.5 Optimization

The optimal conditions were predicted using the Quantum XL software in the same range than the experimental runs and their CSF was calculated. As expected, the maximum lignin removal can be achieved when relatively harsh pre-treatment conditions are employed, 180 °C, 20 min and 35 mol/m<sup>3</sup> in this study. Coincidentally, these particular pre-treatment conditions were run and resulted in  $\log R_o^* = 1.63$ . The value for lignin removal derived from the CSF simulation, Eq. (8), at those particular conditions was 59.8%, while the RSM was slightly different (66.9%). It should be noted that, unlike the RSM, the CSF in the range of the experimental data showed a linear relationship and thus no maximum. The software predicted that the optimized conditions for total xylose in the liquid fraction are a reaction temperature, residence time and SA concentration of 152 °C, 25 min and 35 mol/m<sup>3</sup> respectively, yielding a total xylose of 67.3%. At these conditions,  $\log R_o^* = 0.78$ ; total xylose recovery (56.9%) was estimated through the CSF, Eq. (6.4). In this case, the results derived from the software and those from the CSF deviate from the experimental results. The optimal conditions for cellulose-to-glucose conversion were 140

°C, 0 min and 35 mol/m<sup>3</sup>, with a 83.9% yield. The CSF logarithm at those particular conditions was -0.02. Cellulose-to-glucose conversion was determined using the CSF model, Eq. (6.6), and the maximum determined as 71.7%. For all cases, the SEE-values for the models derived from Quantum XL (Table 6.19) were lower than from the CSF models (Table 6.17), showing that the software models fit better to the experimental results. The experimental runs gave optimums of 71.6% for total xylose recovery (152 °C, 25 min, 35 mol/m<sup>3</sup>) and 79.2% for cellulose-to-glucose conversion (140 °C, 0 min and 35 mol/m<sup>3</sup>), which is in agreement with the values calculated via the RSM model.

Both approaches (CSF and RSM) provide valuable information concerning the pre-treatment's efficiency. The CSF is a simple tool when comparing the acetone organosolv pre-treatment with other fractionation treatments. Whereas the RSM can depict the extent to which each of the independent variables contribute to the outcome.

Enzymatic digestibility is one of the most important parameters for the evaluation of the pre-treatment efficiency. The cellulose-to-glucose conversion of barley straw was significantly improved after acetone organosolv pre-treatment. Even under the mildest conditions, a 67% increase in C-to-G conversion was achieved. Based on the statistical data provided by the RSM (Table 6), changes in catalyst (H<sub>2</sub>SO<sub>4</sub>) concentration and temperature had a significant impact on cellulose conversion, which is in accordance with previous studies (Goh et al., 2011). However, at high temperature (T > 150 °C) SA addition had a negative effect on cellulose conversion. This could be attributed to glucose loss in the pulp (mostly to amorphous cellulose) resulting in more structured (crystalline) cellulose at severe conditions (high temperature acidic medium). Residual lignin content has been characterized as an inhibiting factor that influences enzymatic hydrolysis (Wildschut et al., 2013), which is in accordance with the findings from this study concerning mild and moderate pre-treatment conditions. Under severe conditions the negative effect of residual cellulose crystallinity prevailed despite lignin removal. Moreover, a number of parameters could also affect enzymatic hydrolysis. The most important are probably the inhibition due to the presence of xylan, xylose, and xylooligomers (Qing et al., 2010), high cellulose crystallinity, high degree of polymerization of cellulose, low accessible surface area, low swelling capacity and low cellulase adsorption (Hendriks et al., 2009).

According to the biorefinery concept, maximum xylose recovery was also important and thus one of the goals of the optimization of acetone organosolv pre-treatment. Using the combined severity factor (Table 6.13), the optimum conditions in terms of pentose recovery corresponded to a 0.61 < CSF < 1.25. Hemicellulose fraction, as derived from

Tables 6.14 and 6.15, appears to be the most reactive major biomass constituent with very small amounts of xylan traced after severe pre-treatment (Surek and Buyukkileci, 2017). Also, for the xylose recovery, SA concentration was found to be the most statistically important of the three parameters analyzed (Table 6.19).

## **6.2.6 Adsorption capacity**

The purpose at this point is to evaluate the acetone organosolv pretreated barley straw as a novel and low cost potential adsorbent for basic dye removal (i.e. Methylene Blue). The effect of the organosolv pretreatment conditions, i.e., catalyst concentration, reaction temperature and time, were investigated.

### **6.2.6.1 Adsorption kinetics**

Many kinetic models have been proposed to elucidate the mechanism of dye adsorption. The rate and mechanism of adsorption is controlled by various factors like physical and/ or chemical properties of sorbent in addition to mass transfer process. Thus, the experimental data of the kinetics of MB adsorption onto modified barley straw were interpreted with the pseudo-first-order and the pseudo-second-order kinetic models. However, these kinetic models are insufficient to fully identify the diffusion mechanisms involved in the adsorption process (Chen et al., 2010). Hence, the Weber-Morris intra-particle diffusion model was applied to further understand the intra-particle diffusion mechanisms.

The models were evaluated by the coefficient of determination factor ( $R^2$ ) and the Standard Error of Estimate (SEE), which measures the differences in the amount of dye taken up by the adsorbent predicted by the models and the actual  $q$  found experimentally. The calculated kinetic constants along with the coefficient of determination ( $R^2$ ) and Standard Error values (SEE) for each model are summarized in Tables 6.20 and 6.21.

**Table 6.20** Pseudo-first-order kinetic model parameters.

Experiment	$\log R_o^*$	$k_1$ ( $\text{min}^{-1}$ )	$q_e$ (mg/g)	$R^2$	SEE
1	-1.97	0.061	10.8	0.981	0.444
2	-1.37	0.069	10.1	0.961	0.575
3	-1.31	0.059	10.1	0.971	4.65
4	-0.82	0.054	9.29	0.966	0.514
5	-0.78	0.104	11.5	0.967	0.553
6	0.08	0.086	10.3	0.952	0.613
7	0.45	0.105	10.5	0.974	0.446
8	0.45	0.102	10.8	0.974	0.466
9	0.42	0.105	10.0	0.970	0.459
10	0.60	0.047	9.37	0.988	0.317
11	0.61	0.062	9.54	0.976	0.436
12	0.68	0.055	8.61	0.990	0.262
13	1.25	0.043	6.45	0.965	0.366
14	1.28	0.055	8.61	0.990	0.262
15	1.63	0.003	18.3	0.991	0.148
Untreated	(-)	0.045	8.21	0.980	0.353

By comparing the results presented in Tables 6.20 and 6.21 , it can be seen that the pseudo-second-order model has higher  $R^2$  values compared to those of the pseudo-first-order model, suggesting that the pseudo-second-order model is more accurate to understand the kinetics for the entirety of the process.

**Table 6.21** Pseudo-second-order kinetic model parameters.

<b>Experiment</b>	<b><math>\log R_o^*</math></b>	<b><math>k_2</math> (g mg<sup>-1</sup> min<sup>-1</sup>)</b>	<b><math>q_e</math> (mg/g)</b>	<b><math>R^2</math></b>	<b><i>SEE</i></b>
1	-1.97	0.006	12.8	0.997	0.154
2	-1.37	0.008	11.7	0.989	0.285
3	-1.31	0.006	11.9	0.993	0.242
4	-0.82	0.006	11.0	0.988	0.289
5	-0.78	0.012	12.7	0.996	0.188
6	0.08	0.011	11.6	0.988	0.293
7	0.45	0.014	11.7	0.998	0.118
8	0.45	0.013	12.0	0.997	0.156
9	0.42	0.014	11.1	0.995	0.175
10	0.60	0.004	11.5	0.996	0.164
11	0.61	0.007	11.2	0.995	0.185
12	0.68	0.015	11.4	0.991	0.252
13	1.25	0.006	8.0	0.981	0.252
14	1.28	0.006	10.3	0.997	0.142
15	1.63	0.00005	35.8	0.991	0.149
Untreated	(-)	0.005	10.1	0.992	0.217

In addition, the plots of MB adsorption versus contact time for selected experiments are shown in Figures 6.31, 6.32, 6.33 and 6.34. The materials were picked based on the pretreatments' severity factor ( i.e low, medium, high value) but also including the untreated barley straw. In all cases the adsorption was found to be quick at the first period of the process and then the rate of adsorption be slower and stagnates with the increase in contact time.

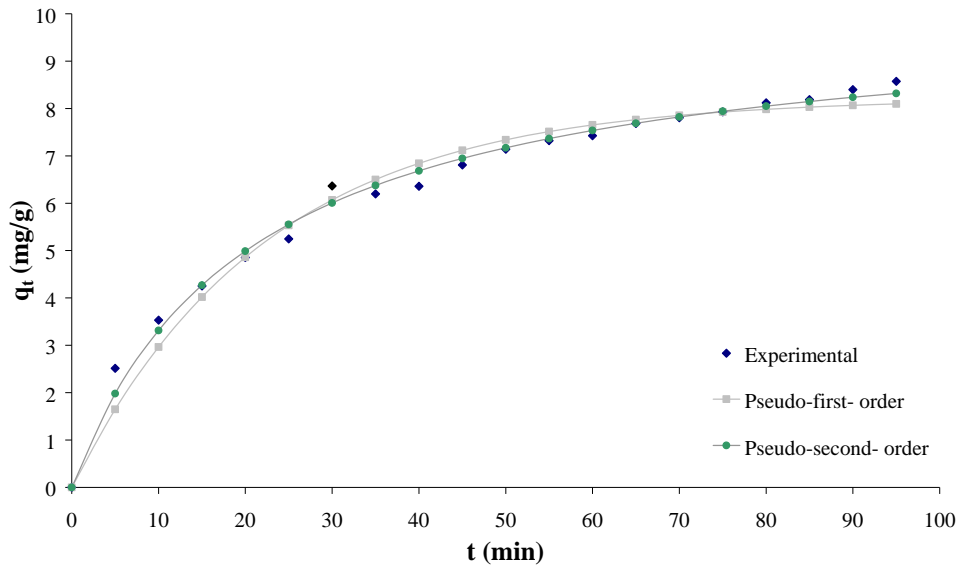


**Fig. 6.31** Curves of kinetic models for untreated barley straw.

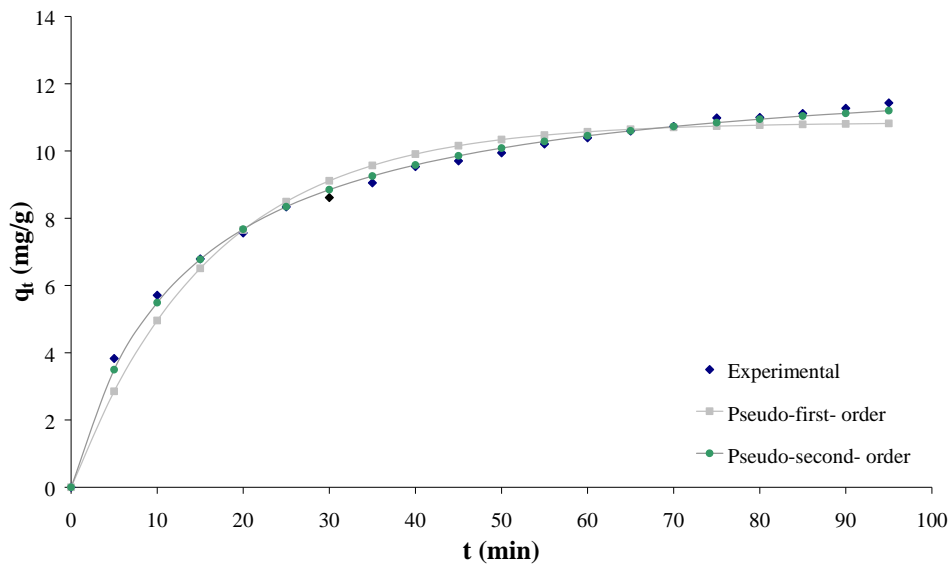


**Fig. 6.32** Curves of kinetic models for pretreated barley straw at 140 °C for 0 min with 10 mol/m<sup>3</sup> H<sub>2</sub>SO<sub>4</sub> (exp1).

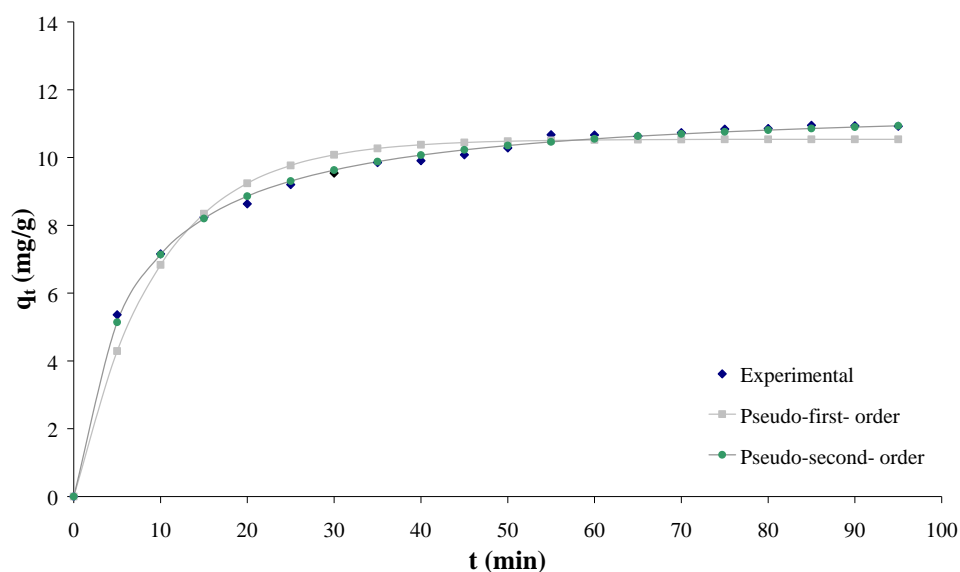


**Fig. 6.33** Curves of kinetic models for pretreated barley straw at 160 °C for 20 min with 23 mol/m<sup>3</sup> H<sub>2</sub>SO<sub>4</sub> (exp7).

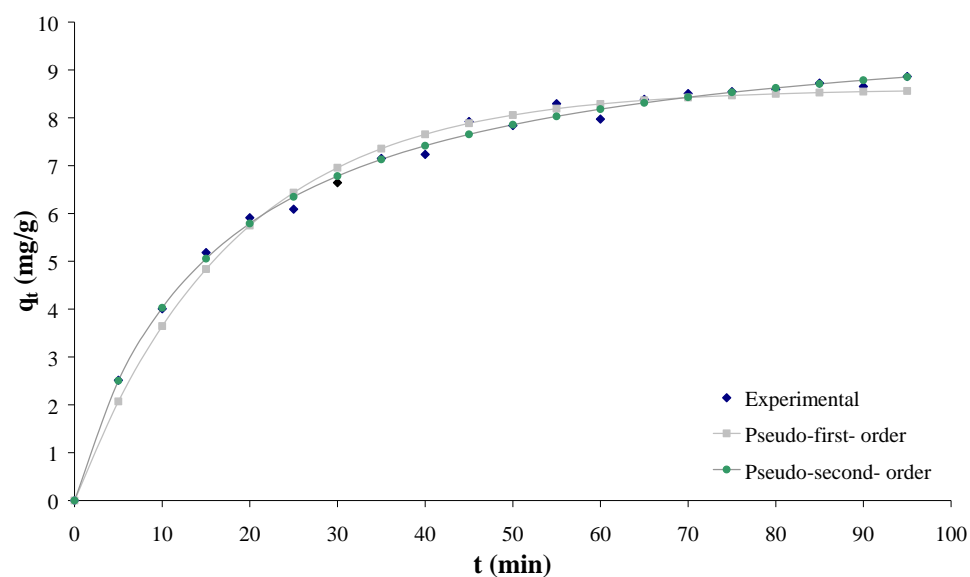


**Fig. 6.34** Curves of kinetic models for pretreated barley straw at 160 °C for 40 min with 35 mol/m<sup>3</sup> H<sub>2</sub>SO<sub>4</sub> (exp13).

Based on the  $R_i$  values presented in Table 6.22 it can be described the initial adsorption behaviour of the sorbent when the intra-particle diffusion model is applied. Almost all the pretreated materials together with the untreated barley straw belong to zone 2 (intermediate initial adsorption) with values  $0.5 < R_i < 0.9$ . The results are in agreement with previous

studies regarding adsorption on raw or modified materials (Cicek et al., 2007) but also with the results presented previously here (see 6.1.4.1).

**Table 6.22** Initial adsorption factor  $R_i$  and kinetic behavior based on the intra-particle diffusion model.

Experiment	$\log R_o^*$	C (mg/g)	$k_p$ ( $\text{mg g}^{-1} \text{min}^{-0.5}$ )	$R_i$	$R^2$	SEE
1	-1.97	2.07	1.06	0.819	0.929	0.795
2	-1.37	2.34	0.958	0.783	0.918	0.779
3	-1.31	1.88	0.992	0.826	0.942	0.667
4	-0.82	1.54	0.918	0.844	0.957	0.525
5	-0.78	3.82	0.983	0.682	0.820	1.25
6	0.08	2.92	0.931	0.737	0.878	0.942
7	0.45	3.56	0.893	0.674	0.807	1.19
8	0.45	3.59	0.925	0.680	0.812	1.21
9	0.42	3.38	0.854	0.679	0.810	1.12
10	0.60	1.09	0.954	0.887	0.961	0.520
11	0.61	1.86	0.928	0.815	0.930	0.689
12	0.68	3.56	0.877	0.674	0.819	1.12
13	1.25	0.63	0.657	0.906	0.976	0.277
14	1.28	1.35	0.861	0.848	0.928	0.650
15	1.63	0	0.427	1.0	0.938	0.575
Untreated	(-)	0.881	0.837	0.897	0.970	0.398

The Tables show that the three models give a good correlation to experimental data. However, the correlation coefficients for the pseudo-second-order kinetic model are closer to one than those of the Lagergren first order and the intra-particle model. Hence, the adsorption can be approximated more properly by the pseudo-second-order kinetic model. This result suggests that boundary layer resistance was not the rate limiting step (Ho and McKay, 1999). Similar modeling results are also found in the kinetic studies on sorption of Methylene Blue and Eriochrome Black T by *Scolymus hispanicus* L. (Barka et al., 2011), Brilliant Green by rice husk ash (Mane et al., 2007) and C.I Reactive Red 194 and C.I Reactive Blue 53 by cupuassu shell (Cardoso et al., 2010) .

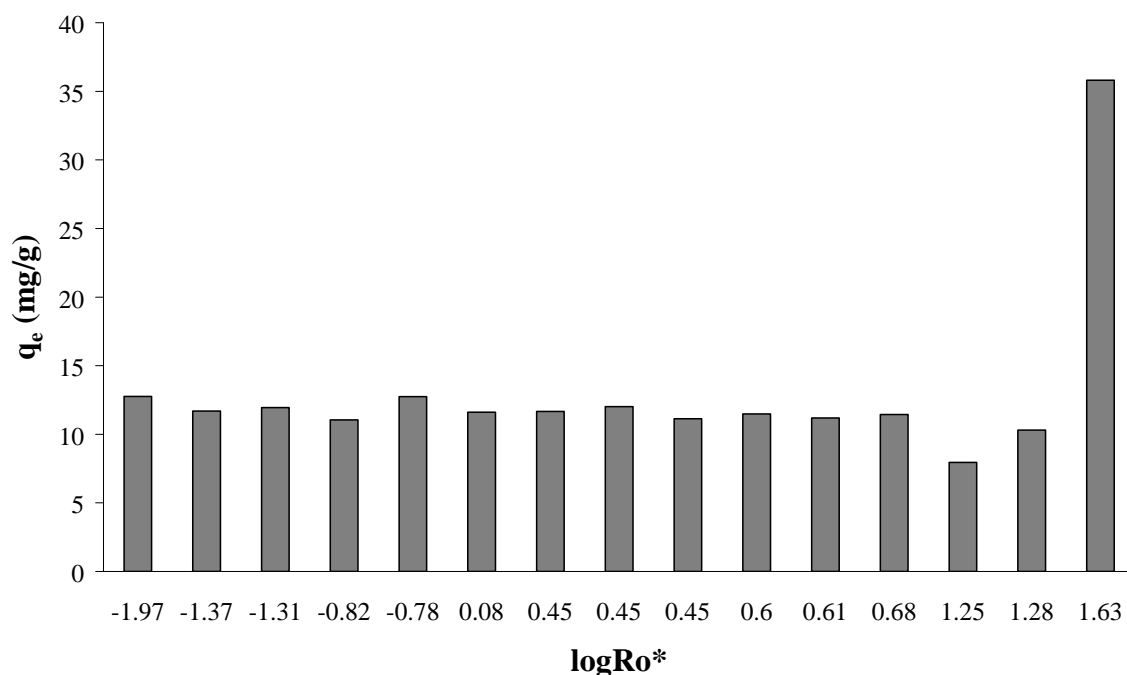


**Fig. 6.35** Kinetic parameter  $q_e$  according to the pseudo-second order model with respect to the CSF.

The effect of organosolv pretreatments' combined severity factors on the amount of dye adsorbed at equilibrium time ( $q_e$ ) is shown in Fig. 6.35. The highest  $q_e$  is to be found at the most severe pretreatment conditions ( $\log R_o^* = 1.63$ ) whereas for all other experiments  $q_e$  values are really close to each other and only slightly increased compared to the untreated barley straw.

### 6.2.6.2 Adsorption isotherm

As already mentioned, the adsorption isotherm is significant for the explanation of how the adsorbent will interact with the adsorbate and for the evaluation of the adsorption capacity. Since they play such an important role in understanding the mechanism of adsorption several isotherm models have been presented in literature over the years (Srinivasan and Viraraghavan, 2010). In this part the experimental data will be analysed using the Freundlich, Langmuir and Sips isotherm models. The models were also evaluated, as previously stated in the adsorption kinetic, by the coefficient of determination factor ( $R^2$ ) and the Standard Error of Estimate ( $SEE$ ).

Freundlich isotherm model is an empirical equation based on sorption on heterogeneous surface or surface supporting sites of varied affinities. Thus its two constants  $K_F$  is related to adsorption capacity and  $n$  is the heterogeneity factor. The Freundlich constants are given

in Table 7.12 along with the  $R^2$  and  $SEE$  values. The magnitude of  $n$  gives a measure of favourability of adsorption. The values of  $n$  between 1 and 10 (i.e.  $1/n$  less than 1) represents favourable and easy adsorption. According to Table 6.23 the  $1/n$  values in all experiments range from 0.36 to 0.80, thus indicating the adsorption as favourable, except from exp1, exp11, exp12 and exp13 where it is easy to adsorb.

**Table 6.23** Parameters of Freundlich isotherm model of MB adsorption on modified and untreated barley straw with regard to the CSF.

Experiment	$\log R_o^*$	$K_F ((\text{mg g}^{-1})(\text{L mg}^{-1})^{1/n})$	$n$	$R^2$	$SEE$
1	-1.97	3.85	1.81	0.974	2.84
2	-1.37	9.36	2.75	0.930	5.09
3	-1.31	8.02	2.76	0.961	3.09
4	-0.82	7.34	2.48	0.959	3.53
5	-0.78	2.66	2.12	0.980	1.28
6	0.08	4.77	2.23	0.974	2.08
7	0.45	3.26	2.12	0.975	1.88
8	0.45	3.26	2.12	0.976	1.91
9	0.45	3.21	2.10	0.971	2.02
10	0.6	4.41	2.65	0.980	1.35
11	0.61	1.85	1.80	0.997	0.51
12	0.68	1.92	1.90	0.951	1.98
13	1.25	1.53	1.24	0.981	2.78
14	1.28	2.89	2.15	0.966	1.62
15	1.63	2.56	2.23	0.953	1.75
Untreated	(-)	3.33	1.69	0.980	2.73

As shown in Table 6.24 the experimental data agreed well with the Langmuir isotherm model fitted relatively well to for both organosolv pretreated sorbents and untreated material  $R^2 > 0.964$ . The monolayer saturation capacities of pretreated wheat straw were found to vary significantly based on the organic solvent, but also the pretreatment's conditions (reaction time and temperature). The nature of the sorption was determined by the dimensionless separation factor  $R_L$ . As previously states (ch. 4.3.2), there are four possibilities for the  $R_L$  value:  $0 < R_L < 1$  favourable;  $R_L > 1$  unfavourable;  $R_L = 1$  linear,  $R_L$

= 0 irreversible. The values of  $R_L$  obtained in this study were between 0 and 1, indicating that the adsorption of MB onto modified but also untreated barley straw is favourable.

**Table 6.24** Parameters of Langmuir isotherm model of MB adsorption on modified and untreated barley straw with regard to the CSF.

Experimen t	$\log R_o^*$	$q_m$ (mg/g)	$K_L$ (L/mg)	$R^2$	SEE
1	-1.97	93.7	0.011	0.964	4.73
2	-1.37	50.6	0.117	0.991	1.73
3	-1.31	40.8	0.129	0.984	1.93
4	-0.82	48.1	0.083	0.987	1.96
5	-0.78	29.1	0.036	0.987	1.18
6	0.08	37.3	0.070	0.993	1.08
7	0.45	36.9	0.035	0.993	0.98
8	0.45	38.0	0.033	0.993	0.96
9	0.45	37.3	0.034	0.994	0.93
10	0.6	26.7	0.086	0.976	1.47
11	0.61	34.9	0.023	0.987	1.19
12	0.68	32.1	0.022	0.933	2.38
13	1.25	162	0.006	0.983	2.61
14	1.28	27.7	0.047	0.993	0.75
15	1.63	24.6	0.043	0.991	0.77
Untreated	(-)	66.8	0.024	0.982	2.57

Although the above isotherm models have been widely used for the adsorption of various pollutants from aqueous solutions these two equations are hard to simultaneously describe the adsorption data well. In this regard the combination of the Freundlich and Langmuir model known as the Sips model comes into prominence. The heterogeneity factor of  $n_s$  close to 0 displays heterogeneous sorbent (the Sips isotherm becomes Freundlich), while  $n_s$  close to or even 1 the Sips isotherm equation reduces to the Langmuir equation; that is, adsorption takes place on homogeneous surface. As derives from Table 6.25 and Figures 6.36, 6.37, 6.38, 6.39 in many cases the  $n_s$  values are really close to 1 revealing that the adsorption takes place on homogeneous surface (Chatterjee et al., 2010). The plots of  $q_e$

versus  $C_e$  for selected experiments are shown in Figures 6.36, 6.37, 6.38 and 6.39. The materials were picked based on the pretreatment's severity factor ( i.e low, medium, high value) but also including the untreated barley straw.

**Table 6.25** Parameters of Sips isotherm model of MB adsorption on modified wheat straw and untreated barley straw with regard to the CSF.

Experiment	$\log R_o^*$	$q_m$ (mg/g)	$K_S$ (L/mg)	$n_s$	$R^2$	SEE
1	-1.97	101	0.008	1.38	0.953	3.97
2	-1.37	50.3	0.119	0.985	0.991	1.82
3	-1.31	47.6	0.077	1.31	0.991	1.55
4	-0.82	52.2	0.065	1.15	0.988	1.94
5	-0.78	40.7	0.014	1.37	0.989	0.972
6	0.08	43.4	0.046	1.22	0.996	0.854
7	0.45	41.2	0.026	1.14	0.994	0.931
8	0.45	41.7	0.025	1.12	0.994	0.945
9	0.45	39.6	0.029	1.08	0.994	0.953
10	0.6	42.3	0.018	1.68	0.988	1.06
11	0.61	39.1	0.016	1.14	0.987	1.14
12	0.68	47.7	0.738	1.35	0.943	2.23
13	1.25	150.2	0.007	0.979	0.983	2.75
14	1.28	28.5	0.044	1.04	0.993	0.784
15	1.63	24.0	0.046	0.962	0.991	0.802
Untreated	(-)	66.9	0.024	1.05	0.982	2.65

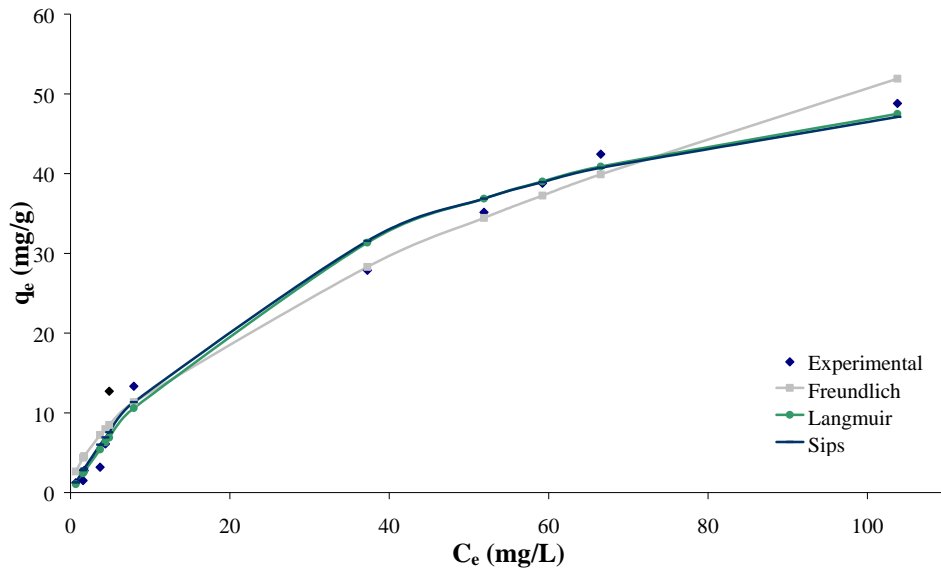


**Fig. 6.36** Plots for isotherm models for untreated barley straw.

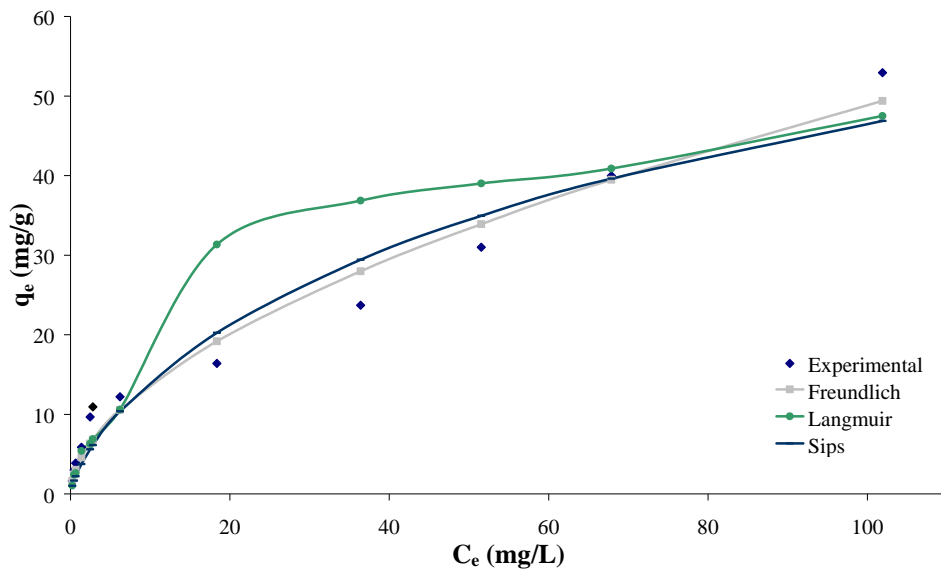


**Fig. 6.37** Plots for isotherm models for pretreated at 140 °C for 0 min with 10 mol/m<sup>3</sup> H<sub>2</sub>SO<sub>4</sub> (exp1) barley straw.

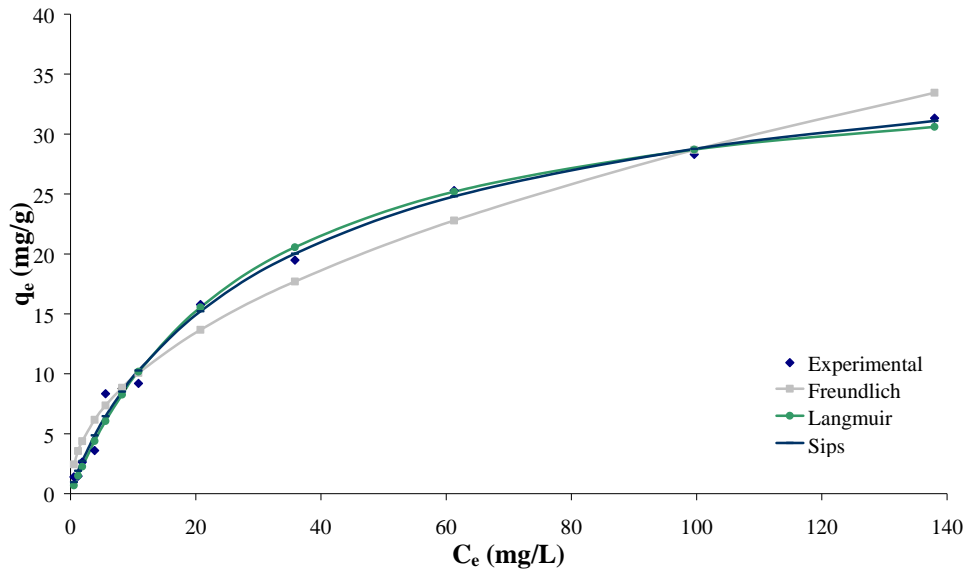


**Fig. 6.38** Plots for isotherm models for pretreated at 160 °C for 20 min with 23 mol/m<sup>3</sup> H<sub>2</sub>SO<sub>4</sub> (exp7) barley straw.

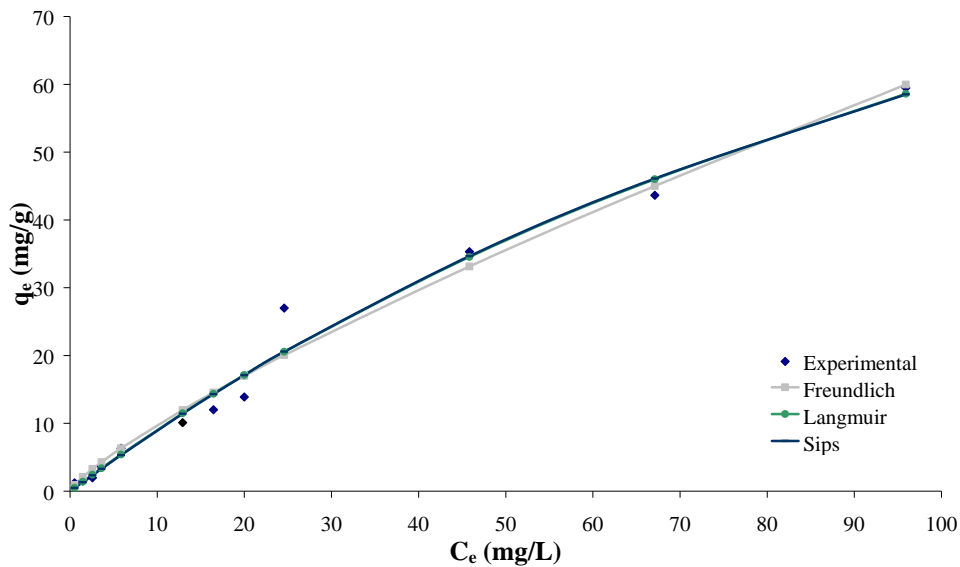


**Fig. 6.39** Plots for isotherm models for pretreated at 160 °C for 40 min with 35 mol/m<sup>3</sup> H<sub>2</sub>SO<sub>4</sub> (exp13) barley straw.

Based on the  $R^2$  and  $SEE$  values, the Sips model is the best isotherm model for the sorbents derived from the experimental processes presented herein. The Sips model showed in Table 7.14 presents the lowest  $SEE$  along with the highest  $R^2$  values, which means that the  $q$  fit by this isotherm model was closer to the  $q$  measured experimentally when compared with the other isotherm models.

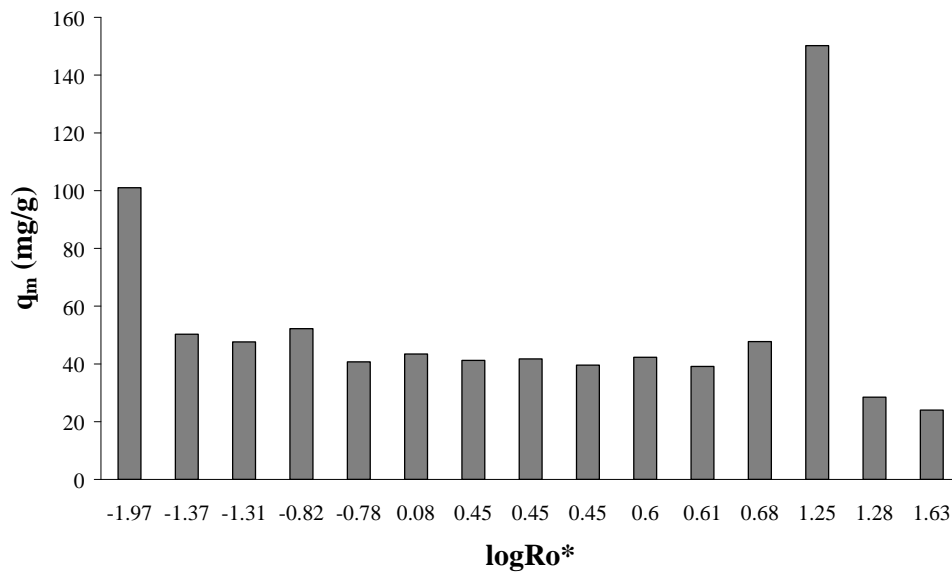


**Fig. 6.40** Sips plots for the adsorption of MB by acetone organosolv pretreated barley straw.

An overall comparison of the maximum adsorption capacity, according to the Sips model, is presented in Fig. 6.40. The maximum adsorption potentials of sorbent for MB were found after acetone organosolv pretreatment of barley straw at 160 °C for 40 min catalyzed by 35 mol/m<sup>3</sup> H<sub>2</sub>SO<sub>4</sub>. It should be noted that only some pretreatments have enhanced the adsorption capacity of barley straw.

## 7 Conclusions - Aspects for further research

### 7.1 Conclusions

Agricultural residues (wheat and barley straw) were used within the biorefinery concept. The organosolv pretreatment process was chosen for the efficient solubilisation or separation of its major constituents. Along with the production of fermentable sugars the co-production of adsorbent materials was investigated. The pretreated materials adsorption capacity was calculated and simulated based on the most commonly used models in literature. Ethanol, methanol and acetone were selected as the most commonly used solvents in literature, whereas butanol due to its rarity. Moreover, diethylene glycol a new organic solvent was introduced. Sulfuric acid served as catalyst for all the pretreatments.

In the case of wheat straw all five organic solvents were evaluated with regard to the effectiveness of the process, in terms of delignification, xylan hydrolysis and enzymatic digestibility. The pretreatments' temperatures were 160 °C and 180 °C, the reaction was carried out for 20 min and 40 min and the sulfuric acid concentration was 23 mol/m<sup>3</sup>.

Regardless the organic solvent ethanol concentration was increased significantly by the pretreatments. To be more precise, pretreatment conditions of 180 °C, 40 min and ethanol as solvent resulted in the highest ethanol concentration of 32.59 g L<sup>-1</sup>, which corresponded to 67.24% of the maximum theoretical yield (relating to glucose). It should be noted that the new organic solvent, introduced herein, diethylene glycol at a lower reaction temperature (160 °C) for 40 min also resulted in a high ethanol concentration of 29.75 gL<sup>-1</sup>, corresponded to 65.28% of theoretical yield with a significantly higher pulp yield (51.1%) than ethanol's (38.9%).

Based on the kinetic experiments the adsorbency of the pretreated material was increased. All three models (Lagergren, Pseudo-second and intra-particle) had good correlation with the experimental data. However, based on the SEE values, the pseudo-second-order kinetic model provided the best fit to the data for all modified wheat straw adsorbents. The two organosolv pretreatments that stood out were ethanol at 180 °C for 20 min and acetone at the same conditions.

Unlike kinetic adsorption experiments according to the isothermal experiments only some pretreatments have enhanced the adsorption capacity of wheat straw. The basic

difference lays in the duration of the experiments (kinetic experiments 120 min, isothermal 7 days). Thus it was observed that the pretreated materials, in most cases, could adsorb only as much for a short period of time. Nevertheless, when adsorbent materials are used for waste-water cleaning fast and no long-term adsorption is of most importance. According to the Sips model (which had the best fit), wheat straw pretreated with butanol or acetone at 180 °C for 20 min exhibited maximum adsorption capacity.

Although acetone organosolv pretreatment (in the previously mentioned conditions) resulted in moderate ethanol concentration, compared to ethanol pretreatment, it represents a very promising process. Its low price and boiling point, which facilitates recycle, render acetone very appealing among the other organic solvents. Thus acetone organosolv pretreatment conditions were simulated and optimized for the pretreatment of barley straw. The key variables selected were temperature (140–180 °C), residence time (0–40 min) and sulfuric acid concentration (10–35 mol/m<sup>3</sup>). The RSM based on a Box-Behnken experimental design and the CSF were the two approaches evaluated for the organosolv fractionation of barley straw and the enzymatic hydrolysis of the cellulosic residues data correlation. Moreover, the most significant parameters were identified to optimize the pretreatment to achieve the maximum total xylose in the liquid phase and cellulose-to-glucose conversion.

The RSM design of experiments was proved to be more accurate than the CSF approach. The ratio of cellulose-to-glucose conversion was higher when  $\log R_o^*$  was near to zero. Specifically, the optimal conditions for cellulose enzymatic digestibility were 140 °C, 0 min and 35 mol/m<sup>3</sup> ( $\log R_o^* = -0.02$ ), resulting in a 83.9% yield. Concerning the total xylose in the liquid phase, a higher yield was achieved at  $\log R_o^*$  values around 1. Maximum recovery was found to be 67.3% at 152 °C for 25 min and 35 mol/m<sup>3</sup> of SA ( $\log R_o^* = 0.78$ ). To reach the maximum values for both total xylose in the liquid phase and cellulose-to-glucose conversion a compromise was necessary. Considering that the formation of degradation products should be avoided, pretreatment with a CSF logarithm from 0.5 to 0.7 was chosen as the most suitable. Thus, pre-treatment at 140 °C for 20 min and a 35 mol/m<sup>3</sup> SA concentration ( $\log R_o^* = 0.6$ ) could provide not only high total xylose recovery (66.7%) but also important enzymatic digestibility (75.4%).

Similarly to the previously mentioned results acetone pretreated barley straw adsorption can also be approximated more properly by the pseudo-second-order kinetic model. The highest  $q_e$  was found at the most severe pretreatment conditions ( $\log R_o^* = 1.63$ ) whereas for all other experiments  $q_e$  values were really close to each other and only slightly increased

compared to the untreated barley straw. In all cases the adsorption was found to be quick at the first period of the process and then the rate of adsorption be slower and stagnates with the increase in contact time.

Finally, based on the isothermal experiments, maximum adsorption potentials of sorbent for MB were found after acetone organosolv pretreatment of barley straw at 160 °C for 40 min catalyzed by 35 mol/m<sup>3</sup> H<sub>2</sub>SO<sub>4</sub>. Just like in the previously described cases Sips isotherm model described the experimental data the best and only some pretreatments have enhanced the adsorption capacity of barley straw.

## 7.2 Aspects for further research

This study provided an approach for the efficient exploitation of lignocellulosic biomass within the biorefinery concept. However, some aspects might be investigated in future studies.

- The biorefinery concept relies on the complete utilization of most lignocellulosic biomass components. The organosolv pretreatment results into two fractions but the present study focuses mainly on the cellulose enriched solid fraction exploitation. Lignin could be isolated from the liquid fraction of the pretreatment and transform into high-value added products such as phenol, catechols and cresols by base-catalyzed depolymerization. Moreover, hemicellulosic sugars could also be obtained and subsequently treated, for example, by enzymatic hydrolysis to produce ethanol. The possibility to use the solid fraction for papermaking could be also explored.
- Other organic solvents like acetic acid, formic acid glycerol etc. could be used and their experimental results compared to these presented herein. It would be also beneficial to identify the most influential process parameters in order to optimize the process. Apart from temperature, reaction time and catalyst dose (examined herein) solvent concentration, particle size and liquid to solid ratio could be also investigated.
- Other lignocellulosic materials like cotton stalk, tree pruning, rice straw, sawdust etc. could be investigated by experimental measurements relevant to their possible usage for ethanol or adsorbent production

## References

- Adler, E., 1977. Lignin chemistry – past, present and future. *Wood Sci. Technol.* 11, 169–218.
- Agbor, V.B., Cicek, N., Sparling, R., Berlin, A., Levin, D.B., 2011. Biomass pretreatment: Fundamentals toward application. *Biotechnol. Adv.* 29, 675–685. doi:10.1016/j.biotechadv.2011.05.005
- Allen, S.G., Kam, L.C., Zemann, A.J., Antal Jr., M.J., 1996. Fractionation of sugar cane with hot, compressed, liquid water. *Industrial Engineering Chemistry Research* 35, 2709–2715.
- Amiri, H., Karimi, K., Zilouei, H., 2014. Organosolv pretreatment of rice straw for efficient acetone, butanol, and ethanol production. *Bioresour. Technol.* doi:10.1016/j.biortech.2013.11.038
- Anjum, M. F., Tasadduq, I., Al-Sultan, K., 1997. Response surface methodology: A neural network approach. *European Journal of Operational Research*, 101, 65–73.
- Annadurai, G., Juang, R.S., Lee, D.J., 2002. Use of cellulose-based wastes for adsorption of dyes from aqueous solutions. *J Hazard Mater* 92(3), 263–74.
- Antonopoulou, G., Vayenas, D., Lyberatos, G., 2016. Ethanol and hydrogen production from sunflower straw: The effect of pretreatment on the whole slurry fermentation. *Biochem. Eng. J.* 116, 65–74. doi:10.1016/j.bej.2016.06.014
- Araque, E., Parra, C., Freer, J., Contreras, D., Rodríguez, J., Mendonça, R., Baeza, J., 2008. Evaluation of organosolv pretreatment for the conversion of *Pinus radiata* D. Don to ethanol. *Enzyme Microb. Technol.* 43, 214–219. doi:10.1016/j.enzmictec.2007.08.006
- Astner, A.F., Young, T.M., Bozell, J.J., 2015. Lignin yield maximization of mixed biorefinery feedstocks by organosolv fractionation using Taguchi Robust Product Design. *Biomass and Bioenergy.* doi:10.1016/j.biombioe.2014.12.021

- Ayeni, A.O., Banerjee, S., Omoleye, J.A., Hymore, F.K., Giri, B.S., Deshmukh, S.C., Pandey, R.A., Mudliar, S.N., 2013. Optimization of pretreatment conditions using full factorial design and enzymatic convertibility of shea tree sawdust. *Biomass and Bioener.* 48, 130–138. doi:10.1016/j.biombioe.2012.10.021
- Badger, P.C., 2000. In: Jannick J., Whipsey A., editors. *Trends in new crops and new uses*. Alexandria, VA: ASHS Press, p.17-21.
- Banerjee, S., Mudaliar, S., Sen, R., Giri, B., Satupte, D., Chakrabarti, T., Pandey, R.A., 2010. Commercializing lignocellulosic bioethanol: technology bottlenecks and possible remedies. *Biofuels Bioprod. Bioref.* 4, 77-93
- Barakat, A., de Vries, H., Rouau, X., 2013. Dry fractionation process as an important step in current and future lignocellulose biorefineries: A review. *Bioresour. Technol.* doi:10.1016/j.biortech.2013.01.169
- Barka, N., Ouzaout, K., Abdennouri, M., Makhfouk, M. El, 2013. Dried prickly pear cactus (*Opuntia ficus indica*) cladodes as a low-cost and eco-friendly biosorbent for dyes removal from aqueous solutions. *J. Taiwan Inst. Chem. Eng.* 44, 52–60. doi:10.1016/j.jtice.2012.09.007.
- Ba , D., Boyacı, .H., 2007. Modeling and optimization I: Usability of response surface methodology. *J. Food Eng.* 78, 836–845. doi:10.1016/j.jfoodeng.2005.11.024
- Bera, A., Kumar, T., Ojha, K., Mandal, A., 2013. Applied Surface Science Adsorption of surfactants on sand surface in enhanced oil recovery: Isotherms, kinetics and thermodynamic studies. *Appl. Surf. Sci.* 284, 87–99. doi:10.1016/j.apsusc.2013.07.029.
- Bezerra, M.A., Santelli, R.E., Oliveira, E.P., Villar, L.S., Escalera, L.A., 2008. Response surface methodology (RSM) as a tool for optimization in analytical chemistry. *Talanta* 76, 965–977. doi:10.1016/j.talanta.2008.05.019
- Billa, E., Monties, B., 1991. Occurrence of silicon associated with lignin-polysaccharide complexes isolated from gramineae (wheat straw) cell walls. *Food Hydrocolloids* 5, 189–195

- Binod, P., Satyanagalakshmi, K., Sindhu, R., Janu, K.U., Sukumaran, R.K., Pandey, A., 2012. Short duration microwave assisted pretreatment enhances the enzymatic saccharification and fermentable sugar yield from sugarcane bagasse. *Renew Energy* 37, 109–116
- Bobleter, O., Binder, H., Concin, R., Burtscher, E., 1981. The conversion of biomass to fuel raw material by hydrothermal pretreatment. In: Palz, W., Chartier, P., Hall, D.O. (Eds.), *Energy from Biomass*. Applied Science Publishers, London, 554–562.
- Bobleter, O., Niesner, R., Rohr, M., 1976. The hydrothermal degradation of cellulosic matter to sugars and their fermentative conversion to protein. *Applied Polymer Science* 20, 2083–2093.
- Bouchard, J., Nguyen, T.S., Chornet, E., Overend, R.P., 1991. Analytical methodology for biomass pretreatment. Part 2: characterization of the filtrates and cumulative product distribution as a function of treatment severity. *Bioresource Technology* 36, 121–131
- Box, G.E.P., Behnken, D.W., 1960. *Technometrics* 2, 455.
- Box, G.E.P., Wilson, K.B., 1951 *J. R. Stat. Soc. B* 13, 1.
- Brandt, A., Gräsvik, J., Hallett, J.P., Welton, T., 2013. Deconstruction of lignocellulosic biomass with ionic liquids. *Green Chem.* 15 (3), 550–583.
- Brereton, R., 2003. *Chemometrics: Data Analysis for the Laboratory and Chemical Plant*, John Wiley & Sons, Chichester.
- Brosse, N., El Hage, R., Sannigrahi, P., Ragauskas, A., 2010. Dilute sulphuric acid and ethanol organosolv pretreatment of *Miscanthus x giganteus*. *Cell Chem Technol* 44(1–3):71–78
- Brosse, N., Sannigrahi, P., Ragauskas, A., 2009. Pretreatment of *Miscanthus x giganteus* using the ethanol organosolv process for ethanol production. *Ind Eng Chem Res* 48(18):8328–8334
- Bundhoo, Z.M.A., 2018. Microwave-assisted conversion of biomass and waste materials to biofuels. *Renew. Sustain. Energy Rev.* 82, 1149–1177. doi:10.1016/j.rser.2017.09.066

- Calvete, T., Lima, E.C., Cardoso, N.F., Vaghetti, J.C.P., Dias, S.L.P., Pavan, F.A., 2010. Application of carbon adsorbents prepared from Brazilian-pine fruit shell for the removal of reactive orange 16 from aqueous solution: kinetic, equilibrium, and thermodynamic studies. *J. Environ. Manage.* 91, 1695-1706.
- Cardoso, N.F., Lima, E.C., Pinto, I.S., Amavisca, C. V., Royer, B., Pinto, R.B., Alencar, W.S., Pereira, S.F.P., 2011. Application of cupuassu shell as biosorbent for the removal of textile dyes from aqueous solution. *J. Environ. Manage.* 92, 1237–1247. doi:10.1016/j.jenvman.2010.12.010
- Chatterjee, S., Lee, M.W., Woo, S.H, 2010. Adsorption of congo red by chitosan hydrogel beads impregnated with carbon nanotubes, *Bioresour. Technol.* 101 1800–1806.
- Chen, H., Zhao, J., Hu, T., Zhao, X., Liu, D., 2015. A comparison of several organosolv pretreatments for improving the enzymatic hydrolysis of wheat straw: Substrate digestibility, fermentability and structural features. *Appl. Energy* 150, 224–232. doi:10.1016/j.apenergy.2015.04.030
- Chen, H., Zhao, J., Hu, T., Zhao, X., Liu, D., 2015. A comparison of several organosolv pretreatments for improving the enzymatic hydrolysis of wheat straw: Substrate digestibility, fermentability and structural features. *Appl. Energy* 150, 224–232. doi:10.1016/j.apenergy.2015.04.030
- Chen, L., Li, J., Lu, M., Guo, X., Zhang, H., Han, L., 2016. Integrated chemical and multi-scale structural analyses for the processes of acid pretreatment and enzymatic hydrolysis of corn stover. *Carbohydr. Polym.* 141, 1–9. doi:10.1016/j.carbpol.2015.12.079
- Chen, S., Zhang, J., Zhang, C., Yue, Q., Li, Y., Li, C., 2010. Equilibrium and kinetic studies of methyl orange and methyl violet adsorption on activated carbon derived from *Phragmites australis*. *Desalination* 252, 149-156.
- Chen, W.H., Tu, Y.J., Sheen, H.K., 2011. Disruption of sugarcane bagasse lignocellulosic structure by means of dilute sulfuric acid pretreatment with microwave-assisted heating. *Appl Energy* 88, 2726–2734.

- Cheng, Y.S., Zheng, Y., Yu C.W., Dooley T.M., Jenkins B.M., VanderGheynst, J.S., 2010. Evaluation of high solids alkaline pretreatment of rice straw. *Appl Biochem Biotech* 162, 1768-1784.
- Chum, H. L., Johnson, D. K., Black, S., Baker, J., Grohmann, K., Sarkanen, K. V., Wallace, K., Schroeder, H. A., 1988. Organosolv Pre treatment for Enzymatic Hydrolysis of Poplars. I. Enzyme Hydrolysis of Cellulosic Residues. *Biotechnol. Bioeng.*, 31, 643-649.
- Chum, H.H., Johnson, D.K., Black, S.K., Overend, R.P., 1990. Pretreatment- catalyst effects and the combined severity parameter. *Appl. Biochem. Biotechnol.* 13, 24-25.
- Chum, H.L., Johnson, D.K., Black, S.K., 1990. Organosolv pretreatment for enzymic hydrolysis of poplars. 2. Catalyst effects and the combined severity parameter. *Ind. Eng. Chem. Res.* 29, 156–162. doi:10.1021/ie00098a003
- Coenen, G.J., Bakx, E.J., Verhoef, R.P., Schols, H.A., Voragen, AGJ, 2007. Identification of the connecting linkage between homo- or xylogalacturonan and rhamnogalacturonan type I. *Carbohydr Polymers* 70, 224-235.
- De Bhowmick, G., Sarmah, A.K., Sen, R., 2017. Lignocellulosic biorefinery as a model for sustainable development of biofuels and value added products. *Bioresour. Technol.* 0–1. doi:10.1016/j.biortech.2017.09.163
- Delgenes, J.P., Penaud, V., Moletta, R., 2002. Pretreatment for the enhancement of anaerobic digestion of solid waster chapter 8. In *Biomethanization of the organic fraction of municipal solid waste* IWA publishing, 201–28.
- Deniz, F., Ersali, E.T, 2016. Simultaneous bioremoval of two unsafe dyes from aqueous solution using a novel green composite biosorbent. *Microchem. Journ.* 128, 312-319.
- Ding, S.Y., Himmel, M.E., 2006. The maize primary cell wall microfibril: a new model derived from direct visualization. *J Agric Food Chem* 54, 597–606.
- Do, D.D, 1998. *Adsorption Analysis: Equilibria and Kinetics*. Imperial College Press, London.
- Doehlert, D.H. 1970. *Appl. Stat.* 19, 231.

- Dong, L., Wu, R., Zhao, X., Liu, D., 2017. Phenomenological modeling and evaluation of formic acid pretreatment of wheat straw with an extended combined severity factor for biomass fractionation and enzymatic saccharification to produce bioethanol. *J. Taiwan Inst. Chem. Eng.* 0, 1–10. doi:10.1016/j.jtice.2017.09.038
- Festucci-Buselli, R.A., Otoni, W.C., Joshi, C.P., 2007. Structure, organization, and functions of cellulose synthase complexes in higher plants. *Braz J Plant Physiol* 19, 1–13.
- FitzPatrick, M., Champagne, P., Cunningham, M.F., Whitney, R.A., 2010. A biorefinery processing perspective: Treatment of lignocellulosic materials for the production of value-added products. *Bioresour. Technol.* 101, 8915–8922. doi:10.1016/j.biortech.2010.06.125
- Fu, D., Mazza, G., 2011a. Optimization of processing conditions for the pretreatment of wheat straw using aqueous ionic liquid. *Bioresour Technol.* 102, 8003–8010.
- Fu, D., Mazza, G., 2011b. Aqueous ionic liquid pretreatment of straw. *Bioresour Technol.* 102, 7008–7011.
- Galbe, M., Zacchi, G., 2002. A review of the production of ethanol from softwood, *Appl. Microbiol. Biotechnol.* 59 618–628.
- Gilarranz, M.A., Oliet, M., Rodriguez, F., Tijero, J., 1999. Methanol-based pulping of *Eucalyptus globulus*. *Can J. Chem. Eng* 77(3), 515–521.
- Girio, F.M., Fonseca, C., Calvalheiro, F., Duarte, L.C., Marques, S., Bogel-Lukasik, R., 2010. Hemicellulose. *Bioresour. Technol.* 101, 4775-4800.
- Goh, C. S., Tan, H. T., Lee, K. T, Brosse, N., 2011. Evaluation and optimization of Organosolv pretreatment using combined severity factors and response surface methodology. *Biomass Bioener.* 35, 4025-4023.
- Goh, C. S., Tan, H. T., Lee, K. T, Brosse, N., 2011. Evaluation and optimization of Organosolv pretreatment using combined severity factors and response surface methodology. *Biomass Bioener.* 35, 4025-4023.
- Gupta, V.K., Suhas, 2009. Application of low-cost adsorbents for dye removal – A review. *J. Envir. Manag.* 90, 2313–2342.

- Ha, S.H., Mai, N.L., An, G., Koo, Y.-M., 2011. Microwave-assisted pretreatment of cellulose in ionic liquid for accelerated enzymatic hydrolysis. *Bioresour. Technol.* 102 (2), 1214–1219.
- Hameed, B., Ahmad, A., 2009. Batch adsorption of methylene blue from aqueous solution by garlic peel, an agricultural waste biomass. *J Hazard Mater* 164(2), 870–875.
- Hameed, B., Krishni, R., Sata, S., 2009. A novel agricultural waste adsorbent for the removal of cationic dye from aqueous solutions. *J Hazard Mater* 162(1), 305–311.
- Hendriks, A.T., Zeeman, G., 2009. Pretreatments to enhance the digestibility of lignocellulosic biomass. *Bioresour. Technol.* 100, 10-18.
- Himmel, M.E., Adney, W.S., Baker, J.O., Elander R., McMillan J.D, Nieves R.A, et al., 1997. Advanced bioethanol production technologies: a perspective. *Fuels Chem Biomass* 666, 2-45.
- Ho, Y.S., McKay, G., 1999. Pseudo-second-order model for sorption processes. *Process Biochem* 34, 451-65.
- Holzapple, M.T., Humphrey, A.E., 1984. The Effect of Organosolv Pre- treatment on the Enzymatic Hydrolysis of Poplars. *Biotechnol. Bioeng*, 28, 670-676.
- Hörmeyer, H., Tailliez, P., Millet, J., Girard, H., Bonn, G., Bobleter, O., Aubert, JP., 1988. Ethanol production by *Clostridium thermocellum* grown on hydrothermally and organosolv-pretreated lignocellulosic materials, *Appl. Microbiol. Biotechnol.* 29 (6) 528–535.
- Huijgen, W.J.J., Reith, J.H., den Uil, H., 2010. Pretreatment and fractionation of wheat straw by an acetone-based organosolv process. *Ind. Eng. Chem. Res* 49(20), 10132–10140.
- Ibrahim, M.M., El-Zawawy, W.K., Abdel-Fattah, Y.R., Soliman, N.A, Agblevor, F.A., 2011. Comparison of alkaline pulping with steam explosion for glucose production from rice straw. *Carbohydr Polym* 83,720-726.
- Ishii, T., Matsunaga, T., 2001. Pectic polysaccharide rhamnogalacturonan II is covalently linked to homogalacturonan. *Phytochemistry* 57, 969-974.

- Jeong, H., Jang, S.K., Hong, C.Y., Kim, S.H., Lee, S.Y., Lee, S.M., Choi, J.W., Choi, I.G., 2017. Levulinic acid production by two-step acid-catalyzed treatment of *Quercus mongolica* using dilute sulfuric acid. *Bioresour. Technol.* 225, 183–190. doi:10.1016/j.biortech.2016.11.063
- Jiménez, L., De La Torre, M.J., Bonilla, J.L., Ferrer, J.L., 1997. Organosolv pulping of wheat straw by use of acetone-water mixtures. *Process Biochem.* 33, 401-408.
- Johansson, A., Aaltonen, O., Ylinen, P., 1987. Organosolv pulping - methods and pulp properties. *Biomass.* doi:10.1016/0144-4565(87)90071-0
- Kabel, M.A., Bos, G., Zeevalking, J., Voragen, A.G.J., Schols, H.A., 2007. Effect of pretreatment severity on xylan solubility and enzymatic breakdown of the remaining cellulose from wheat straw. *Bioresour. Technol.* 98, 2034–2042. doi:10.1016/j.biortech.2006.08.006
- Kabir, M.M., Rajendran, K., Taherzadeh, M.J., Horváth, I., 2015. Experimental and economical evaluation of bioconversion of forest residues to biogas using organosolv pretreatment. *Bioresour. Technol.* doi:10.1016/j.biortech.2014.07.064
- Kamm, B.; Gruber, P.R.; Kamm, M., 2006. *Biorefineries – Industrial Processes and Products.* Wiley-VCH, ISBN: 3-527-31027-4, Weinheim, Germany.
- Karimi, K., Shafiei, M., Kumar, R., Karimi, K., Shafiei, Á.M., Kumar, R., Gupta, V.K., Tuohy, M.G., n.d. Progress in Physical and Chemical Pretreatment of Lignocellulosic Biomass. doi:10.1007/978-3-642-34519-7\_3
- Karr, W.E., Holtzapple, M.T., 2000. Using lime pretreatment to facilitate the enzymatic hydrolysis of corn stover. *Biomass Bioenergy* 18, 189–199.
- Kassim, M.A., Bhattacharya, S., 2016. Dilute alkaline pretreatment for reducing sugar production from *Tetraselmis suecica* and *Chlorella* sp. biomass. *Process Biochem.* 51, 1757–1766. doi:10.1016/j.procbio.2015.11.027
- Kaur, D., Bhardwaj, N.K., Lohchab, R.K., 2017. Prospects of rice straw as a raw material for paper making. *Waste Manag.* 60, 127–139. doi:10.1016/j.wasman.2016.08.001

- Kim, S., Holtzapfle, M.T., 2005. Lime pretreatment and enzymatic hydrolysis of corn stover. *Bioresour. Technol.* 96, 1994–2006.
- Kim, T.H., Kim, J.S., Sunwoo, C., Lee, Y.Y., 2003. Pretreatment of corn stover by aqueous ammonia. *Bioresour. Technol.* 90, 39–47
- Kim, Y., Mosier, N.S., Ladisch, M.R., 2009. Enzymatic digestion of liquid hot water pretreated hybrid poplar. *Biotechnol Progr* 25, 340-348.
- Klason, P., 1893. Bidrag till kannedomen om sammansattningen af granens ved samt de kemiska processerna vid framställning af cellulosa darur. *Teknisk Tidskrift, Afdelningen for Kemi och Metallurgi* 23(2):17–22.
- Kumar, P., Barrett, D.M., Delwiche, M.J., Stroeve, P., 2009. Methods for pretreatment of lignocellulosic biomass for efficient hydrolysis and biofuel production. *Ind Eng Chem Res* 48, 37-39.
- Lagergren S., 1898. Zur theorie der sogenannten adsorption gelöster stoffe. *Kungliga Svenska Vetenskapsakademiens, Handlingar*, 24, 1-39.
- Laghari, S.M., Isa, M.H., Laghari, A.J., 2016. Delignification of palm fiber by microwave assisted chemical pretreatment for improving energy efficiency. *Malays J Sci* 35, 8–14.
- Laure, S., Leschinsky, M., Fröhling, M., Schultmann, F., Unkelbach, G., 2014. Assessment of an Organosolv Lignocellulose Biorefinery Concept Based on a Material Flow Analysis of a Pilot Plant. *Cellul. Chem. Technol.* 48, 793–798.
- Lee, C., Zheng, Y., VanderGheynst, J.S., 2015. Effects of pretreatment conditions and post-pretreatment washing on ethanol production from dilute acid pretreated rice straw. *Biosyst. Eng.* 137, 36–42. doi:10.1016/j.biosystemseng.2015.07.001
- Lee, J.H., Brown, R.M., Kuga, S., Shoda, S., Kobayashi, S., 1994. Assembly of synthetic cellulose I. *Proc Natl Acad Sci USA* 91, 7425–7429
- Li, C., Knierim, B., Manisseri, C., Arora, R., Scheller, H.V., Auer, M., Vogel, K.P., Simmons, B.A., Singh, S., 2010. Comparison of dilute acid and ionic liquid pretreatment of switchgrass: biomass recalcitrance, delignification and enzymatic saccharification. *Bioresour Technol* 101, 4900–4906.

- Ligero, P., Villauerde, J.J., de Vega, A., Bao, M., 2008. Delignification of *Eucalyptus globulus* saplings in two organosolv systems (formic and acetic acid) preliminary analysis of dissolved lignins. *Ind. Crop Prod* 27(1):110–117. doi:10.1016/j.indcrop.2007.08.008
- Limayem, A., Ricke, S.C., 2012. Lignocellulosic biomass for bioethanol production: Current perspectives, potential issues and future prospects. *Progress in Energ. Combust. Schien.* 38, 449-467.
- Liu, C.-G., Qin, J.-C., Liu, L.-Y., Jin, B.-W., Bai, F.-W., 2016. Combination of ionic liquid and instant catapult steam explosion pretreatments for enhanced enzymatic digestibility of rice straw. *ACS Sustainable Chem. Eng.* 4, 577–582.
- Liu, C.Z., Cheng, X.Y., 2010. Improved hydrogen production via thermophilic fermentation of corn stover by microwave-assisted acid pretreatment. *Int J Hydrog Energy* 35, 8945–8952.
- Lopez, F., Garcia, J.C., Perez, A., Garcia, M.M., Feria, M.J., Tapias, R., 2010. *Leucaena diversifolia* a new raw material for paper production by soda-ethanol pulping process. *Chem Eng Res Des* 88 (1A),1–9. doi:10.1016/j.cherd.2009.06.016
- Lopez, F., Perez, A., Garcia, J.C., Feria, M.J., Garcia, M.M., Fernandez, M., 2011. Cellulosic pulp from *Leucaena diversifolia* by soda-ethanol pulping process. *Chem Eng J* 166(1):22–29. doi:10.1016/j.cej.2010.08.039
- Lynd, L.R., Elander, R.T., Wyman, C.E., 1996. Likely features and costs of mature biomass ethanol technology. *Applied Biochemistry and Biotechnology* 57/58, 741–761.
- Mane, V. S., I. D. Mall, and V. C. Srivastava, 2007. Kinetic and Equilibrium Isotherm Studies for the Adsorptive Removal of Brilliant Green Dye from Aqueous Solution by Rice Husk Ash,. *J. Environ. Manage.*, 84, 390.
- McIntosh, S., Vancov, T., 2010. Enhanced enzyme saccharification of *Sorghum bicolor* straw using dilute alkali pretreatment. *Bioresour Technol* 101, 6718-6727.
- McKay G, Blair H.S, GARDNER J., 1983. The adsorption of dyes in chitin. III. Intraparticle diffusion processes. *J. Appl. Polym. Sci*, 28, 1767.

- Menon, V., Rao, M., 2012. Trends in bioconversion of lignocellulose: Biofuels, platform chemicals & biorefinery concept. *Prog. Energy Combust. Sci.* 38, 522–550. doi:10.1016/j.peecs.2012.02.002
- Mesa, L., Gonzalez, E., Ruiz, E., Romero, I., Cara, C., Felissia, F., Castro, E., 2010. Preliminary evaluation of organosolv pre-treatment of sugar cane bagasse for glucose production: application of 23 experimental design. *Appl. Energ.* 87(1), 109–114.
- Mesa, L., Gonzalez, E., Ruiz, E., Romero, I., Cara, C., Felissia, F., Castro, E., 2010. Preliminary evaluation of organosolv pre-treatment of sugar cane bagasse for glucose production: application of 23 experimental design. *Appl. Energ.* 87(1):109–114. doi:10.1016/j.apenergy.2009.07.016
- Mielenz J.R., 2001. Ethanol production from biomass: technology and commercialization status. *Curr. Opin. Microbiol.* 4, 324–325.
- Miller, G. L., 1959. Use of Dinitrosalicylic Acid Reagent for Determination of Reducing Sugar, *Anal. Chem.* 31, 426–428.
- Mok, W.S.-L., Antal Jr., M.J., 1992. Uncatalyzed solvolysis of whole biomass hemicellulose by hot compressed liquid water. *Industrial Engineering Chemistry Research* 31, 1157–1161.
- Mok, W.S.-L., Antal Jr., M.J., 1994. Biomass fractionation by hot compressed liquid water. In: Bridgewater, A.V. (Ed.), *Advances in Thermochemical Biomass Conversion*, vol. 2. Blackie Academic & Professional Publishers, New York, pp. 1572–1582.
- Monrroy, M., Ibanez, J., Melin, V., Baeza, J., Mendonca, R.T., Contreras, D., Freer, J., 2010. Bioorganosolv pretreatments of *P. radiata* by a brown rot fungus (*Gloephyllum trabeum*) and ethanolysis. *Enzyme Microb Technol* 47(1–2):11–16. doi:10.1016/j.enzmictec.2010.01.009
- Moral, A., Aguado, R., Mutjé, P., Tijero, A., 2016. Papermaking potential of *Citrus sinensis* trimmings using organosolv pulping, chlorine-free bleaching and refining. *J. Clean. Prod.* 112, 980–986. doi:10.1016/j.jclepro.2015.09.008

- Mou, H., Wu, S., 2016. Comparison of organosolv and hydrotropic pretreatments of eucalyptus for enhancing enzymatic saccharification. *Bioresour. Technol.* 220, 637–640. doi:10.1016/j.biortech.2016.08.072
- Mupondwa, E., Li, X., Tabil, L., Sokhansanj, S., Adapa, P., 2017. Status of Canada's lignocellulosic ethanol: Part I: Pretreatment technologies. *Renew. Sustain. Energy Rev.* 72, 178–190. doi:10.1016/j.rser.2017.01.039
- Myers, R. H., Montgomery, D. C., 1995. *Response surface methodology: Process and product optimization using designed experiments*. New York: John Wiley & Sons, Inc.
- Myers, R.H., Montgomery, D.C., 2009 *Response Surface Methodology: Process and Product Optimization Using Designed Experiments (Wiley Series in Probability and Statistics)*, Wiley, New York.
- Nakamura, A., Furuta, H., Maeda, H., Takao, T., Nagamatsu, Y., 2002. Structural studies by stepwise enzymatic degradation of the main backbone of soybean soluble polysaccharides consisting of galacturonan and rhamnogalacturonan. *Biosci Biotechnol Biochem* 66, 1301-1313.
- Nakamura, A., Furuta, H., Maeda, H., Takao, T., Nagamatsu, Y., 2002b. Analysis of the molecular construction of xylogalacturonan isolated from soluble soybean polysaccharides. *Biosci. Biotechnol. Biochem.* 66:1155-1158.
- Nguyen, T.-A.D., Kim, K.-R., Han, S.J., Cho, H.Y., Kim, J.W., Park, S.M., Park, J.C., Sim, S.J., 2010. Pretreatment of rice straw with ammonia and ionic liquid for lignocellulose conversion to fermentable sugars. *Bioresour. Technol.* 101 (19), 7432–7438
- Norman, A.G., 1934. The biological decomposition of plant materials: part IX. The anaerobic decomposition of hemicelluloses. *Ann Appl Biol* 21, 454–475.
- O'Neill, M., Albersheim, P., Darvill, A., 1990. The pectic polysaccharides of primary cell walls P.M. Dey (Ed.), *Methods in Plant Biochemistry*, 2, Academic Press, London, pp. 415-441
- Ogunsile, B.O., Quintana, G.C., 2010. Modeling of soda: ethanol pulps from *Carpolobia lutea*. *Bioresources* 5(4):2417–2430.

- tt, ., Spurlin, H.M., Grafflin, M.W., 1956. Cellulose and cellulose derivatives. Part I. 2nd edn. Interscience Publishers, New York.
- Overend, R.P., Chornet, E., 1987. Fractionation of lignocellulosics by steam-aqueous pretreatments. *Phil. Trans. R. Soc. London, ser. A* 321, 523-536.
- Palmqvist, E., Hahn-Hägerdal, B., 2000. Fermentation of lignocellulosic hydrolysates. I: inhibition and detoxification. *Bioresour Technol* 74, 17–24.
- Pan, X., Xie, D., Yu, R.W., Saddler, J.N., 2007. Pretreatment of lodgepole pine killed by mountain pine beetle using the ethanol organosolv process: fractionation and process optimization. *Ind. Engin. Chem. Res.* 46 (8), 2609-2617.
- Pan, X.J., Gilkes, N., Kadla, J., Pye, K., Saka, S., Gregg, D., Ehara, K., Xie, D., Lam, D., Saddler, J., 2006. Bioconversion of hybrid poplar to ethanol and co-products using an organosolv fractionation process: optimization of process yields. *Biotechnol Bioeng* 94(5), 851–861. doi:10.1002/Bit.20905
- Pan, X.J., Xie, D., Yu, R.W., Saddler, J.N., 2008. The bioconversion of mountain pine beetle-killed lodgepole pine to fuel ethanol using the organosolv process. *Biotechnol Bioeng* 101(1):39–48. doi:10.1002/Bit.21883
- Park, N., Kim, H.Y., Koo, B.W., Yeo, H., Choi, I.G., 2010. Organosolv pretreatment with various catalysts for enhancing enzymatic hydrolysis of pitch pine (*Pinus rigida*). *Bioresour. Technol.* doi:10.1016/j.biortech.2010.04.020
- Pauly, H., 1918. Aktiengesellschaft für Zellstoff- und Papierfabrikation in Aschaffenburg, assignee. Verfahren zur Gewinnung der das sogenannte Lignin bildenden Stoffe aus Holzarten. German Patent 309551.
- Peng, F., Peng, P., Xu, F., Sun, R.C., 2012. Fractional purification and bioconversion of hemicelluloses. *Biotechnol Adv.* doi:10.1016/j.biotechadv.2012.01.018
- Pérez, S., Samain, D., 2010. Structure and engineering of celluloses. In: Derek H (ed) *Advances in carbohydrate chemistry and biochemistry*, vol 64. Academic Press, New York, pp 25–116.

- Pettersen, R.C., 1984. The chemical composition of wood. In: Rowell RM, editor. The chemistry of solid wood. Advances in chemistry series, vol. 207. Washington, DC: American Chemistry Society, p.115-116.
- Popper, Z.A., Fry, S.C., 2007. Xyloglucan–pectin linkages are formed intraprotoplasmically, contribute to wall-assembly, and remain stable in the cell wall. *Planta* 227, 781-794.
- Procentese, A., Raganati, F., Olivieri, G., Elena Russo, M., Marzocchella, A., 2017. Pretreatment and enzymatic hydrolysis of lettuce residues as feedstock for bio-butanol production. *Biomass and Bioenergy* 96, 172–179. doi:10.1016/j.biombioe.2016.11.015
- Qing, Q., Guo, Q., Zhou, L., Gao, X., Lu, X., Zhang, Y., 2017. Comparison of alkaline and acid pretreatments for enzymatic hydrolysis of soybean hull and soybean straw to produce fermentable sugars. *Ind. Crops Prod.* 109, 391–397. doi:10.1016/j.indcrop.2017.08.051
- Qureshi, A.S., Zhang, J., Bao, J., 2015. High ethanol fermentation performance of the dry dilute acid pretreated corn stover by an evolutionarily adapted *Saccharomyces cerevisiae* strain. *Bioresour. Technol.* 189, 399–404. doi:10.1016/j.biortech.2015.04.025
- Rabemanolontsoa, H., Saka, S., 2016. Various pretreatments of lignocellulosics. *Bioresour. Technol.* doi:10.1016/j.biortech.2015.08.029
- Redlich, O., Peterson, DL., 1959. A useful adsorption isotherm. *J. Phys. Chem.* 63, 1024–1026.
- Reisinger, M., Tirpanalan, Ö., Huber, F., Kneifel, W., Novalin, S., 2014. Investigations on a wheat bran biorefinery involving organosolv fractionation and enzymatic treatment. *Bioresour. Technol.* doi:10.1016/j.biortech.2014.07.068
- Ridley, B.L., O'Neill, M.A., Mohnen D., 2001. Pectins: structure, biosynthesis, and oligogalacturonide-related signalling. *Phytochemistry* 57, pp. 929-967.
- Rodriguez, A., Jimenez, L., 2008. Pulping with organic solvents other than alcohols. *Afinidad* 65(535), 188–196.

- Royer, B., Cardoso, N.F., Lima, E.C., Vaghetti, J.C.P., Simon, N.M., Calvete, T., Veses, R.C., 2009. Applications of Brazilian pine-fruit shell in natural and carbonized forms as adsorbents to removal of methylene blue from aqueous solutions-Kinetic and equilibrium study. *J. Hazard. Mater.* 164, 1213–1222. doi:10.1016/j.jhazmat.2008.09.028
- S. Vieira, R. Hoffman, *Estatística Experimental*, Atlas, São Paulo, 1989.
- Saeed, A., Sharif, M., Iqbal, M., 2010. Application potential of grapefruit peel as dye sorbent: kinetics, equilibrium and mechanism of crystal violet adsorption. *J Hazard Mater* 179(1), 564–72.
- Samiey, B., Dargahi, M., 2010. Kinetics and thermodynamics of adsorption of Congo red on cellulose, *Central Eur. J. Chem.* 8, 906–912.
- Sánchez, C., 2009. Lignocellulosic residues: biodegradation and bioconversion by fungi. *Biotechnol Adv* 27,185–194.
- Sapci, Z., 2013. The effect of microwave pretreatment on biogas production from agricultural straws. *Bioresour Technol* 128, 487–494.
- Seidl, P.R., Goulart, A.K., 2016. Pretreatment processes for lignocellulosic biomass conversion to biofuels and bioproducts. *Curr. Opin. Green Sustain. Chem.* 2, 48–53. doi:10.1016/j.cogsc.2016.09.003
- Sharma, P., Saika, B.K., Das, M.R., 2014. Removal of methyl green dye molecule from aqueous system using reduced graphene oxide as an efficient adsorbent: kinetics, isotherm and thermodynamic parameters. *Colloids Surf. A Physicochem. Eng. Asp.* 457, 125-133.
- Sidiras, D., Batzias, F., Ranjan, R., Tsapatsis, M., 2011. Simulation and optimization of batch autohydrolysis of wheat straw to monosaccharides and oligosaccharides. *Bioresour. Technol.* 102, 10486–10492. doi:10.1016/j.biortech.2011.08.059
- Sidiras, D., Koukios, E., 2004. Simulation of acid catalysed organosolv fractionation of wheat straw. *Bioresour. Technol.* 94(1), 91-98.

- Sills, D.L., Gossett, J.M., 2011. Assessment of commercial hemicellulases for saccharification of alkaline pretreated perennial biomass. *Bioresour Technol*; 102, 1389-1398.
- Sindhu, R., Binod, P., Pandey, A., 2016. Biological pretreatment of lignocellulosic biomass - An overview. *Bioresour. Technol.* 199, 76–82. doi:10.1016/j.biortech.2015.08.030
- Sips, R., 1948. On the structure of a catalyst surface. *J. Chem. Phys.* 16, 490-495.
- Sluiter, A., Hames, B., Ruiz, R., Scarlata, C., Sluiter, J., Templeton, D., Crocker, D., 2008. Determination of Structural Carbohydrates and Lignin in Biomass, Laboratory Analytical Procedure (LAP), NREL/TP-510-42618, National Renewable Energy Laboratory, Golden, Colorado.
- Snelders, J., Dornez, E., Benjelloun- Mlayah, B., Huijgen, W.J.J., de Wild, P.J., Gosselink, R. J.A., Gerritsma, J., Courtin, C. M., 2014. Biorefining of wheat straw using an acetic and formic acid based organosolv fractionation process. *Bioresour. Technol.* 156, 275-282.
- Srinivasan, A., Viraraghavan, T., 2010. Decolorization of dye wastewaters by biosorbents: A review. *J. Environ. Manage.* 91, 1915–1929. doi:10.1016/j.jenvman.2010.05.003
- Stephen, J.D., Mabee, W.E., Saddler, J.N., 2012. Will second-generation ethanol be able to compete with first-generation ethanol? Opportunities for cost reduction. *Biofuels Bioprod Bioref* 6, 159–76.
- Sun, F.F., Wang, L., Ren, J., Du, F., Hu, J., Zhang, Z., Zhou, B., 2015. The impact of glycerol organosolv pretreatment on the chemistry and enzymatic hydrolyzability of wheat straw. *Bioresour. Technol.* 187, 354-361.
- Sun, J., Dutta, T., Parthasarathi, R., Kim, K.H., Tolic, N., Chu, R.K., Isern, N.G., Cort, J.R., Simmons, B.A., Singh, S., 2016. Rapid room temperature solubilization and depolymerization of polymeric lignin at high loadings. *Green Chem.* 18 (22), 6012–6020.
- Sun, Y., Cheng, J., 2002. Hydrolysis of lignocellulosic materials for ethanol production: a review. *Bioresour Technol* 83, 1–11.

- Swatloski, R.P., Spear, S.K., Holbrey, J.D., 2002. Rogers RD. Ionic liquids: new solvents for nonderivitized cellulose dissolution. *Abstr Pap Am Chem Soc*, 224:U622.
- Taherzadeh, M.J., Karimi, K., 2007. Acid-based hydrolysis processes for ethanol from lignocellulosic materials: a review. *BioResources* 2, 472-499.
- Taherzadeh, M.J., Karimi, K., 2008. Pretreatment of lignocellulosic wastes to improve ethanol and biogas production: A review. *Int J Mol Sci* 9,1621–1651.
- Talebnia, F., Karakashev, D., Angelidaki, I., 2010. Production of bioethanol from wheat straw: An overview on pretreatment, hydrolysis and fermentation, *Bioresour. Technol.* 101, 4744–4753.
- Temkin, M.J., Pyzhev, V., 1940. Kinetics of ammonia synthesis on promoted iron catalysts. *Acta Physiochim URSS* 12, 217–22.
- Teramoto, Y., Lee, S.H., Endo, T., 2008. Pretreatment of woody and herbaceous biomass for enzymatic saccharification using sulfuric acid-free ethanol cooking. *Bioresour Technol* 99(18), 8856–8863. doi:10.1016/j.biortech.2008.04.049
- Teymouri, F., Perez, L.L., Alizadeh. H., Dale, B.E., 2004. Ammonia fiber explosion treatment of corn stover. *Appl Biochem Biotechnol* 116, 951-963.
- Thring, R.W., Chornet, E., Overend, R., 1990. Recovery of a solvolytic lignin: effects of spent liquor/acid volume ratio, acid concentrated and temperature. *Biomass* 23, 289–305.
- Toledano, A., Alegría, I., Labidi, J., 2013. Biorefining of olive tree (*Olea europea*) pruning. *Biomass Bioener.* 35, 503-504.
- Th, J., 1971. State equations of the solid–gas interface layers. *Acta Chem Acad Sci. Hung* 69, 311–28.
- Uju, Shoda Y, Nakamoto A, Goto M, Tokuhara W, Noritake Y, Katahira, S., Nobuhiro, I., Kazunori, N., Chioki, O., Noriho, K., 2012. Short time ionic liquids pretreatment on lignocellulosic biomass to enhance enzymatic saccharification. *Bioresour Technol.* 103, 446–452.

- Vadivelan, V., Kumar, K.V., 2005. Equilibrium, kinetics, mechanism, and process design for the sorption of methylene blue onto rice husk. *J Colloid Interface Sci* 286(1), 90–100
- Vaghetti, J.C.P., Lima, E.C., Royer, B., Brasil, J.L., da Cunha, B.M., Simon, N.M., Cardoso, N.F., Noreña, C.P.Z., 2008. Application of Brazilian-pine fruit coat as a biosorbent to removal of Cr(VI) from aqueous solution. Kinetics and equilibrium study. *Biochem. Eng. J.* 42, 67-76.
- Vaghetti, J.C.P., Lima, E.C., Royer, B., da Cunha, B.M., Cardoso, N.F., Brasil, J.L., Dias, S.L.P., 2009. Pecan nutshell as biosorbent to remove Cu(II), Mn(II) and Pb (II) from aqueous solutions. *J. Hazard. Mater.* 162, 270-280.
- Vera Candiotti, L., De Zan, M.M., Cámara, M.S., Goicoechea, H.C., 2014. Experimental design and multiple response optimization. Using the desirability function in analytical methods development. *Talanta* 124, 123–138. doi:10.1016/j.talanta.2014.01.034
- Wahlström, R., Suurnäkki, A., 2015. Enzymatic hydrolysis of lignocellulosic polysaccharides in the presence of ionic liquids. *Green Chem.* 17 (2), 694–714.
- Wang, H., Wang, J., Fang, Z., Wang, X., Bu, H., 2010. Enhanced bio-hydrogen production by anaerobic fermentation of apple pomace with enzyme hydrolysis. *Int J. Hydrogen Energ* 35, 8303-8309.
- Weber Jr., W.J., Morris, J.C., 1963. Kinetics of adsorption on carbon from solution. *J. Sanit. Eng. Div. Am. Soc. Civil Eng.* 89, 31-59.
- Weinwurm, F., Drljo, A., Waldmüller, W., Fiala, B., Niedermayer, J., Friedl, A., 2015. Lignin concentration and fractionation from ethanol organosolv liquors by ultra- and nanofiltration. *J. Clean. Prod.* 136, 62–71. doi:10.1016/j.jclepro.2016.04.048
- Wildschut, J., Smit, A. T., Reith, J. H., Huijgen, W.J.J., 2013. Ethanol-based organosolv fractionation of wheat straw for the production of lignin and enzymatically digestible cellulose. *Bioresour. Technol.* 135, 58-66.
- Wildschut, J., Smit, A.T., Reith, J.H., Huijgen, W.J.J., 2013. Ethanol-based organosolv fractionation of wheat straw for the production of lignin and enzymatically digestible cellulose. *Bioresour. Technol.* doi:10.1016/j.biortech.2012.10.050

- Wu, F.C., Tseng, R.L., Juang, R.S., 2009. Initial behavior of intraparticle diffusion model used in the description of adsorption kinetics. *Chem. Eng. J.* 153, 1–8. doi:10.1016/j.cej.2009.04.042
- Xu, F., Sun, R.C., Zhan, H.Y., 2003. Progress in non-wood hemicellulose research. *Trans Chin Pul Pap.* 18(1), 145–152.
- Xu, G., Wang, X., Hu, J., 2013. Bioleaching of wheat straw pulp using laccase and xylanase. *BioResources* 8 (3), 3181–3188.
- Xu, J., Chen, H., Kádár Z, Thomsen, A.B., Schmidt, J.E., Peng, H., 2011. Optimization of microwave pretreatment on wheat straw for ethanol production. *Biomass- Bioenergy* 35, 3859–3864.
- Yagub, M.T., Sen, T.K., Afroze, S., Ang, H.M., 2014. Dye and its removal from aqueous solution by adsorption: A review. *Adv. Colloid Interface Sci.* 209, 172–184. doi:10.1016/j.cis.2014.04.002
- Yang, S.H., 2008. *Plant fiber chemistry*. Beijing: China Light Industry Press.
- Yoo, C.G., Nghiem, N.P., Hicks, K.B., Kim, T.H., 2011. Pretreatment of corn stover using low-moisture anhydrous ammonia (LMAA) process. *Bioresour. Technol.* 102, 10028–10034
- Yu, J., Zhang, J., He, J., Liu, Z., Yu, Z., 2009. Combinations of mild physical or chemical pretreatment with biological pretreatment for enzymatic hydrolysis of rice hull. *Bioresour Technol* 100:903–908
- Zavrel, M., Bross, D., Funke, M., Büchs, J., Spiess, A.C., 2009. High-throughput screening for ionic liquids dissolving (ligno-) cellulose. *Bioresour. Technol.* 100, 2580–7.
- Zeitsch, K.J., 2000. *of Sugar Series. The chemistry and technology of furfural and its many by-Products*, vol. 13. New York: Elsevier Science.
- Zhan, H.Y., 2005. *Fiber chemistry and physics*. Beijing: Science Press.
- Zhang JQ, Lin L, Sun Y, Mitchell G, Liu SJ, 2008. Advance of studies on structure and decrystallization of cellulose. *Chem Ind for Prod.*, 28(6), 109–14.

- Zhang, K., Pei, Z., Wang, D., 2016. Organic solvent pretreatment of lignocellulosic biomass for biofuels and biochemicals: A review. *Bioresour. Technol.* doi:10.1016/j.biortech.2015.08.102
- Zhang, M., Qi, W., Liu, R., Su, R., Wu, S., He, Z., 2010. Fractionating lignocellulose by formic acid: characterization of major components. *Biomass Bioenerg* 34(4):525–532. doi:10.1016/j.biombioe.2009.12.018
- Zhang, YHP, Ding, SY, Mielenz, JR, Cui J-B, Elander, RT, Laser, M, Himmel, M., MacMillan, J., Lynd, L.2007. Fractionating recalcitrant lignocellulose at modest reaction conditions. *Biotechnol. Bioeng.* 97, 214-223.
- Zhao, X., Cheng, K., Liu, D., 2009. Organosolv pretreatment of lignocellulosic biomass for enzymatic hydrolysis. *Appl. Microbiol. Biotechnol.* doi:10.1007/s00253-009-1883-1
- Zhao, X.B., Cheng, K.K., Liu, D.H., 2009. Organosolv pretreatment of lignocellulosic biomass for enzymatic hydrolysis. *Appl. Microbiol. Biotechnol.* 82 (5), 815.
- Zheng, Y., Pan, Z., Zhang, R., 2009. Overview of biomass pretreatment for cellulosic ethanol production. *Int J Agric Biol Eng* 2, 51–68
- Zugenmaier, P., 2001. Conformation and packing of various crystalline cellulose fibers. *Prog. Polym. Sci.* 26(9), 1341–417.

## Appendix

The Determination of structural carbohydrates and lignin biomass, presented herein, was based on the National Renewable Energy Laboratory procedure (Sluiter et al., 2008).

### Apparatus

- i. Analytical balance, accurate to 0.1 mg
- ii. Convection drying oven, with temperature control of  $105 \pm 3$  °C.
- iii. Muffle furnace, equipped with thermostat, set to  $575 \pm 25$  °C or equipped with optional ramping program.
- iv. Water bath, set at  $30 \pm 3$  °C.
- v. Autoclave, suitable for autoclaving liquids, set to  $121 \pm 3$  °C.
- vi. Filtration setup, equipped with vacuum source.
- vii. Desiccator containing desiccant.
- viii. HPLC system with refractive detector.
- ix. UV- Visible spectrophotometer, diode array or single wavelength.

### Reagents and Materials

#### ➤ Reagents

- i. Sulfuric acid, 72% w/w (specific gravity 1.6338 at 20°C)
- ii. Calcium carbonate, ACS reagent grade.
- iii. Water, purified, 0.2 µm filtered.
- iv. High purity standards: D-cellobiose, D(+)glucose, D(+)xylose, D(+)galactose, L(+)arabinose, and D(+)mannose.

#### ➤ Materials

- i. QA standard, well characterized, such as a National Institute of Standards and Technology (NIST) biomass standard or another well characterized sample of similar composition to the samples being analyzed.
- ii. Pressure tubes, minimum 90 mL capacity, glass, with screw on Teflon caps and o-ring seals.
- iii. Teflon stir rods sized to fit in pressure tubes and approximately 5 cm longer than pressure tubes.
- iv. Filtering crucibles, 25 mL, porcelain, medium porosity, Coors #60531 or equivalent.
- v. Bottles, wide mouth, 50 mL.

- vi. Filtration flasks, 250 mL.
- vii. Erlenmeyer flasks, 50 mL.
- viii. Adjustable pipettors, covering ranges of 0.02 to 5.00 mL and 84.00 mL.
- ix. pH paper, range 4–9.
- x. Disposable syringes, 3 mL, fitted with 0.2  $\mu\text{m}$  syringe filters.
- xi. Autosampler vials with crimp top seals to fit.

### **Procedure**

1. Prepare the sample for analysis and hydrolyze.
  - 1.1 Place an appropriate number of filtering crucibles in the muffle furnace at  $575 \pm 25$  °C for a minimum of four hours. Remove the crucibles from the furnace directly into a desiccator and cool for a specific period of time, one hour is recommended. Weigh the crucibles to the nearest 0.1 mg and record this weight.
  - 1.2 Place the crucible back into the muffle furnace at  $575 \pm 25$  °C and ash to constant weight. Constant weight is defined as less than  $\pm 0.3$  mg change in the weight upon one hour of re-heating the crucible.
  - 1.3 Weigh  $300.0 \pm 10.0$  mg of the sample or QA standard into a tared pressure tube. Record the weight to the nearest 0.1 mg.
  - 1.4 Add  $3.00 \pm 0.01$  mL (or  $4.92 \pm 0.01$  g) of 72% sulfuric acid to each pressure tube. Use a Teflon stir rod to mix for one minute, or until the sample is thoroughly mixed.
  - 1.5 Place the pressure tube in a water bath set at  $30 \pm 3$  °C and incubate the sample for  $60 \pm 5$  minutes. Using the stir rod, stir the sample every 5 to 10 minutes without removing the sample from the bath. Stirring is essential to ensure even acid to particle contact and uniform hydrolysis.
  - 1.6 Upon completion of the 60-minute hydrolysis, remove the tubes from the water bath. Dilute the acid to a 4% concentration by adding  $84.00 \pm 0.04$  mL deionized water using an automatic burette. Dilution can also be done by adding  $84.00 \pm 0.04$  g of purified water using a balance accurate to 0.01 g. Screw the Teflon caps on securely. Mix the sample by inverting the tube several times to eliminate phase separation between high and low concentration acid layers.
  - 1.7 Prepare a set of sugar recovery standards (SRS) that will be taken through the remaining hydrolysis and used to correct for losses due to destruction of sugars during dilute acid hydrolysis. SRS should include D-(+)glucose, D-(+)xylose, D-(+)galactose, -L-(+)arabinose, and D-(+)mannose. Weigh out the required amounts of each sugar, to

the nearest 0.1 mg, and add 10.0 mL deionized water. Add 348  $\mu$ L of 72% sulfuric acid. Transfer the SRS to a pressure tube and cap tightly.

- 1.8 Place the tubes in an autoclave safe rack, and place the rack in the autoclave. Autoclave the sealed samples and sugar recovery standards for one hour at 121°C, usually the liquids setting. After completion of the autoclave cycle, allow the hydrolyzates to slowly cool to near room temperature before removing the caps.
2. Analyze the sample for acid insoluble lignin as follows.
  - 2.1 Vacuum filter the autoclaved hydrolysis solution through one of the previously weighed filtering crucibles. Capture the filtrate in a filtering flask.
  - 2.2 Transfer an aliquot, approximately 50 mL, into a sample storage bottle. This sample will be used to determine acid soluble lignin as well as carbohydrates, and acetyl if necessary. Acid soluble lignin determination must be done within 6 hours of hydrolysis. If the hydrolysis liquor must be stored, it should be stored in a refrigerator for a maximum of two weeks.
  - 2.3 Use deionized water to quantitatively transfer all remaining solids out of the pressure tube into the filtering crucible. Rinse the solids with a minimum of 50 mL fresh deionized water. Hot deionized water may be used in place of room temperature water to decrease the filtration time.
  - 2.4 Dry the crucible and acid insoluble residue at  $105 \pm 3$  °C until a constant weight is achieved, usually a minimum of four hours.
  - 2.5 Remove the samples from the oven and cool in a desiccator. Record the weight of the crucible and dry residue to the nearest 0.1 mg.
  - 2.6 Place the crucibles and residue in the muffle furnace at  $575 \pm 25$  °C for  $24 \pm 6$  hours.
  - 2.7 Carefully remove the crucible from the furnace directly into a desiccator and cool for a specific amount of time, equal to the initial cool time of the crucibles. Weigh the crucibles and ash to the nearest 0.1 mg and record the weight. Place the crucibles back in the furnace and ash to a constant weight.
3. Analyze the sample for acid soluble lignin.
  - 3.1 On a UV-Visible spectrophotometer, run a background of deionized water or 4% sulfuric acid.
  - 3.2 Using the hydrolysis liquor aliquot obtained in step 2.2, measure the absorbance of the sample at an appropriate wavelength on a UV-Visible spectrophotometer.
  - 3.3 Calculate the amount of acid soluble lignin present using calculation.
4. Analyze the sample for structural carbohydrates.

- 4.1 Using the hydrolysis liquor obtained in step 2.2, transfer an approximately 20 mL aliquot of each liquor to a 50 mL Erlenmeyer flask.
- 4.2 Use calcium carbonate to neutralize each sample to pH 5–6. Avoid neutralizing to a pH greater than 6 by monitoring with pH paper. Add the calcium carbonate slowly after reaching a pH of 4. Swirl the sample frequently. After reaching pH 5–6, stop calcium carbonate addition, allow the sample to settle, and decant off the supernatant. The pH of the liquid after settling will be approximately 7.
- 4.3 Prepare the sample for HPLC analysis by passing the decanted liquid through a 0.2  $\mu\text{m}$  filter into an autosampler vial. Seal and label the vial.
- 4.4 Analyze the calibration standards, CVS, and samples by HPLC using a Shodex sugar SP0810 or Biorad Aminex HPX-87P column equipped with the appropriate guard column.
- 4.5 Check test sample chromatograms for presence of cellobiose and oligomeric sugars.